Modeling of Cooling Towers under Heat Recovery

Matias Peljo

School of Engineering

Thesis submitted for examination for the degree of Master of Science in Technology.

Espoo 29.11.2018

Thesis supervisor:

Prof. Ville Vuorinen

Thesis advisor:

D.Sc. Brad Schofield

Aalto University
School of Engineering

AALTO UNIVERSITY
SCHOOL OF ENGINEERING

ABSTRACT OF THE
MASTER'S THESIS

Author: Matias Peljo

Title: Modeling of Cooling Towers under Heat Recovery

Date: 29.11.2018 Language: English Number of pages: 8+82

Department of Energy Technology

Professorship: Energy Technology

Supervisor: Prof. Ville Vuorinen

Advisor: D.Sc. Brad Schofield

The European Organization for Nuclear Research (CERN) has agreed on a commitment to minimize the environmental impact of the wide range of activities the Laboratory carries out. A key measure is waste heat recovery (WHR), as approximately 75 % of the power consumed in the electricity intensive particle accelerator complex, is dissipated to the sky as waste heat by cooling towers.

A project for installing waste heat recovery to the cooling system of the Large Hadron Collider (LHC) at LHC point 8 has started and is expected to be operational in the beginning of 2020, after the second LHC long shutdown in 2018-2019. The operation of WHR causes a risk of temperature transients in case of unexpected WHR shutdowns. A dynamic simulation model of the cooling towers is needed to verify robustness against these temperature transients. In this Thesis, a thorough literature review of existing evaporative cooling tower modeling methods is performed, and the hybrid modeling method presented by Jin et al. (2007), is implemented to simulate the cooling towers at LHC point 8. The developed model is validated against real operational data. To the authors knowledge, this study is the first published use case of this evaporative cooling tower modeling method.

A selection of anticipated sudden WHR shutdown scenarios are simulated in virtual commissioning environment with real programmable logic controller (PLC) to verify robustness of the cooling system against sudden temperature transients. A conclusion is that the cooling towers and their current control scheme is sufficient in dampening the anticipated temperature transients. This knowledge allows the WHR installation project to proceed.

Keywords: cooling tower, waste heat recovery, dynamic modeling, parameter optimization, CERN

AALTO-YLIOPISTO
INSINÖÖRITIETEIDEN KORKEAKOULU

DIPLOMITYÖN
TIIVISTELMÄ

Tekijä: Matias Peljo

Työn nimi: Jäähdytystornien Mallintaminen ja Lämmön Talteenotto

Päivämäärä: 29.11.2018 Kieli: Englanti Sivumäärä: 8+82

Energiatekniikan laitos

Professuuri: Energiatekniikka

Työn valvoja: Prof. Ville Vuorinen

Työn ohjaaja: D.Sc. Brad Schofield

Euroopan hiukkasfysiikan tutktimuskeskuksella CERN:illä on tavoitteenaan minimoida laboration aktiviteettien ympäristövaikutukset. Tämän tavoitteen saavuttamisessa lämmön talteenotto (LTO) on tärkeässä roolissa, sillä energiaintensiivisessä hiukkaskiihdytinkompleksissa noin 75 prosenttia käytetystä sähkötehosta haihdutetaan taivaalle jäähdytystornien kautta hukkalämpönä.

Toisen pitkän käyttökaton aikana vuosina 2019 - 2020 suuren hadronitörmäyttimen (LHC) pisteelle 8 asennetaan lämmön talteenottojärjestelmä. Lämmön talteenoton käyttö aiheuttaa riskin lämpötilavaihteluiden syntymiselle, jos hukkalämmön vastaanotto katkeaa äkillisesti. Dynaaminen jäähdytystornien simulaointimalli tarvitaan suuren hadronitörmäyttimen toiminnan kannalta kriittisen jäähdytysjärjestelmän luotettavuuden varmistamiseksi. Tässä diplomityössä esitellään kattava kirjallisuuskatsaus jäähdytystornien mallinusmenetelmistä ja implementoidaan Jin et al. (2007) julkaisema hybridi-menetelmä LHC pisteen 8 jäähdytystornien simuloimiseksi. Malli validoidaan järjestelmästä mitattua dataa vasten. Tehdyn kirjallisuusselvityksen perusteella tämä diplomityö on ensimmäinen julkaisu, jossa tätä jäähdystornien mallinusmenetelmää sovelletaan käytössä olevan järjestelmän simuloimiseen.

Järjestelmän lämpötilatransienttien vaimmenuskyvyn tutkimiseksi jäähdytystornimallilla simuloidaan eri vuodenaikoina odetettavissa olevia lämmön talteenoton pysähtymisiä virtual commissioning -ympäristössä, jossa todellinen ohjelmoitava logiikka (Programmable Logic Controller PLC) ohjaa mallia. Simulointien tulokset osoittavat, että nykyinen jäähdytyskapasiteetti ja ohjauslogiikka vaimentavat odotettavissa olevia transientteja tehokkaasti. Tämän tiedon perusteella lämmön talteenottoprojekti voi edetä.

Avainsanat: jäähdytystorni, lämmön talteenotto, dynaaminen mallintaminen, paramterioptimointi, CERN

Acknowledgements

The work of this thesis was carried out between January and October 2018 in Geneva, Switzerland. I want to thank my employer CERN, the European Organization for Nuclear Research, for setting up this truly inspirational and motivational project, which I'm grateful for having a chance to take a part of. I hope the actions at CERN towards a climate neutral laboratory will be successful and will set an example to others.

I'm grateful to my advisor at CERN, Dr. Brad Schofield, for his guidance and his trust in my abilities during this challenging project. It was truly a pleasure to work with him. I naturally also wish to thank my supervising professor Dr. Ville Vuorinen. To my colleagues at the BE-ICS-AP, I will never forget how welcoming you were and how easy it was for me to be part of the team. Thank you for all the expertise help and the nice moments we spent together in and out of the office! I wish to give my endorsement for the community of CERN people, Yacht Club du CERN and CERN Ski Club for keeping me busy in a new place. The moments and opportunities to meet people from all over the world has left a permanent impact on me and created long lasting friendships.

Here by my journey to become a Master of Science is coming to a happy ending. I am truly grateful for the skills I have acquired, the values I've developed and experiences I have had while being a part of these academic institutions as a degree student in Aalto, as an exchange student in Technische Univeristät Berlin and as a Master's Thesis student at CERN. Equally if not more importantly I'm now equipped with experiences and lessons learned from amazing individuals whom I've had a chance to meet in the student community of Aalto while steaming and bathing with Koneinsinöörikilta, starting fires at Slush and taking driving lessons in Autokoulu.

Special thanks to family, friends and Sandra, for supporting me and pushing me forward when I missed you the most and needed encouraging with the Thesis work. Thank you for supporting me during this journey.

Espoo, November 22, 2018

Matias Peljo

Contents

Symbols and abbreviations

Symbols

T_1	general return temperature (°C)
T_2	cooling tower basin temperature (°C)
$\dot{V}$	volumetric flow (m^3/s)
$\dot{m}$	mass flow (kg/s)
i	enthalpy (kJ/kg)
A	area (m^2)
dA	characteristic heat transfer area (m^2)
Q	heat power (kW)
h	heat transfer coefficient (W/m^2K)
h_d	mass transfer coefficient (kg/m^2s)
w	humidity ratio (kg water vapor / kg dry air)
w_{sw}	humidity ratio of saturated air at the air-water interface temperature (kg water vapor / kg dry air)
c_p	specific heat at constant pressure (J/kgK)
c_{pma}	specific heat of air and vapor mixture (J/Kkg dry air)
Me	Merkels number
T_{dp}	Ambient dry-bulb temperature (°C)
T_{wb}	Ambient wet-bulb temperature (°C)
RH	Ambient relative humidity (%)
P	Ambient pressure (mbar)
c_1, c_3, c_4, l	Model parameters (dimensionless)

Subscripts

a	air
w	water
s	saturation
v	vapor

Abbreviations

LHC	Large Hadron Collider
WHR	Waste Heat Recovery
ESS	European Spallation Source
CFD	Computational Fluid Dynamics
UNICOS	UNified Industrial Control System
PLC	Porgrammable Logic Controller

1 Introduction

Dynamic modeling is a common tool to solve engineering and business problems. It involves building models, defining quantitative relations between variables and interpreting phenomena by running numerical simulations on the models. In this Thesis a dynamic cooling tower model is created and simulations ran to gain knowledge of the effect of retrofitting waste heat recovery to the cooling system of the Large Hadron Collider (LHC). Due to the complex and critical nature of the cooling system, thorough understanding of the robustness is required, and only way to gain this knowledge is a dynamic simulation study. In section 1.1 the problem is introduced, and section 1.2 presents how the key concepts of this thesis, process simulation and virtual commissioning are addressed in the literature. The objective of this Thesis is discussed in section 1.3.

1.1 Problem

To minimize the environmental impact of the wide range of activities CERN carries out in the course of its research on fundamentals of physics, an environmental commitment has been agreed on (CERN 2018c). Due to the energy intensity of activities related to high energy physics, waste heat recovery is a key measure to increase the energy efficiency (Claudet 2017). Preparations have started for installing waste heat recovery on the cooling sites, and the project is starting with a pilot at LHC point 8, providing heat released by the LHC magnets and LHCb experiments magnets for the use of the nearby french municipality of Ferney-Voltaire (Claudet 2017). At the early design phase of the heat recovery compatibility refit, CERN has faced questions which raised an interest towards a simulation study: What is the ability of the cooling towers and current control configuration to damp fluctuations in the cooling water temperature caused by external disturbances to the waste heat recovery plant and if any changes on the control configuration are required? The cooling towers supply primary cooling water to cryogenic refrigeration plants, which are complex and sensitive systems and critical for the LHC operations. A simulation model is needed for verification of the existing/updated control system configuration under a possible event of temperature transients caused by a sudden loss of the waste heat recovery.

1.2 Literature survey

Process simulation and virtual commissioning are widely discussed and researched in the literature, supplied as commercial software tools and applied in wide range of industrial applications. Process simulation is an important tool in engineering in different domains. In order to conduct simulation studies, a model is needed, which

builds quantitative relations between inputs and outputs such as flows, distances, costs or temperatures. Simulation is a numerical experiment done with the model. In dynamic simulations models, which output values depend on the past values, are simulated over time, giving and receiving continuous or discrete values or a mixture of them. (Ljung and Glad 1994).

Process simulations consisting of models that require chemical and thermal properties as parameters or variables, can have them incorporated in the simulation software as property models. Property models provide values for densities, enthalpies etc. during the simulation (Gani and Pistikopoulos 2002). Simulation software tools such as EcosimPro, provide property models in libraries including property databases, which can be applied by the modelers in their own models (EcosimPro 2018). Process simulation is used as a tool in many areas of engineering and business. In his Master's Thesis, El Geneidy (2016-06-13) presents a discrete event simulation study of an energy system of a passengers ship. The models and simulations were created to test and analyze overall effect and cost savings of different types of technologies which increase the energy efficiency of a large scale diesel electric marine power system.

Basic idea of virtual commissioning is to connect a real control system with a simulation model of the real system. This practise allows engineers to detect errors and debug programmable logic controller (PLC) -code, which makes the actual commissioning with the real system easier. In manufacturing of products in large scales and under constant pressure to reduce manufacturing costs, many corporations have found virtual commissioning as an effective tool to analyze and optimize processes. Lee and Park (2014) provide an overview of virtual commissioning in manufacturing processes. They identified that the main obstacle for wider application of virtual commissioning is the model building, which requires in depth expertise, both in modeling and control engineering, as the model needs to communicate with the real control system.

For large scale and highly complex systems with large number of correlated variables, dynamic models and complete virtual twins are the only way to improve knowledge of the system. Bradu, Philippe Gayet, and Niculescu (2009) present a process and control simulator of cryogenic refrigeration plants of the Large Hadron Collider. Their model is designed for virtual commissioning, it can fully replace the real system and connect with the existing control and supervision system in use. Thus the simulations can be used for operator training or testing and verifying control algorithms. For critical systems virtual commissioning of control algorithms and programmable logic controller (PLC) -code is a preferred practise (Booth et al. 2018). In their paper Booth et al. (2018) present a study of virtual commissioning procedure applied for a heating, ventilation and air conditioning (HVAC) system of the Compact Muon Solenoid (CMS) cavern, which is one of the four LHC experiments.

1.3 Objective

The objective of this Thesis is to develop a simulation model for the cooling towers which allows virtual commissioning simulations, that are used to study if the control scheme is able to survive a sudden loss of the heat recovery sufficiently. In order to reach this objective two major areas are researched in this Thesis:

1. Develop a simulation model of the cooling towers which dynamically simulates the output water temperature given the input variables that can be used for virtual commissioning
    - Compare published methods and implement a suitable solution
    - Validate the developed model against real operational data
2. Study if the current control scheme is sufficient in keeping the output temperature nominal in the case of sudden loss of heat recovery
    - Simulate the system response under control of a Programmable Logic Controller (PLC) containing the current control configuration

The study is carried out together with Industrial controls and Safety Group at Beams Department (BE-ICS-AP) at CERN, Geneva, Switzerland. In order to accomplish these objectives this Thesis will present the theory and previous research on the heat and mass transfer phenomena in an evaporative counter flow cooling tower, and review modeling methods available in the literature. A model is implemented in EcosimPro -simulation software based on a modeling method presented in the literature. The model is parameterised and validated with the data available from CERN cooling towers. The Thesis presents results of the simulations run with the model parameterised for the cooling system at LHC point 8. The validation of the model concludes that the developed model is accurate and can be reliably used for virtual commissioning simulations to study the overall cooling tower system robustness. From the simulations results it is concluded that the current installed capacity and control algorithm is able to manage the anticipated transients with the waste heat recovery.

2 Background

This chapter presents some key activities and technologies at CERN. The methods to accomplish the key task of CERN, provide head to head collisions of particles traveling at high energy, and obtain and maintain a high luminosity, i.e. the rate of collisions in the experiments, are introduced briefly. Energy intensity of the activities related to high energy physics is discussed, and major contributors to high energy consumption are introduced. The cooling system used at CERN and the project of installing waste heat recovery are presented. The use of waste heat in other similar facilities and the project of installing waste heat recovery to the cooling system at LHC point 8 is presented. Also further possibilities of heat recovery in larger scale in the future are discussed. The motivation for the need of transient cooling tower simulation is presented.

2.1 CERN

CERN, the European Organization for Nuclear Research, founded in 1954, nowadays a collaboration of 22 member states, is a laboratory studying the fundamental structure of the universe (CERN 2018f). At CERN, the biggest machine in the world, the Large Hadron Collider (LHC), among with some of the world's largest and most complex scientific instrumentation are used to accelerate and collide particles close to the speed of light. The LHC, is a 27 km long circular particle collider that accelerates particles in bunches and rotates them in the LHC ring in both directions. The particles are steered to collide head to head in the ATLAS, CMS, LHCb and ALICE experiments. In the collisions energy is transformed into mass and new particles are formed. The detectors in the experiments capture clues of information of the collisions produced by the LHC. (CERN 2018a)

2.1.1 Research at CERN

Particle physics is the main area of research and activities at CERN. The fundamentals of our knowledge of physics and the universe have been predicted by the Standard model of physics since the 1970's, proposing the few basic building blocks of all that exists in the universe and stating the forces keeping them together. The results from LHC and experiments at CERN, now show that the predictions of the Standard model are correct, and it is today considered as a well-tested physics theory. (CERN 2018e)

It is estimated that the Standard model only describes 4 % of the known universe, and beyond this theory there are numerous other theories needed to describe the questions not yet answered, and the phenomena that currently is unobservable. The LHC and the experiments, are used to produce these conditions and detectors are

used to observe them. These are conditions that need high energies, like during the big bang, and can be produced by making particles travel at high energies close to speed of light to collide with each other. Particles collide at the experiments, where novel instrumentation is used to record clues of the phenomena during the collisions. Four main experiments are located around the LHC ring: Atlas, Compact Muon Solenoid (CMS), LHCb and Alice. The Atlas experiment hall, which houses the cavern used for building the experiment underground, is seen in figure (1). (CERN 2018e)

Figure 1: 3:4 Mural on the wall of the Atlas control center at CERN, illustrating the detector lying beneath the ground (Atlas Collaboration 2015).

2.1.2 The accelerator complex

The layout of the CERN accelerator complex is shown in figure (2). The protons colliding in the experiments on the LHC ring, originate from a bottle of hydrogen at the beginning of the chain of particle accelerators. Protons are stripped out from the hydrogen atoms and accelerated to energy of 50 MeV in Linear Accelerator 2 (LINAC 2). The mass of the protons increase by 5 % in LINAC 2, following the Theory of relativity by Albert Einstein, as the speed of the protons approaches the speed of light. Energy of the beam in MeV is for a single proton. The proton beam

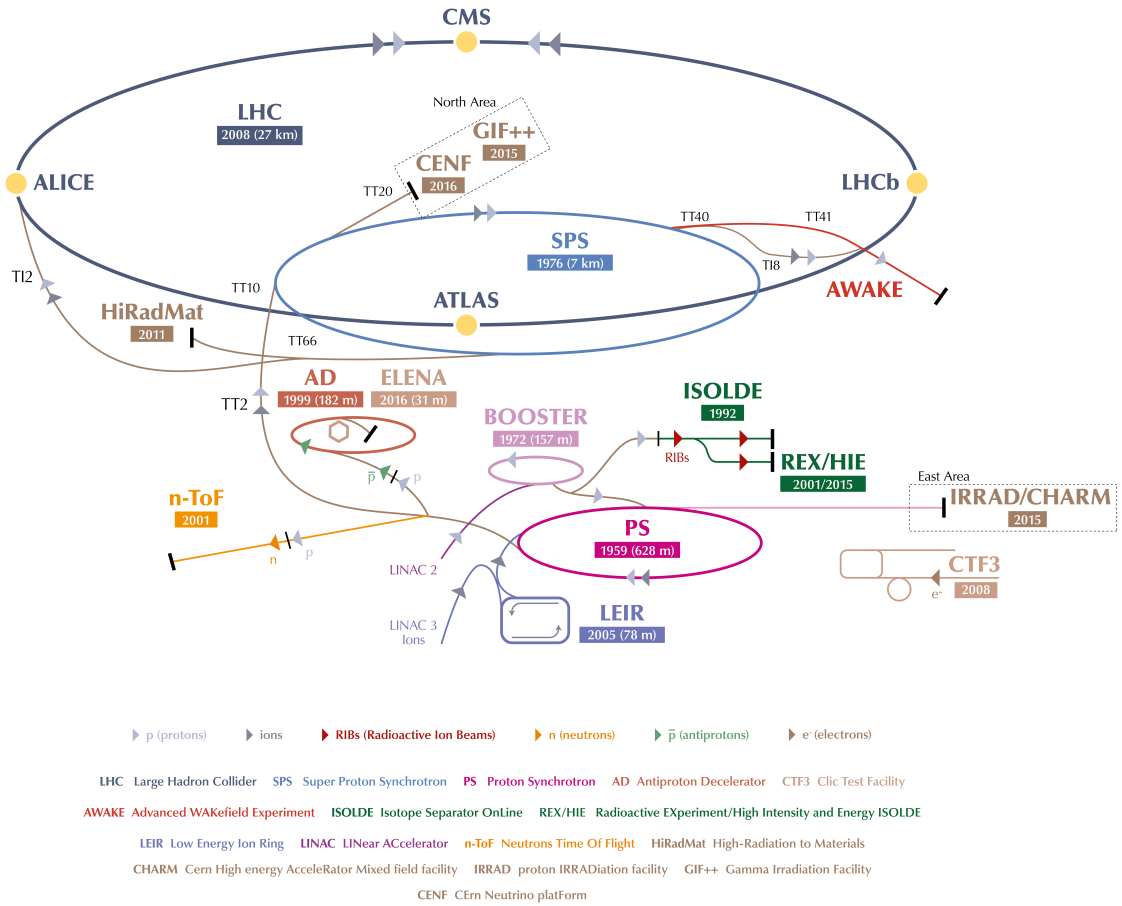

Figure 2: The CERN accelerator complex including linear accelerators, circular accelerators and colliders. The largest circular accelerator, the Large Hadron Collider (LHC), is in a tunnel 100 meters below ground. (CERN 2015).

is then injected in to the Proton Synchrotron Booster (PSB), a circular accelerator, further increasing the energy to 1.4 GeV. From PSB, the beam continues to the Proton Synchrotron (PS), which accelerates the protons to 25 GeV, followed by Super Proton Synchrotron (SPS), which pushes the beam to 450 GeV. Finally the protons are transferred into the two beam pipes travelling opposite direction in the LHC, 100 meters below the ground with parts of it in France and Switzerland. In each beam pipe, the protons travel in 2808 bunches forming what is called the particle beam, every bunch containing $1.15e10^{11}$ protons. A bunch is about 30 cm long and there are 7.5 metres or 25 nano seconds between the bunches. The LHC accelerates the beam for 20 minutes to reach the maximum energy of 6.5 TeV. Total energy of the two beams is about 724 MJ, enough to melt a ton of copper (CERN Outreach -). The beam then circulates for many hours providing continuous collisions in the experiments on the LHC ring, before a new injection of protons from the SPS is again required.

The LHC consists of 16 radio frequency cavities and 2000 dipole magnets. The radio

frequency cavities produce an electric field that is accelerating the particles. The electric field is oscillating (switching direction) at 400Hz, as the bunches come one clockwise after another counter clockwise. This way the cavities alternate between accelerating bunches coming from both directions. The speed and energy of the particles are restricted by two factors, the curvature of the circular accelerator and the magnetic force bending the trajectory of the beam. The dipole magnets produce a magnetic field in to each beam pipe to keep the beam on the circular track. The superconducting dipole magnets reach 8.3 tesla magnetic field, strong enough to bend the trajectory of a high energy beam. The cryogenic temperature conditions at 1.9 Kelvins allow the magnets to carry current of 11,000 amperes with zero resistance, to generate the strong magnetic field. (CERN 2018b)

2.1.3 CERN's impact on society

"My message was that science has no passport, no gender, no race, no culture, no political party. I said that science can play a key role in connecting people and creating a shared future in a fractured world, because science is universal and unifying." -Fabiola Giannotti, director general of CERN, at World Economic Forum 2018, Davos, Switzerland (The New York Times 2018).

Existence of CERN is driving innovation, collaboration, education, open access science, everything extremely important for creating long term circumstances, where our understanding of the physics, and the universe, may enhance. This development has an impact on the society, which will push forward also other domains. At CERN a knowledge transfer group works to promote the technological and human capital developed at CERN, to transfer the knowledge into the society and find applications for CERN innovations outside particle physics. The development driven by ambitions in particle physics, has wide range of applications for example in medicine and bio-medical engineering or aerospace applications. (CERN 2018d)

2.2 Cooling at CERN

This section presents the centralized cooling systems at CERN, that are used to manage the large heat load produced by the accelerator complex and smaller instruments. Cryogenic systems are discussed briefly, and water systems in more detail.

Particle physics as an industry is very electricity intensive. At 2017, the total electricity consumption of CERN accounted for 1132 GWh. This contributes yearly to an electricity bill more than 80 M Swiss francs. Electricity is used in the accelerating equipment, bending magnets and cryogenic cooling installations around the 27 km LHC ring as well as in smaller accelerators, SPS and PS, and linear accelerators feeding the protons to the accelerator complex. Most of the energy used as electricity

is converted into heat losses in various activities. Majority of the electricity is used in science instrumentation and only about 10 % of the total electricity consumption accounts for conventional facilities. The cooling circuits equipped with evaporative cooling towers, are used to dissipate the excess heat generated and keep the equipment in the accelerators and experiments cool. Total heat dissipated by the cooling towers at 2017 was 835.9 Gwh, 74 % of the total electrical energy consumed. Heat dissipation contributors shown in table (1). (CERN Engineering Department 2017b)

Table 1 Sources of waste heat at CERN. (CERN Engineering Department 2017a)

Users	Location of the cooling network	Power dissipated (GWh), 2017
LHC and Experiments	Point 1 (Atlas), 2, 5 (CMS), 6, 8 and 1.8	512
SPS	Point 1	115
North Area	CERN Prévessin site	112
PS and other equipment	CERN Meyrin site	86.9

2.2.1 Cryogenic cooling networks at CERN

To accelerate and keep the particle beams on the circular trajectory, an intensity of 8.3 T magnetic field is required to bend the trajectory of proton traveling 0.999999991 times the speed of light. Such strength of the magnetic field is achieved by creating conditions so cold, that the wiring in the coils of the electric magnets reach superconductivity. The dipole magnets and the strong magnets needed in the experiments, are cooled down to 1.9K throughout the whole LHC ring and in smaller accelerators. The refrigeration process consists of multiple stages of heat exchange and cryogenic heat pumps using first water, then a mixture of helium and oil and finally superfluid helium in 1.9 Kelvin. Water is used to cool the cryoplants, with temperature change of approximately 24 °C - 34 °C. The cooling towers are used to dissipate this thermal energy to the atmosphere and return the cooling water at approximately 24 °C. (CERN 2018h) (CERN 2018g)

Cryogenic cooling networks, each having a cryoplant and one to six cooling towers on ground, are situated at the LHC points 1, 2, 5, 6, 8, and 1.8 around the LHC ring. The eight cooling networks are capable to function autonomously. The distributed architecture helps to manage and detect faults and reduces the scale of the problems. The LHC points and underground facilities are presented in figure (3). At LHC points, vertical cavities connect the underground facilities to surface. Each cryogenic refrigeration network distributes the superfluid helium to a ring sector of about 3.3 km. (Blanco and Ph Gayet 2007)

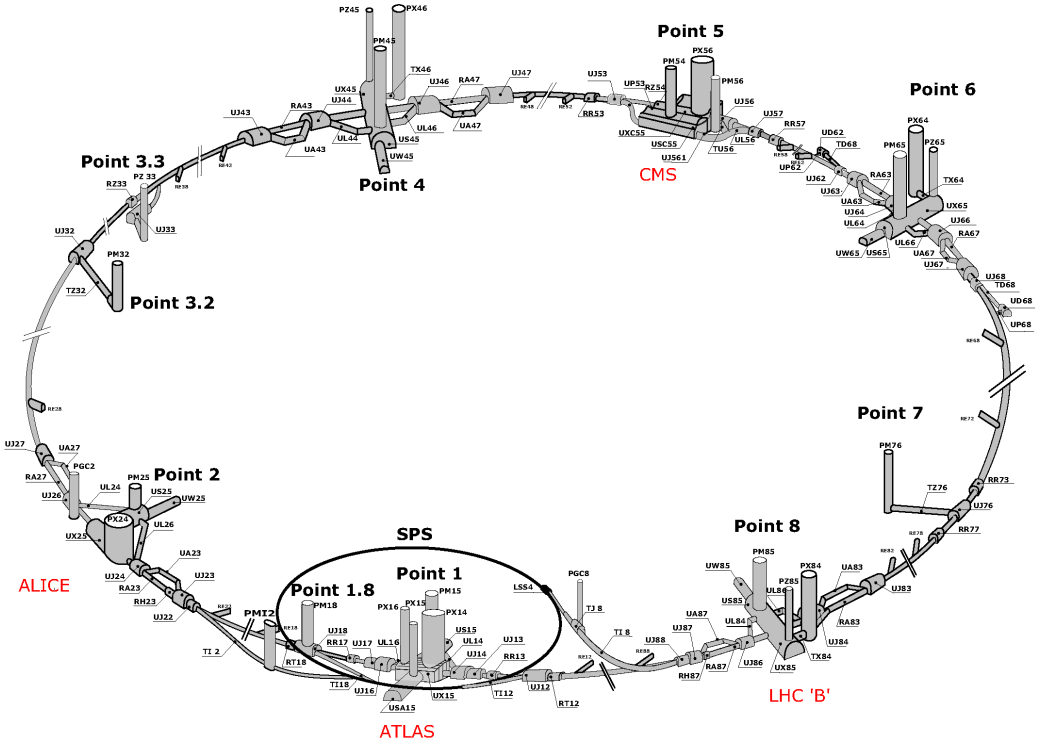

Figure 3: Vertical cavities connect large caverns to surface facilities. The cavers house the experiments which record particle collisions. Cavities where used to construct the experiments like a ship in bottle is made. (CERN Technology Department 2015).

2.2.2 Cooling tower water distribution at LHC point 8

CWER cooling water systems operate primary cooling water and demineralised cooling water. The demineralised cooling water is in a closed circuit and is cooled via a heat exchanger by the primary cooling water. Demineralised water is used to cool the accelerator systems. Primary water is cooled in the towers to design temperature of 24 °C, while the temperature may vary between 20 °C and 26 °C depending on ambient wet-bulb temperature. The primary cooling water circuit is a closed circuit, however periodically raw water is required to add in order to compensate the evaporation in the cooling towers. Raw water is sourced from the Lake Geneva by a pumping station located in Vengeron, Switzerland. The primary water also requires treatment: electric heating to prevent freezing in the winter during shutdown, filtering to remove small particles and Legionella preventive treatment. (Brüning et al. 2004)

At LHC point 8 the primary water circuits connected to the cooling towers in figure (4) are:

I. Circuits for supplying the underground and surface installations

II. Filter circuit using sand filters

III. Anti-freeze circuit

IV. Blowdown circuit

V. Backup circuit

The cooling station at LHC point 8 / LHCb experiment, provides average cooling power of 10 megawatts by five counter flow forced draft evaporative cooling towers, providing total cooling capacity of 47.5 MW (CERN Engineering Department 2017b). Main clients of the cooling at LHC point 8 are cryogenics for cooling down the LHC (I), cryogenics for cooling the magnets at LHCb experiment and other smaller applications requiring cooling (II). The cooling towers have been built on site in two phases. First tower and the machine hall in the early 1980s, and the remaining four towers in the early 1990s. The dimensions of the towers are similar. Currently a tent has been installed in front of the towers, that covers some of the air flow entering the towers. The tent is due to be removed during long shutdown 2 (2019 - 2020), as it reduces the cooling capacity of the towers.

Each cooling tower has a water basin (B) below the tower, and below the cooling tower basins in the machine hall, there is a common basin (C) smaller in volume compared to the tower basins combined. The primary cooling water is feed to the cooling circuits from the common basin. The cooling rate of the cooling tower is controlled by two factors, the cooling towers statues and fan speed. The cooling towers statuses include bypass status, shower status and ventilation status. In bypass mode the input water is passed straight into the cooling tower basin. In showering mode, the input water is lead to the shower nozzles, but the fan is of and air flow is driven by the warm air buoyancy in the tower, i.e. natural draft. In ventilation status i.e. mechanical draft mode, the fan is switched on and the speed of the fan is controlled by the control system. The control configuration is based on feedback control, where mean of the basin temperatures is the controlled value.

Reliability has been a key feature in designing the system. Circuits that supply critical systems, are equipped with a back up pump (indicated with * in figure (2.2.2). During long shutdown 1 (2013 - 2014), two back up cooling towers were added.

Several sensors and indicators are installed to the cooling towers and the control system. The control system is based on UNICOS (Unified Industrial Control System), a control framework developed at CERN. The readings are used for control and supervision of the cooling towers and the primary cooling water circuits. The readings from the sensors are logged to the archive, where it is available since October 2013, also for use of this thesis. (CERN Industrial Controls and Safety Group (ICS) 2018)

Sensors indicated in the figure 4:

T_1 Water temperature before the cooling towers, °C

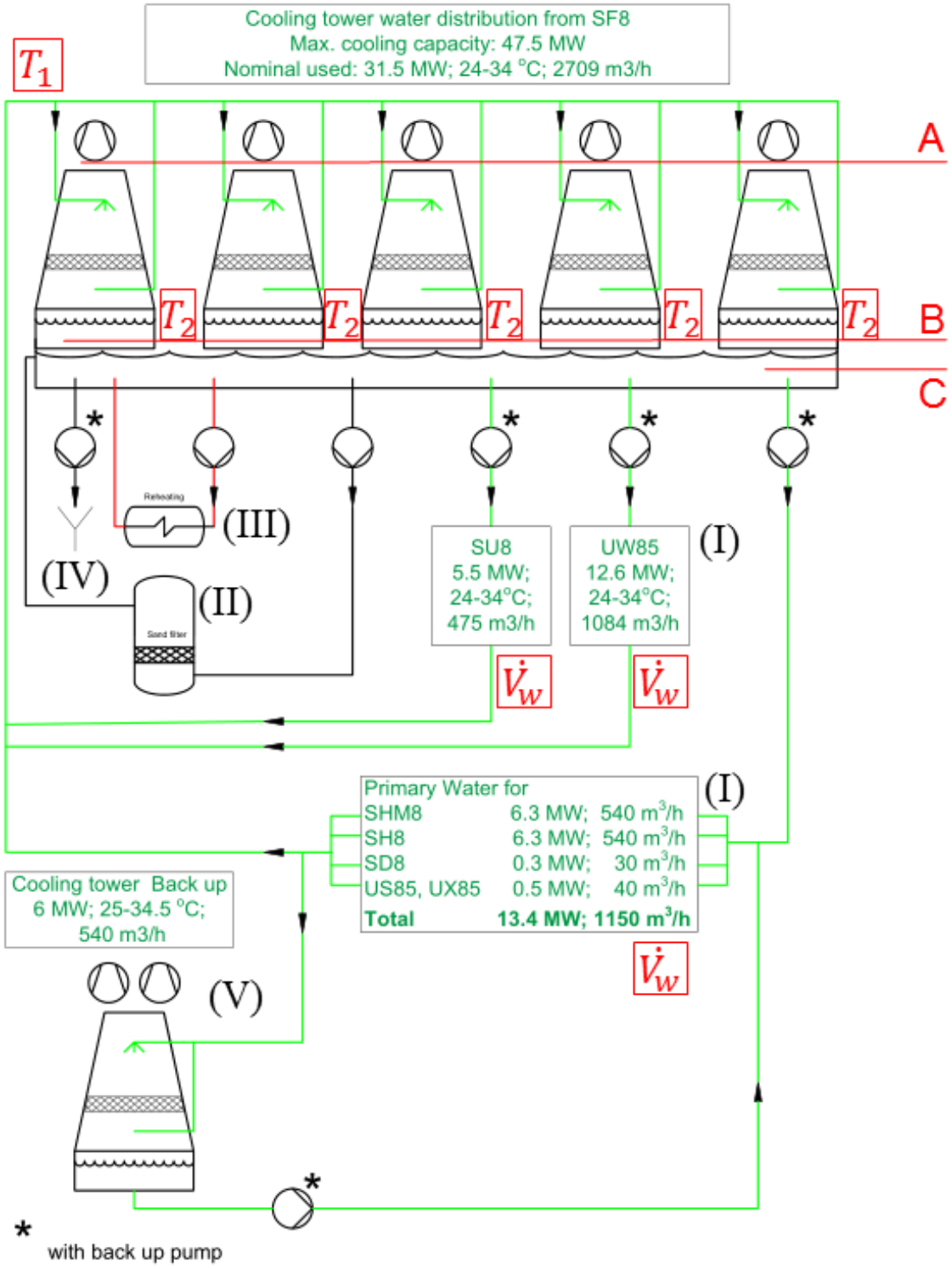

Figure 4: Cooling system at LHC point 8. The common basin collects cooled primary cooling water, from where the cooling water is distributed to clients. (CERN Engineering Department)

Figure 5: Cooling towers at LHC point 8 close to the Geneva Airport and the border of France and Switzerland. A tent has been blocking part of the airflow into the towers, which have increased the primary cooling water temperature during the hottest days.

T_2 Cooling tower basin temperatures, °C

$\dot{V}_w$ Volumetric flow in each of the cooling circuits supplying installations, m^3/h

A Fan speed signal indicator, %

Temperature sensors for the basin temperatures (B), are located in the cooling tower basins approximately 50 centimeters below the surface. This temperature is approximately same as the temperature of the water that leaves the cooling tower basin. Volumetric flow entering the cooling towers is not measured directly, but it can be calculated from the sum of the three flows in the three circuits supplying primary cooling water to the installations and returning it to the cooling towers. The water is then distributed equally to all five towers, given none of the towers is defunct. The cooling power can be calculated from the temperature difference in cooling towers as $Q = \dot{m}_w c_p \Delta T$. c_p is the specific heat capacity of water (kJ/kg) in respective temperature and $\dot{m}_w$ is the mass flow of water (kg/s) calculated using the density of water in respective temperature.

2.3 Waste heat recovery

Many big high energy physics laboratories with similar excess heat management as in CERN, are build before the new millennial during an era when the environmental issues where not as high on agenda as today.

2.3.1 Waste heat recovery at European Spallation Source (ESS), Lund, Sweden

The ESS, European Spallation Source, of which constructions started in 2013 and are due to finish in 2025, claims to be the first large scale physics laboratory of its kind to install waste heat recovery (ESS 2013). A 4-5 km long district heating pipeline will be build to connect the cooling system of the ESS to the district heating network of the city of Lund. For the ESS, the installation of the waste heat recovery, has been a design feature since the early stages of the project. The cooling system and the cryoplants there, are designed to optimize the efficiency of the heat recovery. This is done by cooling the equipment at as high temperature as possible. The configuration there will be consisting of high, medium and low temperature cooling loops. The high temperature loop, will allow the use of a heat exchanger between the district heating water and ESS cooling water, instead of only using heat pumps, which have lower efficiency due to the need of electricity driving them. (Jurns, Bäck, and Gierow 2014)

2.3.2 Waste heat recovery at CERN

CERN has an environmental commitment to minimize the environmental impact of the wide range of activities the Laboratory carries out in the course of its research. Several actions are in practise at this moment to increase the awareness of CERN employees in their everyday work to minimize the environmental impact on use of resources. However at CERN, buildings and conventional facilities represent for only about 10% of total electricity consumption, and the rest is used in the physics research instruments. The majority of this electricity used transforms to waste heat, which is managed by the cooling networks. Designs and agreements together with the surrounding municipalities of the first steps towards waste heat recovery has started at CERN. (Claudet 2017)

The municipality of Ferney Voltaire, which is located about 2 km to the east from the LHC point 8, is collaborating with CERN to recover up to 10 MW of the waste heat. The area has developed a lot, partially due to its proximity of the United Nations quarters and other big employers of Geneva, and high demand on housing in Geneva. A new area for housing and commercial services has been planned right next to the Swiss border in Ferney. The project, La Zone d'Aménagement Concertée (ZAC),

will include construction of 412 000 square meters of estate for housing, services and offices (Mairie de Ferney-Voltaire 2018). The project will also include installation of a grid of 200 meters deep geothermal U-tubes and heat pump facilities to provide clean and renewable heat source for the new quarters. The heat pumps needed for geothermal heating system allow the use of low temperature waste heat from CERN. The collaboration with CERN significantly reduces the amount and cost of geothermal U-tubes needed at ZAC. During the summer months when heating is not needed, the heat from CERN can be stored to the ground. (Mertens 2018)

An incentive to pilot and develop experiences and a proof of concept now on a smaller scale, is the long term future of circular colliders. It has been identified, that to go even further and to study even smaller particles outside the standard model of physics, the energy of the collisions needs be increased. The high performance and success of the LHC machine has lead to discovery of the Higgs Boson, but to go further, the project FCC, Future Circular Collider, has been established. The power of magnetic field is a boundary for accelerating particles to even higher energies, thus increasing the diameter of the circular collider is a valid option. The energy consumption and amount of excess heat generated, would be enormous in the FCC, if being 100 kilometers long as planned. The FCC would go below the high populated areas of Geneva and French Annemasse, providing a great possibility for cooling system optimized for heat recovery similar to the solution currently under construction at the ESS. (Mertens 2018)

2.4 Motivation for developing a dynamic cooling tower model

The simulation model is needed to study the reliability and robustness of the cooling towers for minimizing downtime. At CERN, as in any industrial facility, factory or power plant, downtime is a serious issue. Availability of the LHC machine each year is a percentage of the time excluding technical stops, when the machine was producing stable beams for physics research, or the time planned between the fills. In 2017, the proton physics run was in total 218 days, with availability of 49 %, operations 30 % and downtime 19 % (Todd et al. 2017). Operations includes all planned machine phases carried out in between fills, when the machine is not in downtime or stable beams. Downtime is the unplanned time lost because of faults somewhere in the accelerator complex. In 2017, cryogenics was the second biggest fault causing equipment, with a contribution of 13 % (Todd et al. 2017). Stable primary cooling water supply from the cooling towers is vital for the nominal operation of the cryogenics. One of the key features of the heat recovery project is, that it must be applied without compromising on the reliability of the cooling supply.

After installing heat recovery, the ZAC will start to absorb some of the waste heat at LHC point 8. This will mean that the cooling towers can operate on lower cooling rate. However CERN can't rely on ZAC to provide a constant and secure heat absorption, and CERN has to be able to absorb the heat load immediately, if the

heat recovery stops for any reason. In the case of a sudden stop of heat recovery, the cooling towers will receive a temperature transient back to the normal cooling water return temperature, and it will be the cooling towers responsible for dampening this transient to an acceptable level. It is estimated that delta T of more than five degrees Celsius in ten minutes or temperature more than 25 degrees Celsius are the hard limits for the underlying cryogenic cooling systems. The concern if the towers are able to increase the cooling power effectively enough to damp the temperature transient without risking the cryogenic conditions at the LHC and the experiments. A dynamic cooling tower model enables simulations to study this event.

The installed hardware will determine if the cooling towers will have the reserve capacity to damp the transients, and a simulation model is used to reveal this, but another equally important matter is the software, the control configuration that controls the cooling towers. It needs to be verified, that the control configuration is able to detect and react to the possible temperature transient efficiently, and ensure that fluctuations will be managed and do not start to oscillate out of control. At CERN, virtual commissioning is used as a tool to evaluate control configuration performance. Commissioning a control configuration coded into a programmable logic controller (PLC) with a simulation model instead of the real system, is called virtual commissioning. Virtual commissioning is a proven way to test upgrades to the control configuration or changes to the real system prior the actual commissioning. Virtual commissioning minimizes the delays and ensures a seamless start-up after a technical stop or a long shutdown, the periods reserved for maintenance and upgrading of the LHC machine and the experiments (Booth et al. 2018). To enable virtual commissioning simulations which study the LHC point 8 cooling stations ability to manage temperature transients, a dynamic model of the cooling towers is developed in this thesis.

Model requirements:

- Model represents well the dynamics of the real cooling towers for control design and verification purposes
- Model can be implemented in EcosimPro and operated in the virtual commissioning environment with a real Programmable Logic Controller (PLC).
- Model performs well under ventilation, but also have representation of the free convection mode and bypass mode including smooth transitions between them
- Model is validated with real data

3 Literature review on modeling of evaporative cooling towers

The literature review in this chapter explains the theory on evaporative cooling in cooling towers, and reviews existing research on modeling methods of evaporative cooling towers, to give reader understanding of the context and common approaches to cooling tower modeling and different assumptions made.

Majority of the publications study static modeling cases, and only a few publications presenting dynamic methods were found. Static models able to predict the cooling tower heat dissipation rate in different operating points are able to answer most common problems the designers or operators may have. They are useful for selecting a cooling tower with correct properties for a certain application, as they can estimate the cooling power in different conditions. For transient studies, when information of the cooling tower functioning is needed during a transition from a typical system steady state to another, model is required to have dynamic capabilities to model the response of the cooling tower. (Jin 2011)

At CERN the interest is towards dynamic modeling, as the model will be used for analyzing alternative control strategies, and to validate control algorithms coded into a PLC prior deployment.

3.1 Evaporative cooling towers

Evaporative cooling tower is a device for dissipating excess heat to the outside air. The term cooling tower includes also dry cooling systems, that exchange heat between the process liquid and ambient air, without a direct exposure. This thesis and the publications reviewed here focus on evaporative cooling towers, which have the distinct characteristic of mass transfer to the ambient airflow due to evaporation. Evaporative cooling towers are widely used in industry wherever there is processes that produce vast amounts of heat, and where there are no cold natural water resources available. Close to cold lakes, rivers or seas, cooling is traditionally assessed with flowing natural water, and no additional systems are needed. The most well known cooling tower application is big fossil fuel and nuclear power plants, which are located inland. In the nuclear industry, recent accidents and thus demand on the increase of security level, has led to installation of cooling towers as back up cooling systems also to power stations that have natural water cooling available (Viljakainen 2013). Smaller scale cooling towers are used in various industrial operations and in heating, ventilation and air conditioning (HVAC) -systems to dissipate the waste heat from process to the atmosphere.

Heat transfer in evaporative cooling towers is both convection at the air-water interface and heat absorbed by the evaporating process water due to mass transfer.

Evaporative cooling is very effective, due to the latent heat transfer during the phase transition from water to vapor. Latent heat transfer means the thermal energy transfer in a constant temperature process. The cooling water evaporation rate is only between 1-2 per cent, but it plays a big role in the heat dissipation. The evaporation needs to be compensated by adding new process water. As a result of the evaporation, a theoretical minimum for the leaving cooling water temperature is ambient wet-bulb temperature, and often temperatures less than ambient dry-bulb temperatures are reached. (Gesellschaft 2010)

Evaporative cooling tower consists from the top to bottom: fan, drift eliminators, water spray, cooling tower fill, shower area and basin. Fan is powered by an electrical motor and is used to increase the air flow in the tower to increase cooling capacity. Drift eliminator prevents the smallest mist escaping the cooling tower. The sprays are used to create small droplets in order to increase the convection and evaporation area, and to equally distribute the water across the cooling tower cross section. The cooling tower fill is used to slow down the water and increase time of contact and area with the counter flowing air. (Gesellschaft 2010)

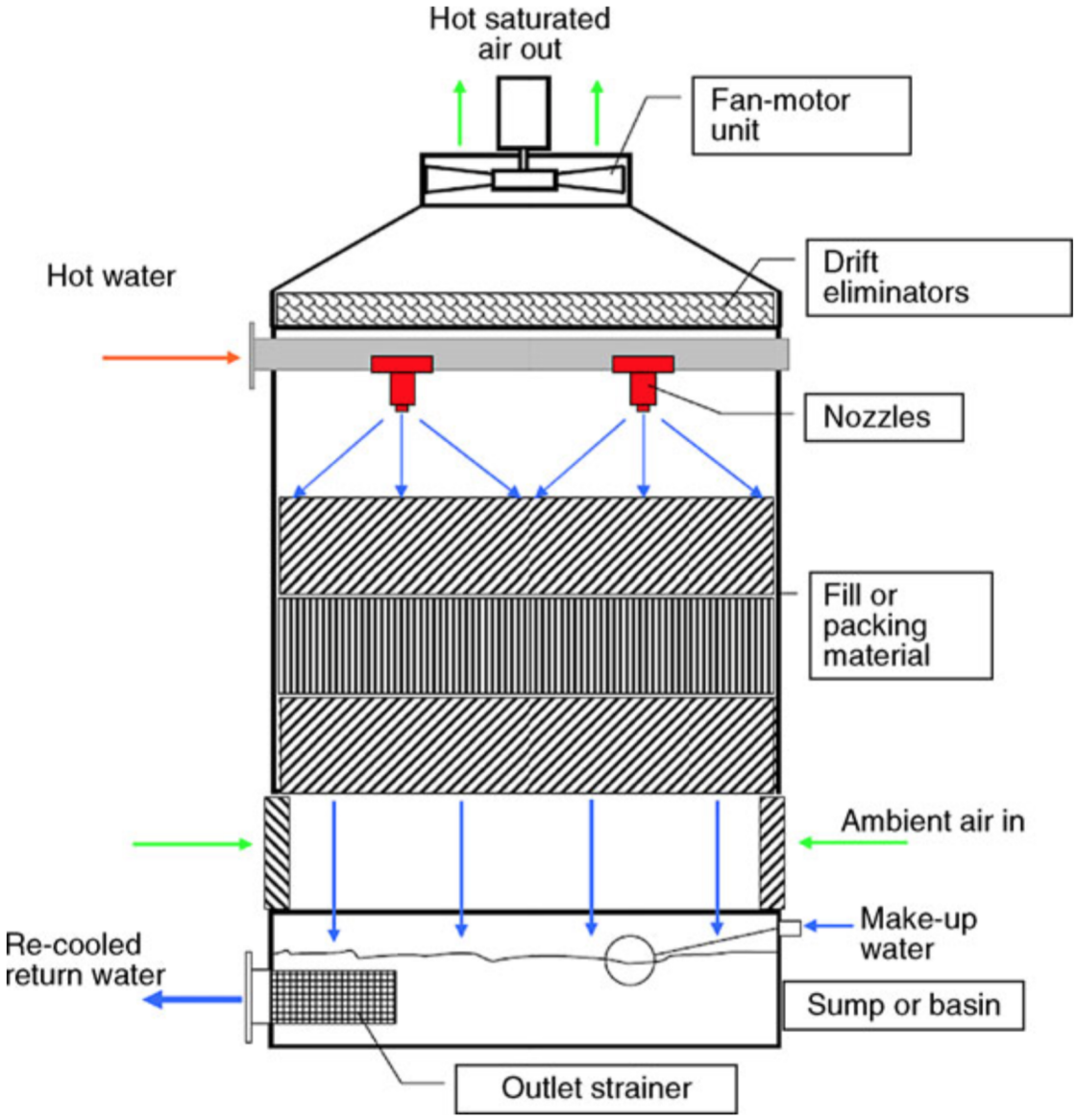

Figure 6: Mechanical draft counter flow evaporative cooling tower. Figure shows the components inside the cooling tower, which are needed to increase cooling capacity and prevent water from escaping the cooling tower. (Gesellschaft 2010).

The large often 100 meters high hyperboloid shaped cooling towers used at power plant applications are natural draft cooling towers. The warm moist air has lower density than the cool and dry outside air, which creates a natural upward current in the cooling tower. The shape and height of the tower are designed for optimal natural draft air flow. The advantage is increased energy efficiency due to the lack of the fan, but natural draft cooling towers are far less compact than the mechanical draft cooling towers.

3.2 Theory of evaporative cooling in cooling towers

Here the theory on evaporative cooling is explained as in Kloppers and Kröger (2005).

The mass balance for the control volume in Figure 7a is

$$d\dot{m}_w = \dot{m}_a dw \tag{1}$$

where w is the humidity ratio of air, kg water vapor/kg dry air.

The energy balance in Figure 7b:

$$\dot{m}_a di_{ma} - \dot{m}_w di_w - i_w d\dot{m}_w = 0 \tag{2}$$

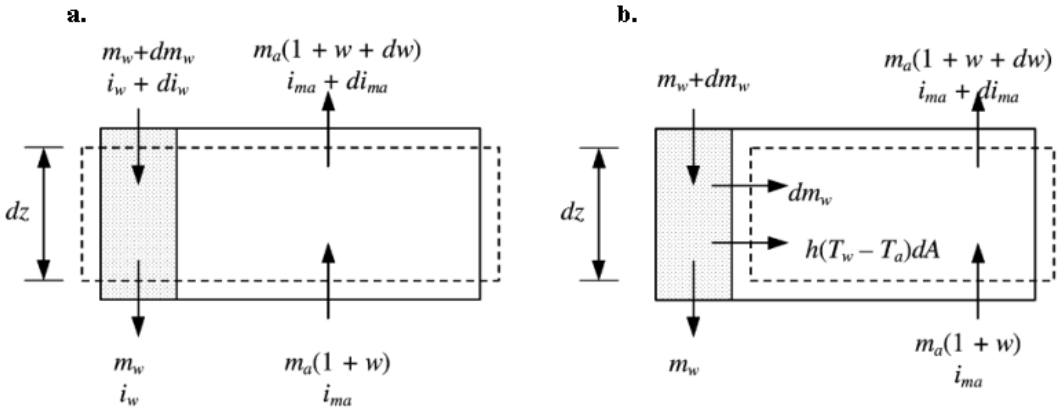

Figure 7: (a) Dashed lines is the control volume for the counter flow. (b) Dashed lines is the control volume for the air side. (Kloppers and Kröger 2005)

The energy balance for the control volume in figure 7a is:

$$m_a di_{ma} - m_w di_w - i_w dm_w = 0 \tag{3}$$

In Figure 7 the heat transferred at the water-air interface is the sum of enthalpy transfer due to the difference in air vapor concentration and enthalpy transfer due to convection.

$$dQ = dQ_m + dQ_c \tag{4}$$

The mass transfer at the interface is

$$d\dot{m}_w = h_d(w_{sw} - w)dA \tag{5}$$

where h_d is the mass transfer coefficient, w_{sw} is the humidity ratio in air-water interface temperature and w is the humidity ratio of the air prior entering the control volume.

Then energy transferred due to mass transfer is

$$dQ_m = i_v d\dot{m}_w = i_v h_d (w_{sw} - w) dA \tag{6}$$

and the energy transferred due to convection in Figure 7b is

$$dQ_c = h(T_w - T_a) dA \tag{7}$$

Temperature difference between water and air can be expressed using enthalpy differences when small differences in specific heat capacities in different temperatures are neglected. (Kloppers and Kröger 2005)

$$T_w - T_a = \frac{i_{masw} - i_{ma}}{c_{pma}} - \frac{(w_{sw} - w) i_v}{c_{pma}} \tag{8}$$

where $c_{pma} = c_{pa} + w c_{pv}$, specific heat capacity of air and vapor mixture.

Substituting Eq. (6) and Eq. (7) into Eq. (4) leads after rearrangement to

$$dQ = h_d \Big[\frac{h}{c_{pma} h_d} (i_{masw} - i_{ma}) + \Big(1 - \frac{h}{c_{pma} h_d}\Big) i_v (w_{sw} - w) \Big] dA \tag{9}$$

where $\frac{h}{c_{pma} h_d}$ is the Lewis number, rate of thermal diffusivity to mass diffusivity.

Equation (9) is the energy transfer in evaporative cooling on the air-water interface expressed by the difference of air enthalpies and humidity rations before and after the cooling tower. When also input water temperature and flow are known, the equation can be used to solve the output water temperature and flow.

The air-vapor mixtures flow in the cooling tower through the geometries of the cooling tower fill and shower area, and the heat transfer between these fluids, are very complex and hard to model. The equation (9) is a first principles representation of the heat transfer in evaporative cooling tower, but it contains parameters and variables that are very hard, if not impossible, to measure accurately, such as coefficients for thermal and mass diffusivity, or the area of the air-water interface. Different simplifying assumptions for solving the equation (9), empirical methods to obtain unknown parameters, or completely different approaches for estimating this phenomenon, are proposed in the literature. Publications studying this area of research are reviewed in the following section.

3.3 Modeling methods presented in the literature

Friderich Merkel was the first to present a calculation model for evaporative cooling towers. The publication from Merkel dates at 1925, and is still used in applications today.

Merkel makes three critical assumptions to simplify the water-air film energy balance equation (9).

1. Lewis number $\frac{h}{h_d c_{pma}}$ equals 1
2. The outlet air is saturated
3. Evaporation rate relative to water mass flow is negligible

The simplified equation (10) for energy transferred into to the air flow is obtained, where i_{masw} is the enthalpy of saturated air in water surface temperature and i_{ma} is the enthalpy of air-water mixture flowing pass the water surface. (Gesellschaft 2010)

$$dQ = \dot{m}_w c_{pw} dT_w = h_d (i_{msaw} - i_{ma}) dA \tag{10}$$

By integrating from equation (10), the formula for a coefficient known as Merkel number is obtained:

$$\int \frac{h_d dA}{\dot{m}_w} = \int \frac{c_{pw} dT_w}{i_{masw} - i_{ma}} \tag{11}$$

$\int \frac{h_d dA}{\dot{m}_w}$ is known as the Merkel number Me, containing the tower specific variables of mass transfer coefficient h_d and the characteristic heat and mass transfer area dA. These are not easy to evaluate due to the complexity of the flow in water films in the cooling tower fill and different sizes of droplets falling through the cooling tower shower area. The variables on the right hand side of the equation (11) are possible to obtain, and are used to calculate the Me.

After having obtained the Me, which is often determined separately for the fill and shower areas, Merkel's equation is solved by iterative procedure from an initial guess for the model variables. Merkel method is essentially a steady state method, as alone, it does not calculate the response of the system. In the masters thesis by Viljakainen (2013), the computational iterative solving procedure for Merkel method is discussed in detail, and an approach for dynamic cooling tower modelling is discussed using Merkel method for heat transfer calculations combined with computational fluid dynamics (CFD) modeling of the two-phase fluid dynamics in the tower components, such as drift eliminators, nozzles, fill material, shower area and basin. It is stated that applying the Merkel method for dynamic modeling is not trouble-free, as the steady-state numerical iteration procedure would need to run on every simulation step.

Poppe method is a more accurate modification of Merkel's method with no assumptions regarding the evaporative mass flow or outlet air saturation. Poppe method is

able to predict the mass flow evaporation rate and leaving airflow properties, and is useful in application where makeup water flow rate of plume visibility is needed to evaluate. Plume is the exhaust cloud of mist of the cooling towers. The model uses number of transfer units approach to eliminate the need for neglecting the mass flow, and an equation proposed by Bosnajacovik, to calculate the Lewis factor. Similarly to Merkel method, Poppe mehtod is iteratively solved, but is computationally more complex than Merkel method. In the iterative procedure for Poppe method, initial guess for outlet air humidity ratio is also required. Numerical Runge-Kutta -integration procedure can be applied together with iterative calculation steps to derive the outlet water temperature. (Gesellschaft 2010)

Fisenko, Brin, and Petruchik (2004) propose a mathematical model of mechanical draft cooling tower performance prediction. In their work, the cooling tower performance is predicted by describing the change of velocity, speed and temperature of the water droplets inside the cooling tower. In their approach to calculate evaporative cooling, the decrease of the droplet size during fall is estimated, and initial size distribution of the water droplets is needed. In a study conducted by Al-Nimr (1998) a mathematical model using an overall heat transfer coefficient, which is assumed constant, is proposed to describe the transient behavior of cooling towers. The temperatures of air and water with respect to time and space as height in the cooling tower is represented as second order differential equations. Using a perturbation technique, a transient solution is obtained. In the publication the performance of the transient model is not experimentally verified.

Neural networks are increasingly popular for solving different problems in all possible areas of research. Their development have accelerated as the computing power is becoming more and more accessible as the hardware and cloud services develop. Neural networks imitate the natural brain to learn patterns from experimental data. The training of the neural network requires vast amounts of data and computing power. Qi et al. (2016) proposes a wavelet neural network (WNN) based model for predicting the evaporative cooling tower performance. They use steady state data from experimental evaporative cooling tower for training the model including air dry-bulb temperature, humidity of the inlet air stream, inlet water temperature, air velocity, water-air mass flow rate ratio, height of the tower and the average droplet diameter.

A combination of physical formulation and empirical parameters is a practical and commonly used engineering approach for complex problems. Hybrid modeling effectively solves problems that are affected by a physical phenomenon too complex to model completely by using first principle physical modeling techniques. Methods applying a combination of physical formulation and empirical parameters, are called hybrid methods or hybrid modeling. Jin et al. (2007) proposes a hybrid method for steady state cooling tower modeling in “A simplified modeling of mechanical cooling tower for control and optimization of HVAC systems”. Their approach is based on the analogy of counter flow evaporative cooling tower to a typical counter flow

heat exchanger. In their work a physical formula is constructed from the principle of heat resistance between the air and water flow interface in the tower. They propose a function for the heat resistance with air and water mass flow rates as its variables. Parameters of the function, which characterize the complex geometry needed to determine the heat resistance and heat transfer area, are optimized against real operational data of steady state operation points or manufactures data. The model originally presented by Jin et al. (2007) is later further extended for dynamic modeling in the PhD thesis by Jin (2011).

3.3.1 Summary

Most of the relevant publications found in literature study methods, that are only applicable for steady state analysis. The greater interest towards steady state modeling than dynamic, is explained by the fact, that they can answer the most common questions and problems that designers and operators of the cooling towers have. The typical operation of cooling towers is steady, and if there are any transients, they are slow and damped by the thermal inertia in the basins, which are often large. Steady state models provide valuable information of the cooling tower performance in different operation conditions in order to design and operate the towers optimally. Correctly sized towers can be chosen when their performance in the applications conditions can be estimated apriori, and the control system can operate the towers at smaller marginal for energy savings.

Also the nature of Merkel and Poppe methods is steady-state, and they require initial guesses and iterative computation to solve the model outputs. As stated by Viljakainen (2013), it is possible to apply iterative steady state computation of the heat transfer in a dynamic simulation supported by dynamic models of the flow components, but the iteration procedure needs to run on every simulation step, thus attention is required for evaluating the complexity and feasibility of the higher computational cost.

To the authors knowledge, the model presented in Jin (2011), is the only dynamic cooling tower model available in the literature, which is validated against dynamic real data. Al-Nimr (1998) presents a mathematical model to describe the dynamic thermal behaviour of cooling towers, however no experimental results are presented to evaluate the accuracy of the model. Majority of the methods found in literature require estimations or detailed geometries often regarding the heat transfer area or amount and size of the water droplets in the towers. These kinds of measures may be possible to acquire in a laboratory environment, but not practical to apply in practise. The method presented by Jin et al. (2007), was identified to best suit the data and information available of the cooling towers at LHC point 8, and was shown in Jin (2011) to work satisfactorily predicting the cooling tower transients. Only the air mass flow requires an estimation, while other variables are directly measured by the CERN LHC logging system.

4 Data and methodology

The first section in this chapter describes the available documentation of the cooling towers and the available data from the LHC data logging system. In the second section, the reasoning of the model selection and theory of the chosen model for simulating the cooling towers are presented.

Careful studying and search for all sources providing useful information of the real system, is important part of model selection and model development (Ljung and Glad 1994). Main sources for this information have been the CERN EDMS - Electronic Document Management System, that contains CERN and subcontractor documents of the installed devices in digital form, if they have originally been stored or created. Main source for empirical data is the LHC logging system, where all sensors and feedback signals are archived, with a short description of the measured variable. The measurement data from sensors and feedback signals of the cooling towers at LHC point 8, is comprehensively archived to LHC logging as part of UNICOS integrated system (Roderick et al. 2009).

The available documentation and data strongly guided the model selection. The cooling towers at CERN are old and unique custom build devices, and detailed manufacturers specifications are not available. However a lot of operational data is available in LHC logging. Finally, the hybrid method using empirical parameters optimized against real operational data, presented by Jin et al. (2007), was found to best suit the purpose of this study, available technical data and measured variables.

4.1 Available data

The model steady state parameter identification requires cooling tower operation points to form the set of observations for the non-linear least squares optimization to obtain the three steady state parameters (Jin et al. 2007). Dynamic data sets are required to identify the dynamic parameter and to validate the model performance to predict transients (Jin 2011). The operation points for steady state identification can be obtained either from the manufacturer data, from historic operational data or by conducting tests (Jin et al. 2007). For cooling towers at SF8, it was soon discovered, that no sufficient manufactures data is available for these decades old on site custom built cooling towers. On the other hand, a lot of precise historic operational data is available in the archive. Testing with different fan speeds was possible, but altering other variables was not, as the towers are continuously under operation and need to provide a constant cooling power.

In this section the available raw data and forming of the cooling tower data sets, that contain the needed variables, are explained. A simple algorithm for finding steady operation points from the dynamic historical data is developed. For air mass

flow there is no direct measurement, and a model is needed to estimate the air mass flow from the fan speed signal. The method for estimating the air mass flow and the necessary assumptions are presented. Uncertainties related to the air mass flow estimation are discussed.

4.1.1 CERN data acquisition system

A CERN-made framework for industrial control applications, UNICOS - Unified Industrial Control System, is used at CERN for supervision and control of many computer controlled systems. (CERN Industrial Controls and Safety Group (ICS) 2018)

The supervision of the control system includes saving data from the sensors and feed back signals connected to the system. The data from the LHC point 8 cooling towers is not saved at regular time interval as it is produced event-based at the source. If the sensor reading goes beyond a certain threshold compared to the last saved reading, a new reading is saved, or if a certain time limit with no change in the reading is passed a new reading is also saved. (Bille, Perty, and Marczukajtis 2002)

The logged data can be queried with Timber, a Java application with a graphical interface where users can search for sensors and select data and time window for a query. Timber provides a possibility to obtain fixed time step averaged data, but for such large data sets, it was computationally faster to only make queries for the raw data, and modify the data with scripts written in R - programming language. (Bille, Perty, and Marczukajtis 2002)

4.1.2 Cooling tower data sets

For parameter optimization and model validation, data sets containing measured input variable and output variable are needed. Output primary cooling water temperatures and fan speed signals are measured directly, while water mass flows in each tower and ambient wet-bulb temperature are calculated as a result from indirect measurements. For air mass flow no direct measurement or a way to calculate it without assumptions exists. Approach for estimating the air mass flow is discussed later in chapter (4.1.4).

Timber was used to make queries of data for both towers during the LHC run 2017 and 2016. Eighth months worth of logged data for both towers and both years. The resulting query is a comma separated data table, with an irregular date-time column, and a column for each measurement. Each row only contains one value, which is for the measurement that triggered the logger. Values for other variables on the row are empty.

A continuous 1 Hz time series is obtained by resampling from the raw data set.

Resampling is done in a way, that a close representation of the occurred real signals is obtained. First the data table is filled with empty rows between the irregular time-stamps, to make the date column continuous with one second time step. Then all empty values are replaced by repeating previous saved non empty value resulting to a square form signals. Error of the re sampled values is the trigger threshold of each variable. The thresholds of the data logger are well justified, and the square form data shows well the events and transients that occurred, as when ever there are relevant slopes in the data, the density of the time-stamps increase due to the thresholds triggering the saving of new readings.

Ambient wet-bulb temperature is a factor of ambient dry-bulb temperature, relative humidity and pressure. Ambient wet-bulb temperature is calculated with a function `wetbulb.temp` found in R-library bigleaf (Knauer et al. 2018). The function calculates wet-bulb temperatures from measured ambient dry-bulb temperatures, humidities and pressures. Water mass flows are calculated from the sum of the measured flows in the three client circuits divided by number of five towers as in figure (2.2.2) on page 9. Individual cooling tower data sets for each of the towers are constructed from the common and individual measured and calculated variables listed in table (2). A cooling tower data sets from different time windows are referred in many occasions in this thesis, as they are the base source data for parameter identification and validation. A short snippet of a cooling tower data set is given in table 3.

Table 2 Common data for the five cooling towers.

Measured variable	Symbol	Range (*unit*)
Individual		
Status	$STATUS$	0-6
Speed signal	$SPEED$	0-100 (%)
Basin temperature	T_2	15-25 ($°C$)
Common		
Flow to user 1	F_1	0-300 (m^3/h)
Flow to user 2	F_2	0-300 (m^3/h)
Flow to user 3	F_3	0-300 (m^3/h)
General return temperature	T_1	24.0-32.0 ($°C$)
Ambient		
Dry-bulb temperature	T_{db}	0-35 ($°C$)
Relative humidity	RH	0-100 (%)
Pressure	P	950-1050 ($mbar$)

Table 3 Snippet of cooling tower time-series data set.

Datetime	T_1 ($°C$)	$\dot{m}_w$ (kg/s)	T_{wb} ($°C$)	T_2 ($°C$)	$SPEED$ (%)	$STATUS$	$\dot{m}_a$ (kg/s)
2018-07-03 12:59:10	28.08	114.69	20.00	21.16	79.74	4.00	123.26
2018-07-03 12:59:11	28.08	114.69	20.00	21.16	81.97	4.00	123.95
2018-07-03 12:59:12	28.08	114.69	20.00	21.16	81.97	4.00	123.95
2018-07-03 12:59:13	28.08	114.69	20.00	21.16	84.33	4.00	124.69
2018-07-03 12:59:14	28.08	114.69	20.00	21.16	84.33	4.00	124.69
2018-07-03 12:59:15	28.08	114.69	20.00	21.16	86.55	4.00	125.39

4.1.3 Steady state extraction

A simple algorithm was developed to extract steady states from the dynamic historical data (appendix). The algorithm runs in R and goes through the data and finds steady periods of user defined limitations for "steady" for each variable. The algorithm then calculates the averages over time windows where all of the variables were steady and saves the result as a steady state. The definition for a system steady state is always a case specific matter and varies on the application and accuracy required.

Steady states are found by running the steady state extraction algorithm over the cooling tower time series data sets. To obtain well performing cooling tower parameters, and to validate them, a wide range of different steady states are required for both identification and validation.

Data from the LHC run in 2017 is used for identification of the model steady state parameters and data from 2016 LHC run is used for steady state validation, from May to December for both of the towers and both years, to obtain 4 time series data sets each containing data from 8 months in total. The cooling systems runs also outside the LHC run with less load due to limited activities, but the data tends to have more faults and missing values during these technical stops. These data sets are large, each containing 21 168 000 rows, and are heavy to manage for a normal desktop computer. Thus the data was split in to half and the steady states where extracted for shorter periods and then combined.

Table 4 Snippet of cooling tower steady state data set.

Datetime	T_1 ($°C$)	$\dot{m}_w$ (kg/s)	T_{wb} ($°C$)	T_2 ($°C$)	$SPEED$ (%)	$STATUS$	$\dot{m}_a$ (kg/s)
2017-05-01 15:29:59	27.38	136.46	7.97	23.06	0.00	3.00	38.57
2017-05-02 08:38:59	27.54	120.68	7.14	23.27	0.00	3.00	32.33
2017-05-02 09:16:59	27.40	121.57	7.38	23.18	0.00	3.00	32.80
2017-05-02 11:19:59	27.40	120.98	8.08	23.02	0.00	3.00	34.69
2017-05-02 13:48:59	27.32	122.81	8.56	23.47	0.00	3.00	31.70
2017-05-02 17:52:59	27.35	121.30	7.76	23.80	0.00	3.00	27.99

Table 5 ETR-880.

	$m_w(kg/s)$	$T_1(°C)$	$T_2(C°)$	$T_{wb}(C°)$	SPEED (%)	STATUS	Count
Identification, 2017							
Entire set	100.7 - 181.3	25.1 - 31.5	12.2 - 29.1	0.4 - 23.7	0 - 100	3 - 4	900
T_{wb} higher half	102.3 - 180.9	26.3 - 31.5	17.8 - 29.1	16.2 - 23.7	0 - 100	3 - 4	450
T_{wb} lower half	100.7 - 181.3	25.1 - 29.7	12.2 - 27	0.4 - 16.2	0 - 100	3 - 4	450
Validation, 2016							
Entire set	114.1 - 167.9	24.7 - 31.3	19.8 - 27.6	-0.5 - 24.2	0 - 100	3 - 4	800
T_{wb} higher half	114.6 - 160.8	25.9 - 31.3	19.8 - 27	16.2 - 24.2	0 - 100	3 - 4	400
T_{wb} lower half	114.1 - 167.9	24.7 - 29.7	21.7 - 27.6	-0.5 - 16.2	0 - 0	3 - 3	400

Table 6 ETR-881.

	$m_w(kg/s)$	$T_1(°C)$	$T_2(C°)$	$T_{wb}(C°)$	SPEED (%)	STATUS	Count
Identification, 2017							
Entire set	100.7 - 181.2	25.1 - 31.4	14.5 - 27.6	-0.5 - 23.7	0 - 100	3 - 4	700
T_{wb} higher half	102 - 181.2	26.3 - 31.4	18 - 27.6	15.9 - 23.7	0 - 100	3 - 4	350
T_{wb} higher half	100.7 - 180.8	25.1 - 29.6	14.5 - 27.4	-0.5 - 15.9	0 - 100	3 - 4	350
Validation, 2016							
Entire set	113.7 - 167.6	24.8 - 31.3	14 - 24.5	1 - 24.2	0 - 100	3 - 4	600
T_{wb} higher half	113.7 - 160.9	25.7 - 31.3	18.1 - 24.5	15.9 - 24.2	100 - 100	4 - 4	300
T_{wb} lower half	114.5 - 167.6	24.8 - 29.7	14 - 22	1 - 15.9	0 - 100	3 - 4	300

The steady state extraction algorithm is run for the data sets and resulting ranges of steady states are presented in tables (5) and (6). The time window to define a steady condition is 30 minutes. The length of the steady time window was chosen as 30 minutes, to avoid detection of false steady states, as the dynamics of the basin are slow - it takes about 10 minutes on average for the water to completely change in the cooling tower basin, and between 30 and 45 minutes for the temperature to fully stabilize after big transients in the input variables. To identify as a global system steady state, all variables are required to declare as steady for the period of the time window. Consecutive steady states are discarded as they are similar to each other.

4.1.4 Air mass flow estimate

In the monitoring system for the cooling towers, no air flow meter or output temperature sensor is included, and thus a way to estimate the airflow is required. Jin et al. (2007) proposes that the air flow through the tower can be estimated from the frequency driving the motor. The rotations per minute (RMP) of an alternating current electric motor follows proportionally the frequency of the variable frequency drive (VDF). According to the fan affinity laws, flow is proportional to the shaft

RPM (Engineering ToolBox 2003). This information is not yet enough to calculate the air mass flow through the tower, but enough to state that the flow is linear to the frequency driving the motor, thus linear to the fan speed signals available in the cooling tower data sets. The magnitude of the flow is determined by the geometry of the fan. Jin et al. (2007) do not provide further details, how the air mass flow estimate is calculated and which assumptions are needed.

At LHC point 8, the variable frequency drive is controlled by a fan speed signal of 0-100 %. The frequency output of the VFD is proportional to the speed signal and between 33-50 Hz. According to sources at CERN, the reduction gear used between the engine and fan, does not allow very low speeds, thus the minimum frequency has been needed to set at 33 Hz. They also agreed that this is shame, as the range of adjustment under forced convection flow is now smaller. The minimum fan speed is high, and the difference to the free convection mode is large.

Using the assumption of Merkel, that the output air is saturated, and an additional assumption, that the output air temperature is close to the water input temperature, the approximate air mass flow in the tower is obtained from the moist air flow - water flow energy balance Eq. (10) on page 21. Using a set of steady state air flow estimate - fan speed signal -data points, the parameters for the linear model between the fan speed control signal and air flow can be obtained by an ordinary linear regression for ETR-880 and ETR-881.

Parameters k and c for a linear model, Eq. (12), for the air mass flow - speed signal, are obtained by linear regression from a set of historical air mass flow estimate - speed signal steady operation points. For tower ETR-880, x steady states and for ETR-881 x steady states from May - December 2017 where used as data for fitting the linear model.

$$\dot{m}_a = k * SPEED + c \tag{12}$$

The set of data points is separated into two subsets, the other containing all the points when fan is off and the tower is in free convection mode, and the other containing points fan being on. First set is used to find a median of the air mass flow estimate under free convection mode, and the second is used to identify the air mass flow estimation model parameters.

The assumption of air temperature being close to the water input temperature, is a rough approximation and not widely used in the literature. It is recognized in the literature, that the output air temperature is close to the input water temperature, but when the air flow increases, or if the ambient temperature decreases, the output air temperature decreases and is not strictly regulated by the input water temperature (Naphon 2005). In this study however, it is not important to find the exact validated airflow, but rather use the best possible estimate for the relation between the fan speed control signal and the air mass flow. The assumption of fully saturated air at

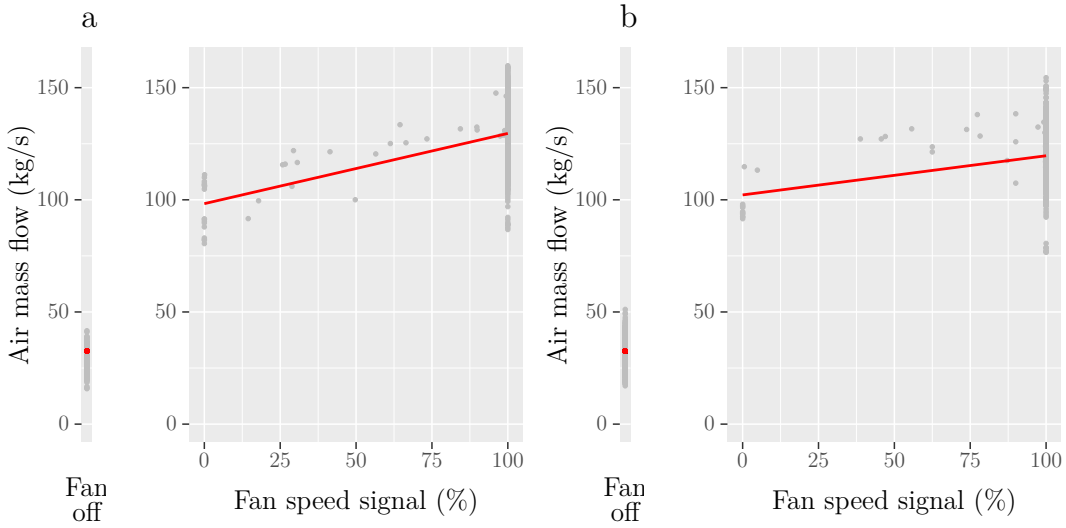

Figure 8: Linear model fit for air mass flow in towers ETR-880 (a) and ETR-881 (b). Plots clearly show the large step in airflow at fan start up.

the air outlet is widely used in the literature.

The sensitivity of the temperature assumption was examined by lowering the temperature and calculating the air mass flow estimation and air flow parameters for the steady states used for steady state parameter identification and validation. Lowering the air flow output temperature below the T1 temperature by 5 or 10 % showed very little or no improvement on validation root mean squared error (RMSE) for warm temperatures, and 0.05 - 0.1 C improvement for cool temperatures. Further decrease of the temperature estimate started significantly increasing the RMSE. This supports the hypothesis that the temperature assumption is accurate on warm weather and decreases in accuracy in chilly weather, as the air in the tower does not heat up as high as the input cooling water temperature T_1. Based on testing the estimation of air flow is feasible and leads to acceptable accuracy of the cooling tower model. The resulting air mass flow estimation model also supports the recognized characteristic of the towers, that the air flow increases significantly, when switching from free convection mode to forced draft mode, due to the high minimum speed of the fan.

4.2 Chosen model

In the work by Jin et al. (2007), a static model for cooling tower modeling is developed based on the analogy between cooling tower and a classical counterflow heat exchanger. The approach proposes that the convective and evaporative heat transfer in the cooling tower can be described by overall heat resistance. They propose that the overall heat resistance is a function of air and water mass flows. Parameters of the function are optimized against real data.

Pros:

+ Simple method, possible to implement in the available time frame of technical student internship at CERN and resources (data and competences required)
+ Based on the results presented in the literature, the method has good potential to be applied successfully for the use case at CERN
+ No need to CFD model flow components, such as nozzles, cooling tower fill and basin
+ No iterative computation needed for solving the equations, fast computing times, well suited for using EcosimPro as a development platform

Cons:

– The publication does not describe in detail the measurement set up used for air flow properties
– Uncertainties in the airflow estimate expected to affect the model accuracy
– Paramter identification restricted to the available operational data

4.2.1 Steady state cooling tower model

The heat dissipation rate can then be calculated using the overall heat resistance R as

$$Q = \frac{T_1 - T_{wb}}{R} \tag{13}$$

where the overall heat resistance R consist on heat resistance of the water side and heat resistance of the air side.

$$R = R_w + R_a \tag{14}$$

According to Jin et al. (2007), the heat transfer at the water-air film can be considered as forced convection, and equations for calculating the heat resistances R_w, R_a are proposed as:

$$\frac{1}{R_w} = \dot{m}_w^{e_1} \left[\frac{4^{e_1} C}{\pi^{e_1}} \cdot \frac{C_{pw}^{e_2} \cdot k^{1-e_2}}{\mu^{e_1-e_2} \cdot D^{1+e_1}} \right] A_w = b_1 \dot{m}_w^{e_1} \tag{15}$$

$$\frac{1}{R_a} = \dot{m}_a^{e_1}\left[\frac{4^{e_1}C}{\pi^{e_1}} \cdot \frac{C_{pa}^{e_2} \cdot k^{1-e_2}}{\mu^{e_1-e_2} \cdot D^{1+e_1}}\right] A_a = b_2 \dot{m}_a^{e_1} \tag{16}$$

Substituting equations (15) and (16) into equation (13) an equation for the heat transfer is obtained:

$$Q = \frac{b_1 \dot{m}_w^{e_1} \cdot b_2 \dot{m}_a^{e_1}}{b_1 \dot{m}_w^{e_1} + b_2 \dot{m}_a^{e_1}}(T_1 - T_{wb}) = \frac{c_4 \dot{m}_w^{l}}{1 + c_3 \frac{\dot{m}_w}{\dot{m}_a}^{l}}(T_1 - T_{wb}) \tag{17}$$

where $c_4 = b_1$, $c_3 = \frac{b_1}{b_2}$ and $l = e_1$ are model parameters.

Thus Jin et al. (2007) are proposing that the heat resistances R_w and R_a are functions of the mass flows $\dot{m}_w$ and $\dot{m}_a$ respectively. They propose and experimentally validate, that the equation (17) can be used to estimate steady state heat dissipation rate of a counter flow evaporative cooling tower. Method for optimizing the model parameters c_3, c_4 and l against manufactures steady state performance data, or real operational steady state data as in Jin et al. (2007), is studied in detail in section 4.3 at page 34.

4.2.2 Dynamic cooling tower model

In a PhD thesis by Jin (2011), the steady state model by Jin et al. (2007) is revisited and the model is further developed for dynamic modeling. Jin (2011) proposes that the dynamic change of temperature for an infinitesimal water element in the cooling tower, can be expressed as

$$\rho_w V_w C_{pw}\left(\frac{\partial T_w}{\partial t} + u_w \frac{\partial T_w}{\partial z}\right) = -q \tag{18}$$

where the heat exchange quantity q for an infinitesimal water element is expressed as a function of the temperature change in time and space.

The temperature of the water element inside the cooling tower is measured in different heights, and based on this work, the change of temperature for the cooling water in the cooling tower is linear to the height of the cooling tower and can be expressed by:

$$T_w = T_1 - \frac{T_1 - T_2}{H} z \tag{19}$$

By derivation with respect to z we obtain the change of temperature in space for the cooling tower with boundary variables:

$$\frac{\partial T_w}{\partial z} = -\frac{T_1 - T_2}{H} \tag{20}$$

Combining this into equation (18), we have the cooling tower heat rejection q_{ct} as a function of change of temperature in time over the height of the cooling tower H:

$$\rho_w V_w C_{pw}(\frac{dT_w}{dt} - u_w \frac{T_1 - T_2}{H}) = -q_{ct} \tag{21}$$

And after rearrangement

$$\frac{dT_w}{dt} = \frac{-q_{ct}}{\rho_w V_w C_{pw}} - u_w \frac{T_2 - T_1}{H} \tag{22}$$

where q_{ct} is substituted by the static cooling tower model Eq. 17.

$$\frac{dT_w}{dt} = -\frac{c_2 \dot{m}_w^l(t)}{1 + c_3 \left[\frac{\dot{m}_w(t)}{\dot{m}_a(t)}\right]^l}[T_1(t) - T_{wb}(t)] - u_w \frac{T_2 - T_1}{H} \tag{23}$$

where $c_2 = \frac{c_4}{\rho_w V_w C_{pw}} = c_1 \frac{c_4}{C_{pw}}$.

Also u_w/H is substituted with $c_1 \dot{m}_w(t)$ resulting:

$$\frac{dT_2(t)}{dt} = -\frac{c_2 \dot{m}_w^l(t)}{1 + c_3 \left[\frac{\dot{m}_w(t)}{\dot{m}_a(t)}\right]^l}[T_1(t) - T_{wb}(t)] - c_1 \dot{m}_w(t)[T_2 - T_1] \tag{24}$$

where, $c_1 = \frac{1}{H p_w A_w}, c_2 = \frac{b_w A_w}{p_w V_w C_{pw}}, c_3 = \frac{b_w A_w}{b_a A_a}$ and l are model parameters.

$$\frac{dT_2}{dt} = c_1 \phi(t) \tag{25}$$

where,

$$\phi(t) = -\frac{\frac{c_4}{C_{pw}} \dot{m}_w^l(t)}{1 + c_3 \left[\frac{\dot{m}_w(t)}{\dot{m}_a(t)}\right]^l}[T_1(t) - T_{wb}(t)] - \dot{m}_w(t)[T_2(t) - T_1(t)] \tag{26}$$

where c_1, l, c_3 and c_4 are parameters optimized against operational data.

In the engineering model proposed by Jin (2011), leaving wet-bulb temperature $T_{wb,o}$ and leaving cooling water temperature T_2 are used as boundary conditions for the

heat rejection rate term q_{ct} instead of using entering cooling water temperature T_1 and ambient wet-bulb temperature T_{wb}. Commonly in practice, sensors are only installed and maintained for readings that are necessary for the control and monitoring of the cooling tower performance, and leaving air conditions are not important to measure. These practices are also recognized by the authors of Jin et al. (2007), and they obtain the heat rejection rate by using T_1 and ambient T_{wb} as boundary conditions. At CERN sensors for the leaving air conditions do not exist, thus the model is implemented and characterized by using boundary conditions similar to Jin et al. (2007).

4.3 Parameter identification

This section presents the procedure for identifying the unknown parameters of the model. First is presented the method used in Jin et al. (2007) for optimizing the steady state parameters of the model. Then is presented the method used in Jin (2011) for identifying an optimal dynamic parameter c_1.

4.3.1 Steady state parameter identification

When stating that $\frac{dT_2(t)}{dt} = 0$ we can rewrite the equation 11 as:

$$\dot{m}_w(T_2 - T_1) = -\frac{\frac{c_2}{c_1}\dot{m}_w^l}{1 + c_3\left[\frac{\dot{m}_w}{\dot{m}_a}\right]^l}(T_1 - T_{wb}) \tag{27}$$

The cooling tower heat dissipation rate can be calculated with the following equation:

$$Q = C_{pw}\dot{m}_w(T_2 - T_1) \tag{28}$$

thus:

$$Q = C_{pw}\frac{\frac{c_2}{c_1}\dot{m}_w^l}{1 + c_3\left[\frac{\dot{m}_w}{\dot{m}_a}\right]^l}(T_1 - T_{wb}) \tag{29}$$

where:

$$c_4 = C_{pw}\frac{c_2}{c_1} \tag{30}$$

We obtain the steady state model expression as in Jin et al. (2007):

$$Q = \frac{c_4 \dot{m}_w^l}{1 + c_3 \left[\frac{\dot{m}_w}{\dot{m}_a}\right]^l}(T_1 - T_{wb}) \tag{31}$$

Jin et al. (2007) proposes that the the parameters c_3, c_4 and l are empirically determined by minimizing the sum of squared residuals:

$$MIN \sum_{i=1}^{N} (Residual)^2 = MIN \sum_{i=1}^{N} \left(\frac{c_4 \dot{m}_w^l}{1 + c_3 \left[\frac{\dot{m}_w}{\dot{m}_a}\right]^l}(T_1 - T_{wb}) - Q_{observation} \right)^2 \tag{32}$$

Eq. (32) is a non-linear least squares problem, a non-linear unconstrained optimization problem. Solving non-linear optimization problems is not a simple task as they may have multiple local optimums. Jin et al. (2007) uses Levenberg-Mardquardt algorithm (LMA) for finding an optimal solution. Levenberg-Mardquardt algorithm is commonly used for solving non-linear least squares problems. The LMA method combines Newton's algorithm and steepest descent algorithm, which safeguards against faults occurring while using only either of the algorithms alone. The resulting algorithm is slower, but more robust method for finding the optimum. (Bazaraa, Sherali, and Shetty 2006)

$$[\epsilon_k I + H(x_k)](x_{k+1} - x_k) = -\nabla f(x_k) \tag{33}$$

In LMA method, Eq. (33), $H(x_k)$ is the Hessian matrix of the objective function, the parameter ϵ_k defines the weight of steepest descend algorithm versus Newton's algorithm. When ϵ_k large, LMA will behave similar to the steepest descent algorithm, and when ϵ is small, the LMA will reduce to Newton's algorithm Eq. (34). (Bazaraa, Sherali, and Shetty 2006)

$$x_{k+1} = x_k - H(x_k)^{-1} \nabla f(x_k) \tag{34}$$

4.3.2 Dynamic parameter identification

After identifying the steady state parameters, in Jin (2011) ordinary linear least squares method is used to identify the dynamic parameter c_1 from step response test data. Parameter c_1 determines how fast the dependent output variable T_2 responses to the changes in any of the input variables.

Ordinary linear least squares method (36) fits a linear model (35) to measured real data by finding the parameter θ that minimizes the sum of squared residuals.

$$y = X\hat{\theta} \tag{35}$$

$$\hat{\theta} = (X^T X)^{-1} X^T y \tag{36}$$

Applying the OLS for the cooling tower model, the left hand side of the equation (38) forms the vector y and right hand side forms the vector X multiplied by scalar $\frac{T_s}{2}\hat{\theta}$. T_s is the one second sampling inter wall.

$$\int_0^{nT_s} \frac{dT(t)}{dt} dt = \hat{\theta} \int_0^{nT_s} \phi(t) dt \tag{37}$$

$$T(nT_s) - T((n-1)T_s) \approx \frac{T_s}{2}\hat{\theta}[\phi(nT_s) + \phi((n-1)T_s)] \tag{38}$$

where $n = 1, 2, 3, ...$

The resulting factor $\hat{\theta}$, is the optimal value for parameter c_1, that gives the optimized modeled response for the step response in the data, compared to the real response.

4.4 Model assumptions and uncertainties

The method used as an engine for calculating the heat transfer and the dynamics of a cooling tower in the model developed in this thesis, is a simplified representation of the real system, that applies empirical parameters. The accuracy should not be compared to cases modeled by physical modelling techniques, which applies first principle calculations of the physics that describe the phenomena and the system, and can predict the process exactly how it is in reality. However in practise, such accuracy is often not required or all the information required to build such model are too expensive to acquire.

The parameters of this model are determined empirically, by iteratively optimizing the resulting model output compered to real observed values, to find optimal parameters. The algorithm used for steady state parameter optimization is not able to find the global optimum for the parameters, but is shown in the publication by Jin et al. (2007) to reach satisfactory results.

Necessary assumptions regarding estimating the air mass flow are needed. The estimate decreases in accuracy when ambient temperature lowers or fans speed

increases. The estimate anticipated to have more uncertainty under free convection mode, as air flow in the tower is more exposed to factors outside the scope of the data such as wind, while the fan is not regulating the air flow.

5 Cooling tower model, LHC point 8

This chapter includes construction of a model for the five cooling towers at LHC point 8 based on the theory presented in the section (4.2) and applying of the parameter identification methods described in section (4.3), for parametrisation of the model. A validation against real operational data is presented, and sensitivity of the model variables and parameters are studied. The model of the five towers is constructed from two differently parameterised towers. All the five towers are similar in their dimensions, but ETR-880 was build and has started operating before the four newer towers, and has slightly different setting in the fan blade inclination. For three of the four newer towers the air flow is restricted due to the tent, which is currently installed in front of the air inlets. However it is not necessary to parameterise each tower separately, as the four new towers are the same in their dimensions and performance. Thus the parameter identification is carried out for ETR-880 and ETR-881, while ETR-882, ETR-883 and ETR-884 are treated as identical to ETR-881.

The validation procedure presented in this chapter includes two different approaches to validate the model and parameter selection, and to analyze the model error. Model steady state performance is studied by collecting a set of steady states outside the parameter identification time window, and calculating root mean squared residuals and mean residual, and by visualizing the histogram of the residuals, to study residual normality. Dynamic validation for validating the model performance for capturing dynamics in the real system, is done by visualizing real observed and simulated basin temperatures and calculating root mean squared error under transients in general return temperature or fan speed signals found from historical operation data.

Model sensitivity is studied by a classical one-by-one spider plots. Each model variable and parameter is multiplied by a factor and the effect on model output is visualized in the plots.

5.1 Characteristics of the model

The cooling tower model created here has been designed to optimize the modelling effort and simplicity relative to available research and methods found in the literature, and the questions and problems where the model is hoped to give answers. The model should be able to predict transients in the cooling tower output temperature with an accuracy sufficient for control design. After studying the problem regarding loss of heat recovery and resulting transients, data and methods available, it was stated that most critically the model would need to be able to predict the cooling tower basin temperatures while the fan is on and increase of cooling capacity resulting from ramping up fans. It was recognized that modeling the free convection mode is far more complex, and it was accepted that with the chosen approach the model accuracy will be reduced when the fan is off. Ramping up fans is the action that

the control system can execute for damping temperature transients, and is also an action which can be dynamically validated due to its frequent occurrence in the historical operation data. Fast temperature transients are not available in the data, and the model can not thus be validated in really fast temperature transient, only a slower transient for dynamic validation of the model under temperature transients was found.

For operating as a virtual twin of the cooling network for control verification, the model will also need to comply with setting towers to bypass. The bypass mode is modelled as energy balance assuming perfect mixing. The dynamic calculation of the basin temperature thus consists of two alternate models, the model for calculating the evaporative cooling, in the tower while showering, and the model for calculating the energy balance and temperature rise of the basin when switched to bypass.

5.2 Model implementation in EcosimPro

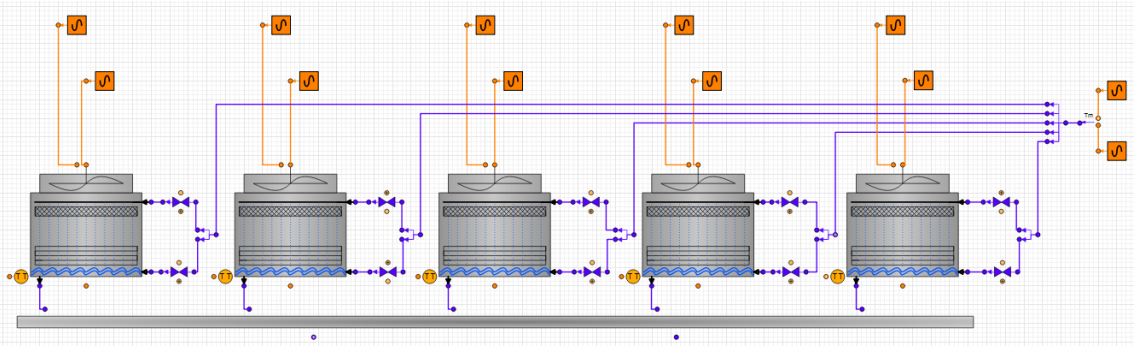

Figure 9: Model in EcosimpPro with signal sources in orange. EcosimPro allows user to define ports for the components, which are then connected using the graphical interface.

EcosimPro allows users too freely write their own components in their EL-programming language, and to define symbols for these components. Simulation models are created in EcosimPro in user friendly graphical interface, where components are added and connected to each other via ports. A simulation model schematic of the system in LHC point 8 with connections is shown in figure (9).

The engine for calculating the evaporative cooling in the `cooling_tower` -component are the equations (25) and (26) written in EL-language into the `CONTINUOUS` -part of the component code as:

```
CONTINUOUS Tout' = c1 * phi

phi = -((c4 / Cp) * (mw ** l)) / (1 + c3 * ((mw / ma) ** l)) * (Tin
- Twb) - mw * (Tout - Tin)
```

The component has two flow inlet ports, for shower and bypass, and three signal inlet ports for ambient wet-bulb temperature, fan speed signal and fan on - off switch signal. The component has two output ports, one for the flow leaving the cooling tower basin, and one for transmitting the temperature signal of the cooling tower basin.

The perfect mixing cooling tower basin model for calculating the output temperature, and an estimate of the dynamics, is based on the energy balance:

```
M_l * Cp_b * Tb' = f_in_bypass.mh - mh_b_out
```

where `mh` is power or enthalpy flow, `M_1` is mass of water in the basin, `Cp_b` is the specific heat capacity of the water in the basin and `Tb'` is the rate of change of temperature in the basin.

An `IF` -sequence is used for alternating between the evaporative cooling and bypass calculation:

```
shower_flow = delay(f_in_shower.m, 1)
SEQUENTIAL
 IF (shower_flow > 0) THEN
  f_out.T = Tout
 ELSE
  f_out.T = Tb
 END IF
END SEQUENTIAL
```

In order for the component to smoothly switch between the two alternate dynamic calculation methods for the basin temperature, the current basin temperature is passed from one to another when a change from bypass to showering or vice versa is detected. For this a similar sequence is also written into the `DISCRETE` -part of the component code:

```
DISCRETE
 --Detecting weather water is entering through shower of bypassed
 WHEN (f_in_shower.m > 0) THEN
  Tout = Tb
 END WHEN

 WHEN (f_in_bypass.m > 0) THEN
  Tb = Tout
 END WHEN
```

While the code in continuous part will apply in every simulation step, the code in discrete part only runs once in the event of a certain action. In this case, the detection of `(f_in_shower.m > 0)` or `(f_in_bypass.m > 0)`, triggers the passing of the current basin temperature from the model to another, and then continues from there again in the continuous part. This detail ensures smooth transitions between bypass and showering.

Additionally the component code contains definitions of its ports and all its variables and initial values in parts `PORTS`, `DATA`, `DECLS` and `INIT`.

The model can be used in two ways: by feeding in real data and comparing the model output for real basin tamperature T_2 for validating the model, or by feeding in simulated data that is inside the range of model validation, for simulations.

The `SourceDataFile` -component in the `CONTROL` -library by EcosimPro, is used to read the cooling tower data sets for simulating real data. First the data set has been modified in R to contain a time column in seconds and saved as a space separated text files, which the `SourceDataFile` -component reads. The simulation can then run in EcosimPro and read values for the model variables each second from the source text data file. `AnalogSource` -component can be used to simulate steps, ramps or constant signals to be fed for the `cooling_tower` -components. The simulation results are plotted by EcosimPro or saved in a csv -table, for further analysis.

5.3 From data to model parameters

5.3.1 Optimization of the steady state parameters

The optimization of the steady state parameters was carried out using the method proposed in Jin et al. (2007) and described in the steady state parameter optimization section. Data used are the steady operation points identified by the steady state extraction algorithm.

Table 7 Identified steady state parameters. Warm temperature parameters are used for wet-bulb temperatures above 17 °C, and low temperature parameters for below 17 °C.

ETR-880	Entire set	T_{wb} higher half	T_{wb} lower half
c3	0.94	0.70	0.71
c4	0.80	0.47	0.61
l	1.43	1.53	1.45
RMSE (°C)	0.90	0.59	0.75

Parameters identified are shown in tables (7) and (8). The RMSE, is the root mean

Table 8 Identified steady state parameters. Warm temperature parameters are used for wet-bulb temperatures above 17 °C, and low temperature parameters for below 17 °C.

ETR-881	Entire set	T_{wb} higher half	T_{wb} lower half
c3	0.49	0.59	0.57
c4	0.23	0.22	0.40
l	1.63	1.66	1.52
RMSE (°C)	0.65	0.62	0.54

squared residuals between modelled steady state cooling water output temperatures and observed cooling water output temperatures, for the steady states used for optimization.

5.3.2 Dynamic parameter: a step response test

For identifying the dynamic parameters, step response tests were carried out on 3.7.2018 for the towers ETR-880 and ETR-881. Tests included fan speed ramp ups from off to 50 %, 50 % to 100 %, off to 100 % and 0 to 100 %. When the fan is off, the air flow in the tower is due to natural convection. Fan at 0 %, is for 33 Hz variable frequency drive output and 100 % is 50 Hz. The increase in air flow from off to 0 % is large compared to the increase from 0 % to 100 %. This was noticed during the testing, as the temperature of the basin had a large drop after off to 0% and smaller drop after 0 % to 100 %. After this discovery, more effort where put in to studying the relation between air flow and speed signal, which eventually lead to use of the linear model for airflow - speed signal, instead of feeding the pure speed signal to the model. It was stated earlier, that the fan ramp up from off to 100 %, is the most interesting event regarding the cooling tower verification analysis. Therefore off to 100 % is selected as the event for identifying the dynamic parameter c_1.

The test was carried out manually at the cooling site of LHC point 8. The testing was possible, due to little influence of a single tower on the cooling water temperature returned by the the tower complex, as long as the the test for the two towers where carried out one by one. The operator of the cooling system at LHC point 8, could manually take control of the fans over the control system. The system needs to reset in steady state before and after the transient to obtain sufficient data. The time available for testing was limited, and before the transient the steady state is short. 30-45 minutes was waited before and after the transient, which is enough for the system to reach the steady state. Other variables: water mass flow, ambient wet-bulb temperature and entering cooling water temperature, stayed approximately constant during the testing.

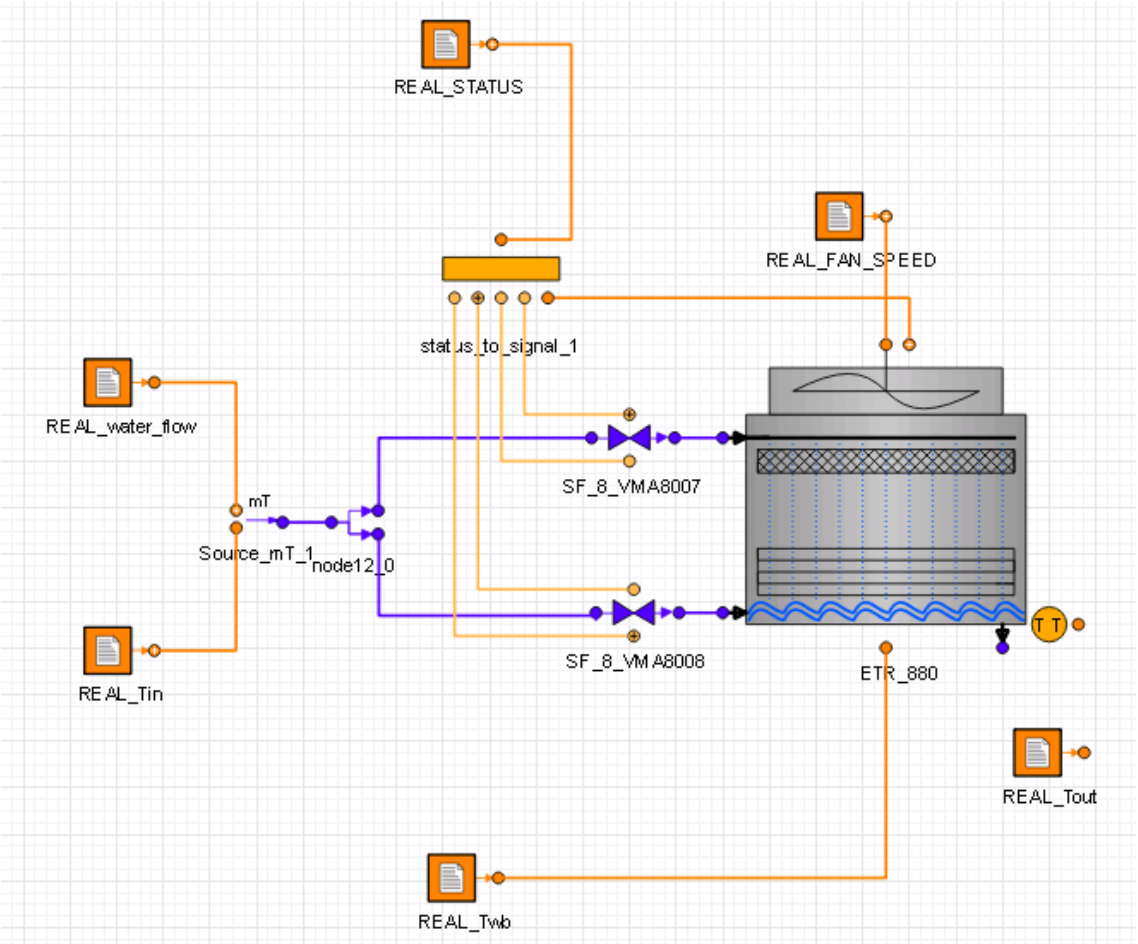

Figure 10: Ecosim model of single cooling tower for validating towers ETR-880 and ETR-881. $\text{REAL}_{T}out$ – *componentreadsdataofmeasuredoutputtemperatureforvalidatingthemodel.*

The data was then parsed and subset to cooling tower data sets for both towers ETR-880 and 881. For both towers, the dynamic parameter c_1 was then obtained with a identification procedure explained in section 4.3.2. Results are presented in table (9). The root mean squared error (RMSE) is the simulated step response, with the identified parameter c_1. Simulation results are presented in figures (11).

Table 9 Identified dynamic parameters.

Tower	c_1	RMSE
ETR-880	9.26e-06	0.72
ETR-881	8.01-06	0.68

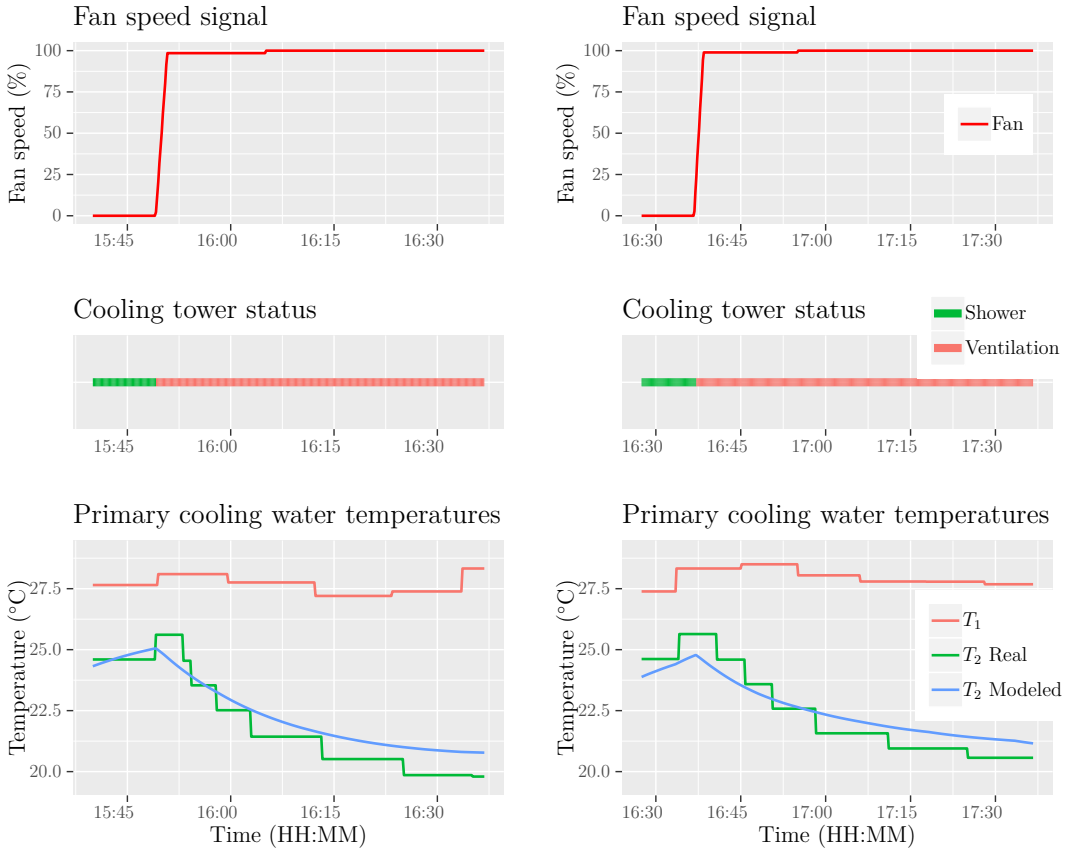

(a) ETR-880 **(b)** ETR-881

Figure 11: (a) Step response test for ETR-880, (b) Step response test for ETR-881. Plots of the real step response and the output of the identified dynamic model.

The figures (11a) and (11b) show that the model is able to imitate the transients well, and predict the steady states before and after the cooling towers with accuracy of approximately 1 degree Celsius. The good imitation of the transient phase indicates that the data from the tests contains sufficient information to describe the inertia of the system, and the linear model parameter c_1 regression works well.

5.4 Model validation

Model validation is a very important and valuable analysis for parties making conclusions based on the simulations run with this cooling towers model. The transients simulated by the model aim to represent the real system, and it is important to study and understand the reliability of this representation. The accuracy of the model needs to be presented clearly and with transparency, to avoid false conclusions of the simulation results.

Key measures of the model accuracy are steady state root mean squared error (RMSE), steady state residual distribution and dynamic RMSE. As model relies on parameter optimization against real operational data, it is important not to use same data for parameter identification and model validation. A cross-validation approach is used, and all validation data are outside the time frame used for parameter identification, May - December 2017.

5.4.1 Dynamic validation

For dynamic model validation, periods of data containing transients were simulated and visualized. The figures contain three plots from top to bottom fan speed signal, cooling tower status and temperatures. Temperatures include real input and output temperatures and modeled output temperature. Here three time periods are simulated with both towers ETR-880 and ETR-881.

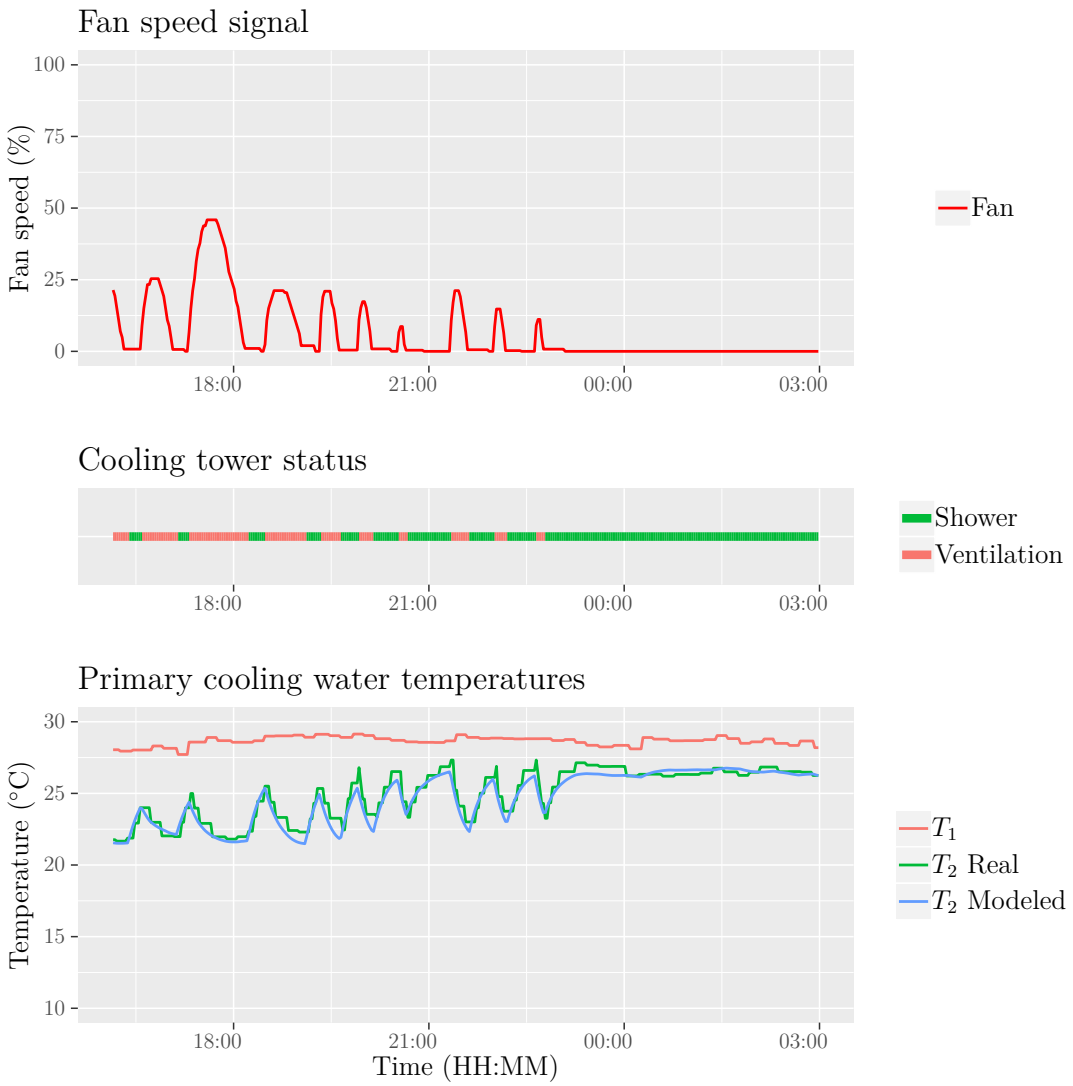

Figure 12: Validation plot ETR-880, rmse = 0.5488 $°C$, mean T_{wb} = 17.58 $°C$. As seen, the T_2 Modeled represents the T_2 Real accurately during fan speed dynamics.

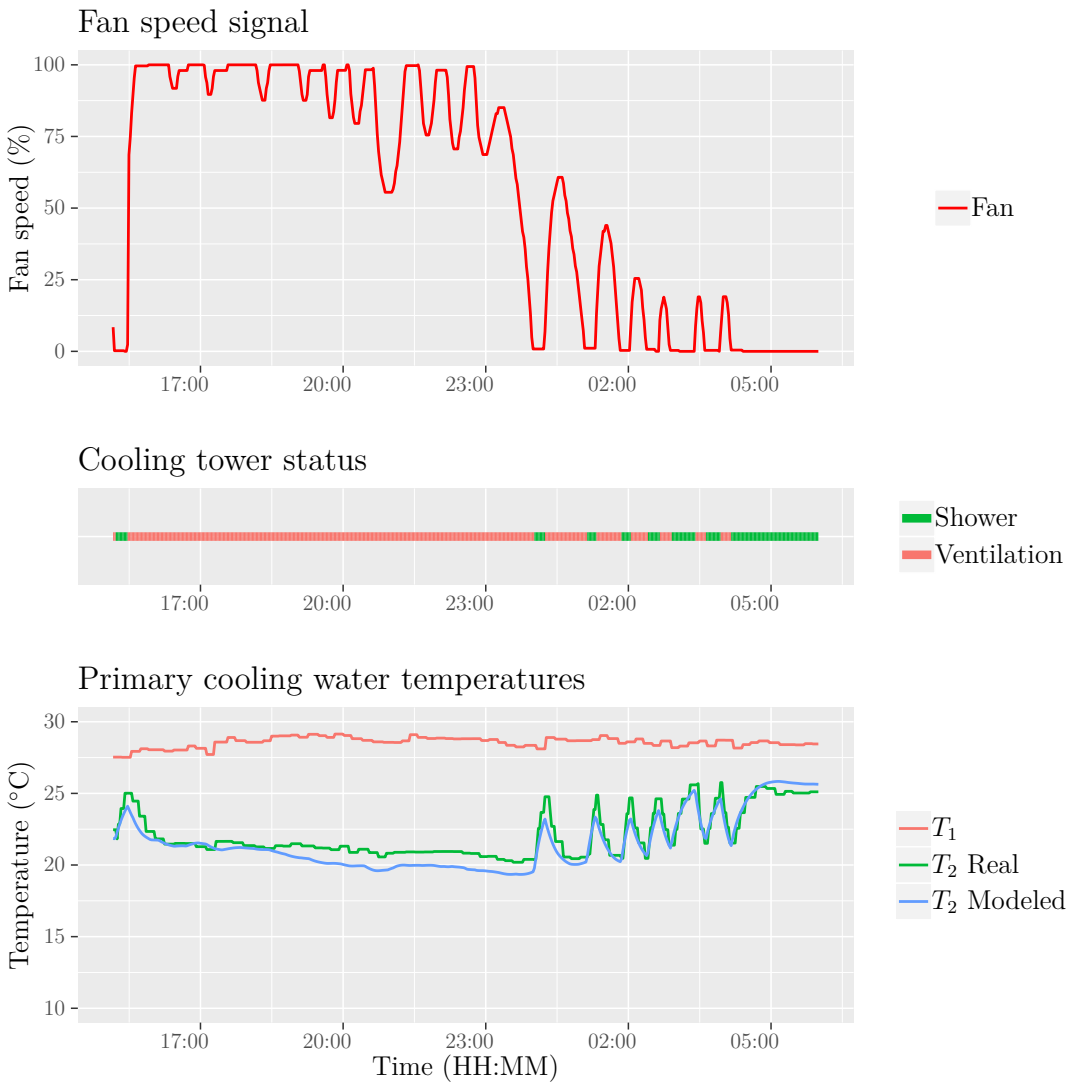

Figure 13: Validation plot ETR-881, rmse = 0.8157 $°C$, mean T_{wb} = 17.19 $°C$. It is seen that the model represents the dynamics well while having occasional offset of 1 $°C$.

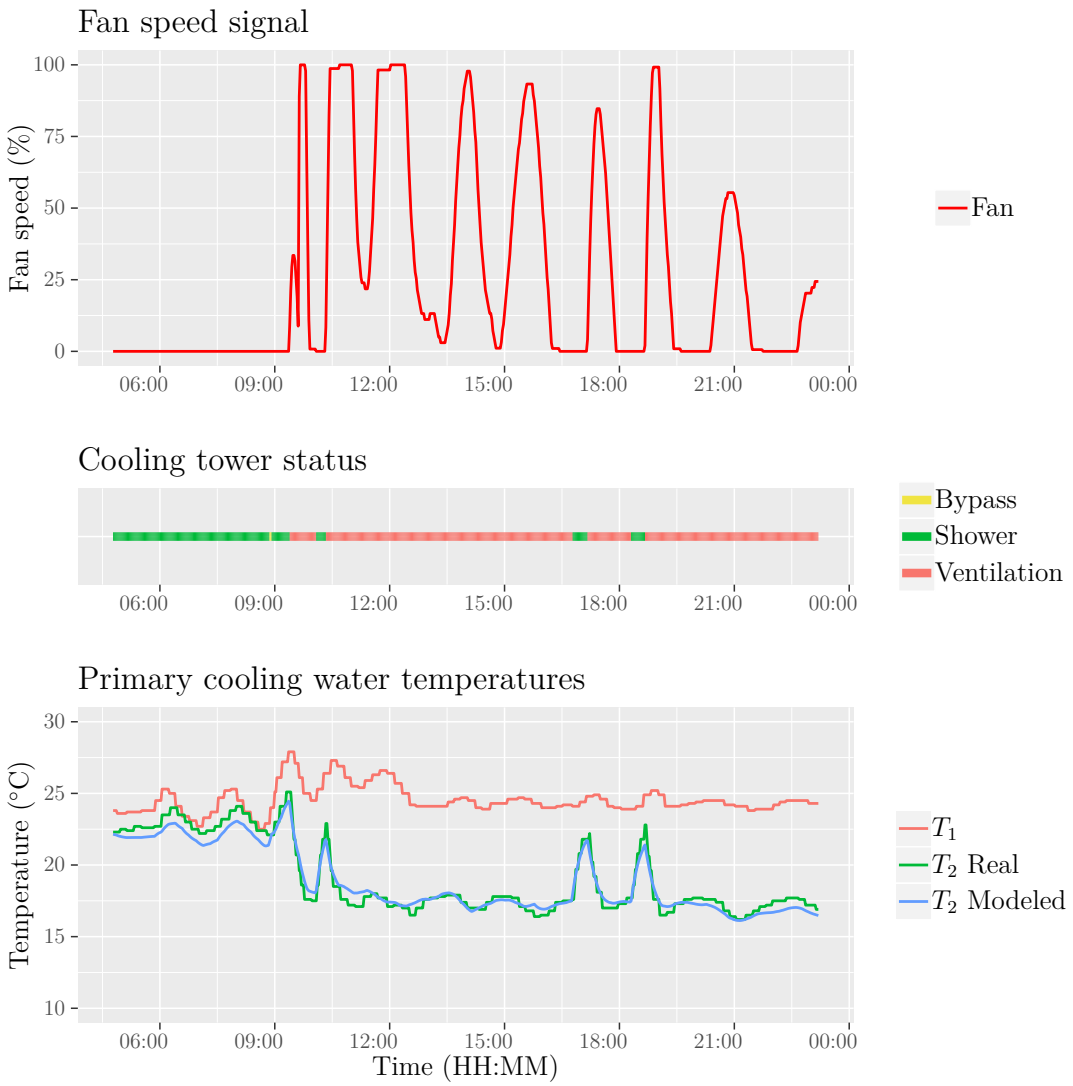

Figure 14: Validation plot ETR-880, rmse = 0.4905 $°C$, mean T_{wb} = 13.57 $°C$. The model captures the dynamics well with minor offset.

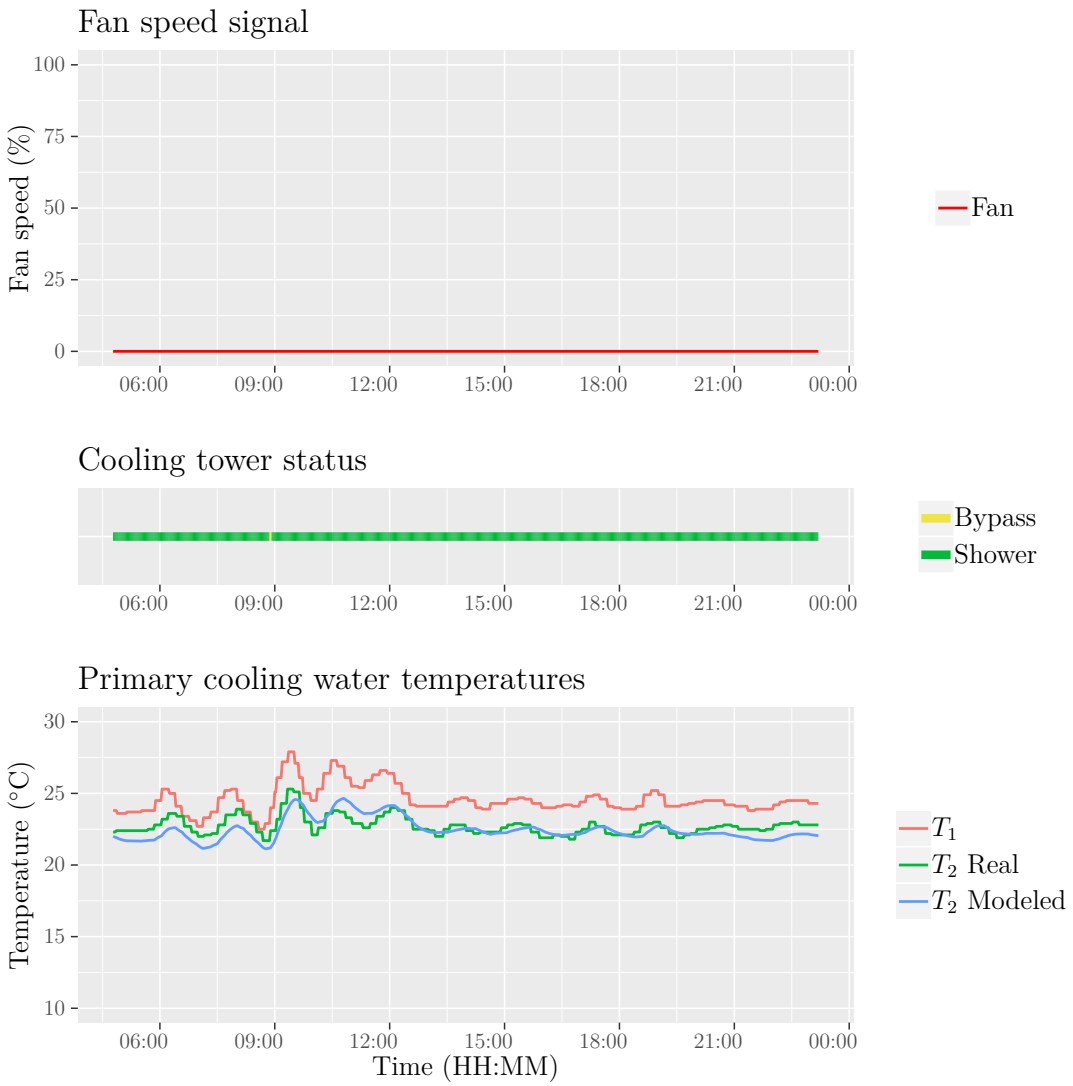

Figure 15: Validation plot ETR-881, rmse = 0.6464 $°C$, mean T_{wb} = 13.57 $°C$. Low wet-bulb temperature validation plot showing the model performance after dynamics in the input temperature.

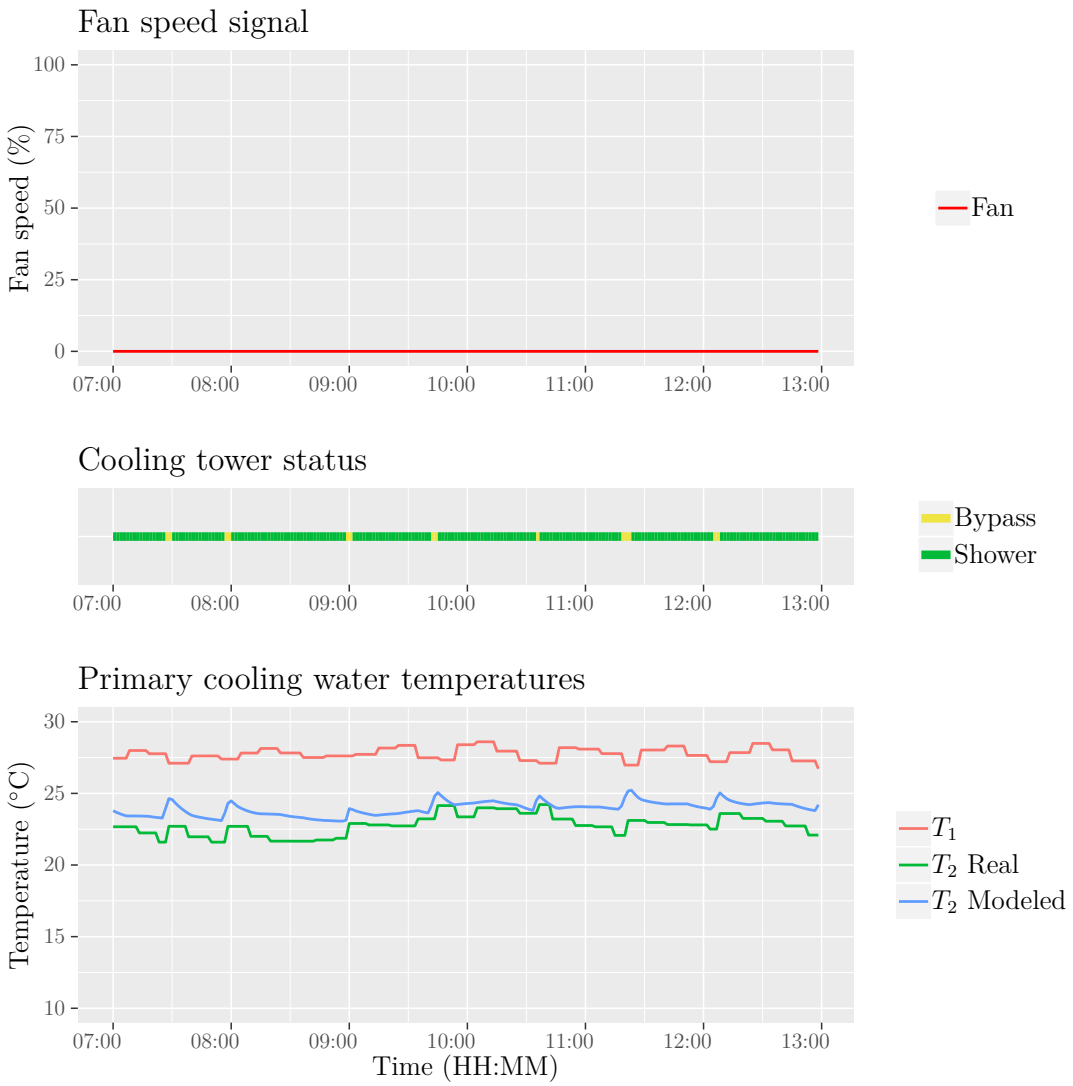

Figure 16: Validation plot, rmse = 1.26 $°C$, mean T_{wb} = 0.83 $°C$. The dynamics of the bypass is modeled well, while the offset is due to the uncertainty related to free convection air flow.

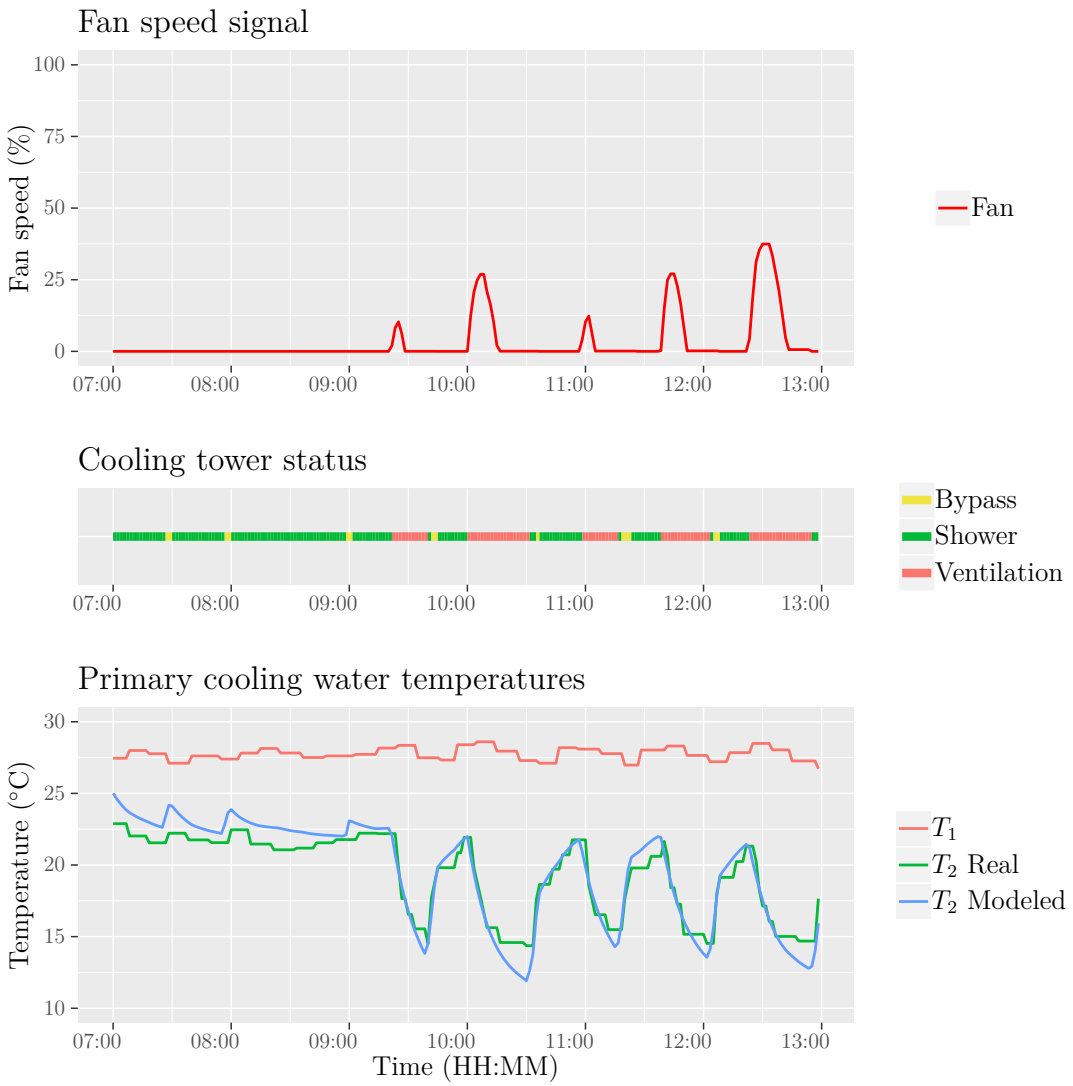

Figure 17: Validation plot, rmse = 1.04 $°C$, mean T_{wb} = 0.83 $°C$. It is seen that the model represents well dynamics related to both bypass and fan speed.

Simulations with real data in figures (16), (17), (14), (15), (12) and (13) show that the model is able to predict the output water temperature T_2 well with RMSE less than 1 °C. The model is able to predict well the response of the dynamics in the input temperature as in figure (14). The response of the control actions, changes in fan speeds signals or cooling tower status, is reproduced with very good accuracy. The figures show that the temperature dynamics followed by the fan start ups or speed signal variations are captured well. In figures (12) and (13) the effect of switching between bypass and showering is captured well. In general all the dynamics are imitated well as the shapes of the T_2 *Real* and T_2 *Modeled* are very similar, while some small offset is almost always present. Bigger errors up to 2.5 $°C$ exist in figure (13). These errors may be due to measurement error in the cooling tower basin and imperfections in the mixing of the basin or uncertainty regarding the fixed air mass

low estimation for showering mode.

5.4.2 Steady state validation

By examining the steady state performance of the model, a wider understanding of the model reliability in the frames of available data can be obtained. Visual evaluation of the model residual normality, is a common way to study the feasibility of the model or parameter selection. Unnormally or uncontinuously distributed residuals indicate errors that may be explained by some reoccurring event in the data. Residuals which distribution is approximately bell shaped, indicate that the model and parameter selection is correct and error is explained as random noise, and does not have problems related to model selection.

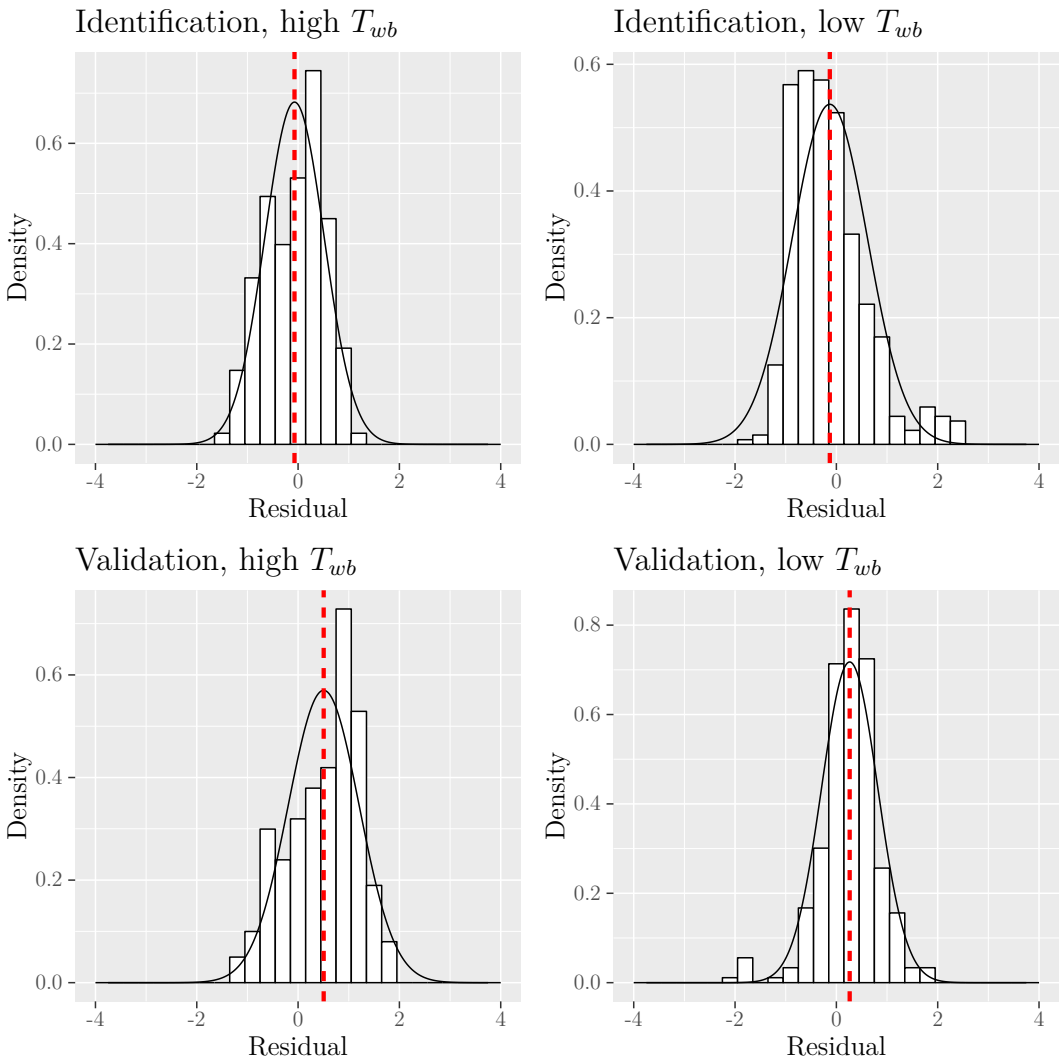

Figure 18: ETR-880 residual normality test showing the approximately bell shaped histogram for model residuals for both identification and validation data sets and both high and low wet-bulb temperature parameters.

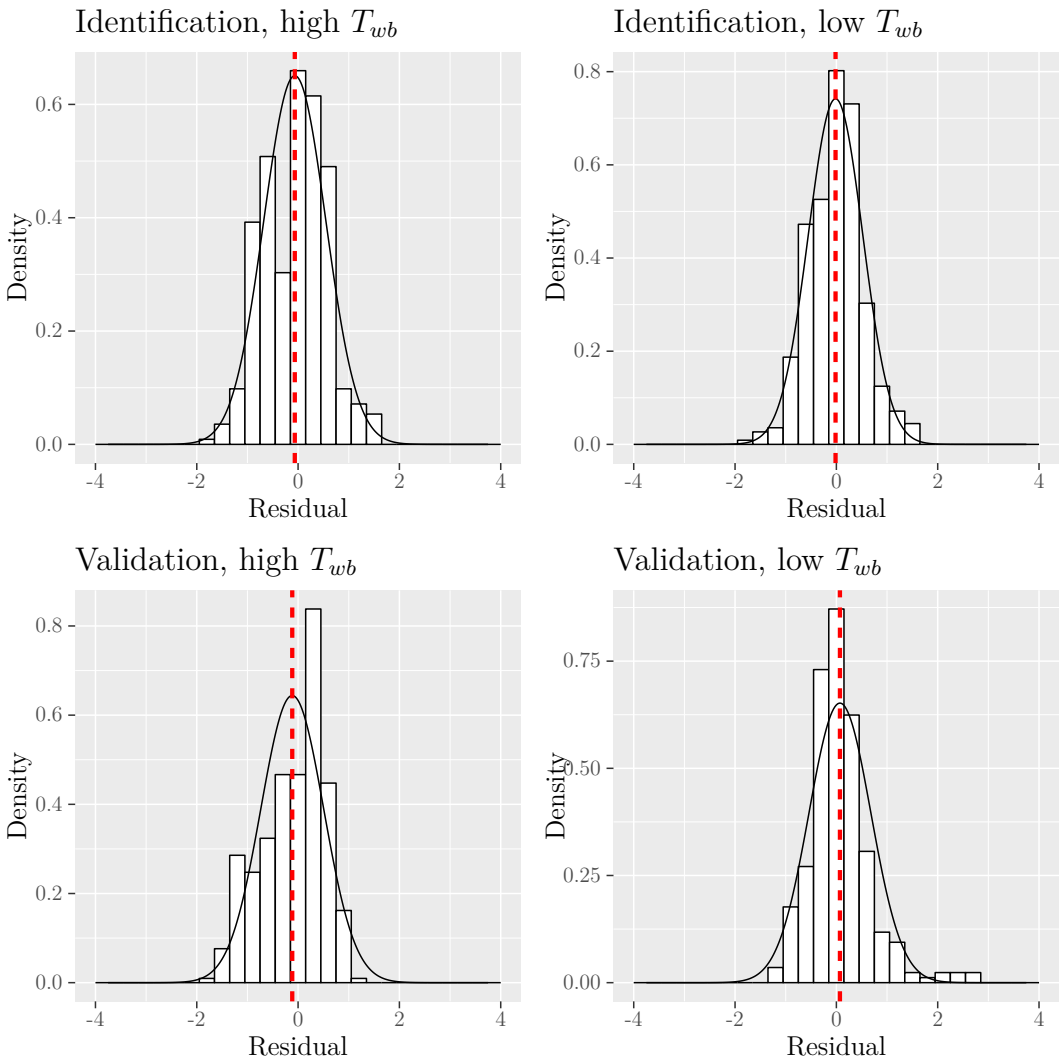

Figure 19: ETR-880 residual normality test showing the approximately bell shaped histogram for model residuals for both identification and validation data sets and both high and low wet-bulb temperature parameters.

The model residual densities of towers ETR-880 and ETR-881 are presented in (18) and (19). The density histograms are presented separately for warm and chilly temperatures and identification and validation steady state data sets. The upper row contains the steady states extracted from year 2017 for parameters identification and the second row contain the steady states extracted from year 2016 for validating the identified parameters. Use of different time period to obtain data for parameter identification than data for validation, is called cross-validation. The model is expected to have better accuracy for the identification data and worse but sufficient accuracy for the validation data.

Bases on the results presented in figures (18) and (19), the steady state accuracy is good. The residuals have highest occurrences between -1 and +1 °C and the error is

never much higher than +2 or -2 °C. Both figures indicate a minor systematic error to the negative side, meaning the model tends to slightly underestimate the cooling performance on average. The residual density histograms are approximately bell shaped. This shows that the model selection is correct, model is able to represent the characteristics of the real system and the error is random, and is not explained by some missing feature in the model architecture.

Table 10 Steady state RMSE.

ETR-880	Entire set	T_{wb} higher half	T_{wb} lower half
Identification RMSE ($°C$)	0.90	0.59	0.75
Validation RMSE ($°C$)	0.95	0.69	0.78

Table 11 Steady state RMSE.

ETR-881	Entire set	T_{wb} higher half	T_{wb} lower half
Identification RMSE ($°C$)	0.65	0.62	0.54
Validation RMSE ($°C$)	0.82	0.63	0.61

The resulting root mean squared error (RMSE) is the mean of the squared residuals over a steady state data set. The tables (10) and (11) present the different RMSE obtained for different sets. In general the RMSE is very satisfying, indicating that the overall model steady state accuracy is good and the parameters obtained work well. It is is seen that as expected, the error is higher for the cross-validation data which is outside the parameter identification time frame. It was found useful to identify two separate parameters for low and high temperatures, as this decreases the model error. In tables (10) and (11) the T_wb *higher half* and *lower half* RMSE are lower than the *Entire set* RMSE.

5.5 Sensitivity Analysis

The uncertainties and possible systematic errors in the sensor readings contribute to the modeling error, not only the errors resulting from the simplifications in the modeling approach. While the sensors measuring the system can be considered accurate, it is useful to study the model outputs sensitivity to each of these variables. Main sources for these uncertainties are the measurement errors in the model variables T_{wb}, T_1, $\dot{m}_w$ and in the estimation of $\dot{m}_a$. The sensitivity of the steady state parameters is also examined. Sensitivity analysis aims to study the influence of these uncertainties relative to each other.

To illustrate the sensitivity of the model, classical one-by-one spider charts are presented to show the absolute change in model estimation T_2, when model input variables or parameters are changed by multiplying them one-by-one by factors from 0.9 to 1.1. The y axis shows the absolute change in the output variable T_2.

Spider charts visualize the correlation between each variable and model output. All the variables show linear or close to linear effect. T_1 and T_{wb} are strictly linear with a correlation of exactly 1 to the dependent variable, but $\dot{m}_w$ and $\dot{m}_a$ show small non-linearity with a correlation slightly below 1. All but variables $\dot{m}_a$ have positive correlation.

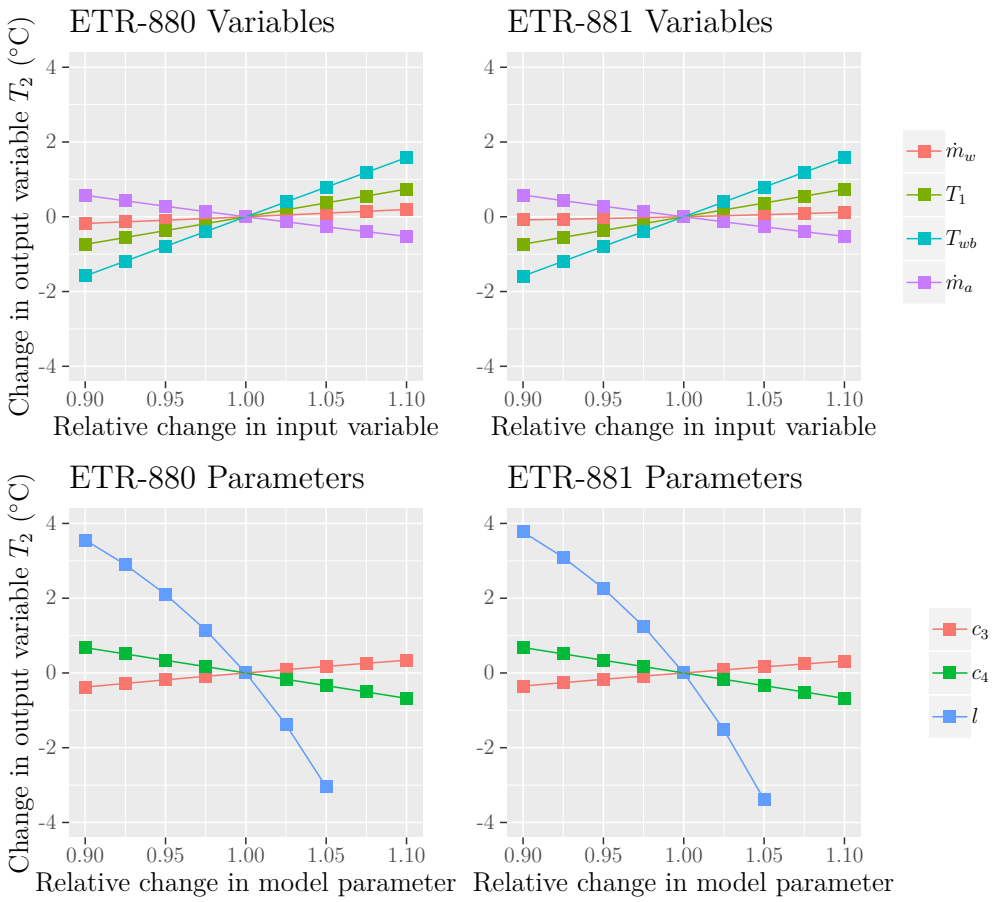

Figure 20: Model sensitivity for both towers ETR-880 and ETR-881 at 21 °C T_{wb}. Model is most sensitive to wet-bulb temperature and parameter l.

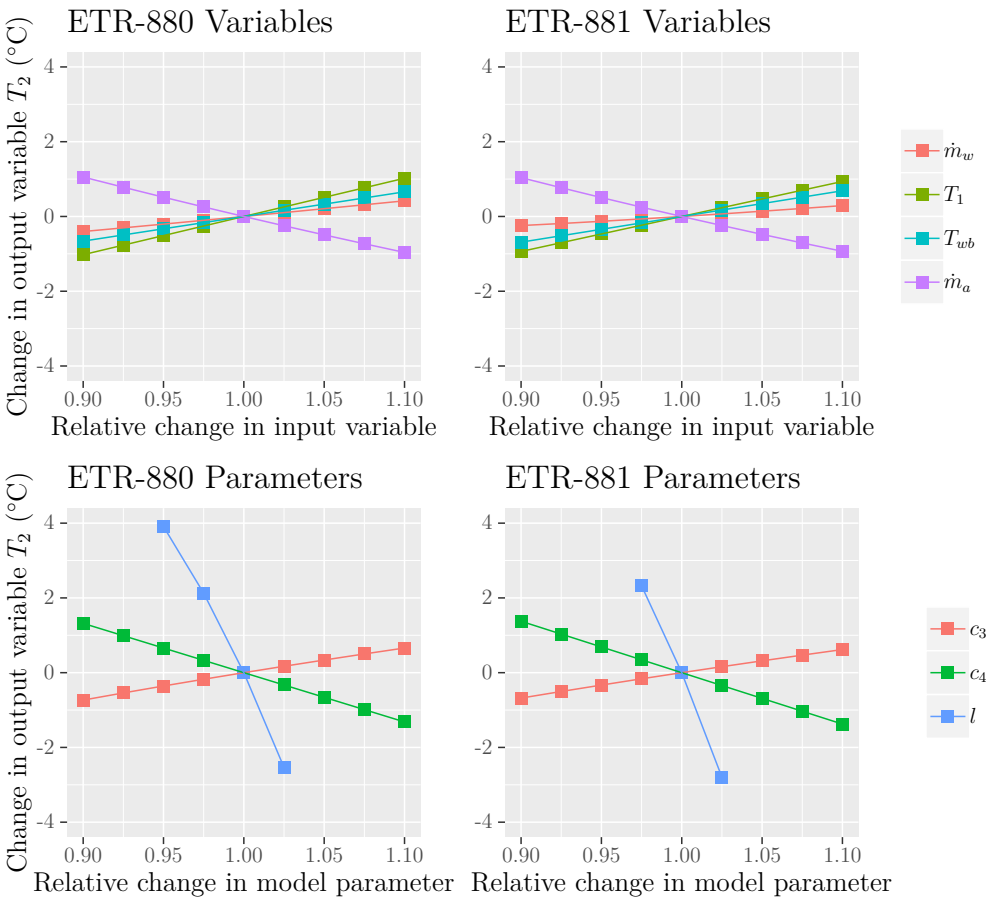

Figure 21: Model sensitivity for both towers ETR-880 and ETR-881 at 21 °C T_{wb}. Model is most sensitive to air mass flow and parameter l.

The spider plots show clear order in the relevancy of each parameter and the ambient wet-bulb temperature having highest relevancy in warm weather. On low temperatures the order of relevancy is changed and the air flow becomes the most relevant. It follows the hypothesis that the towers output temperature range that the operator is able to control is much wider in low temperatures, when the wet-bulb temperature is not limiting the lower limit of this range very high. As shown by the spider plots, air flow has increased relevancy on low temperatures. From model parameters, the l has clearly the highest relevancy. This is due to l being an exponent in the model algorithm. All parameter sensitivities become higher in low temperatures, thus the model is more sensitive to poor parameter selection in low temperatures.

6 Simulation of sudden heat recovery loss

The resulting accuracy of the cooling tower model developed in this thesis was studied in the previous chapter. It was found that the model imitates the real system well and can be used for simulations where the model variables are kept within the model validation ranges (tables 5 and 6). This chapter shows the use of the model in practice, by presenting results from simulations run with the model for studying the cooling towers robustness against input temperature fluctuations. The simulations are run both in open and closed control loop manner. In the open control loop simulations, manually selected control actions are used to react to the temperature transients immediately. In the closed control loop simulations, a real PLC running current control algorithms is controlling the cooling towers in a virtual commissioning environment. The observed phenomena in the simulations is the output cooling water temperature from the cooling tower complex, mean T_2, which is supplied to the cooling clients. Most importantly the simulation study the response in mean T_2 to a temperature step in T_1. It is estimated that that in mean T_2 a delta T of more than five degrees Celsius in ten minutes or temperature more than 25 degrees Celsius are the hard limits for the underlying cryogenic cooling systems.

Conditions for the simulations are based on anticipated scenarios of sudden loss of heat recovery. Scenarios are defined by an engineering team at CERN responsible of waste heat recovery installation. The scenarios define anticipated operating conditions of the clients and waste heat recovery, and expected maximum worst case wet-bulb temperatures for each season. Clients are users of the primary cooling water at LHC point 8, which are the Large Hadron Colliders (LHC) and LHCb experiments cryogenic refrigeration stations. Client heat load defines the increase of the primary cooling water temperature at client side and WHR absorption rate defines the decrease of the temperature in the WHR heat exchanger, before the water enters the cooling towers. The anticipated heating requirement and use of WHR by the municipality is lower during the summer, thus the temperature steps to expect during summer time are smaller, Primary cooling water flow is kept stable at the design value. WHR -loss scenario that generates most pressure for the cooling towers and the control system is during high WHR -absorption, and when the clients are at full power and ambient wet-bulb temperature is high. Then less reserve cooling capacity is available and the step up transient in temperature of the primary cooling water the towers receive after a WHR -loss event is high.

6.1 Open loop simulation in EcosimPro

Open control loop simulations were run on scenarios, which don't require active control to keep the basin temperatures steady within 20-24 C nominal range. Open control loop simulation has no connection to the PLC, and control actions to damp the temperature transient are taken manually. With open control loop simulations

model functionality could be verified and understanding of the towers ability to damp transients could be gained already prior to implementation of the virtual commissioning environment.

For the simulations, a simplified representation of the client flow circuit was created in EcosimPro, with constant client heat load Q_{LHC} with no thermal inertia or time constants. The time constant, the time for the cooling water to run through the circuit, can be neglected in this context, as it is fast compared to the volume and circulation time of the cooling tower basins. A simple component for the heat recovery heat exchanger was created, which takes a power Q_{WHR} from the general return primary cooling water and stops at a given time, creating a temperature step up in the general return temperature T_1.

The simulation model used is shown in figure (22). The cooling tower model parameters are set as attributes of the `cooling_tower` -component in EcosimPro. In EcosimPro, simulations are declared by creating an `.exp` -experiment file in EL -language for the simulation model. The simulation model can contain components, that do actions of which time of occurrence (seconds from start of the simulations), can be declared in the component attributes. These actions or anything that the user wants to occur during the simulation, can also be programmed in to the experiment `.exp` -file, which also declares the start an stop times and initial values of the simulation.

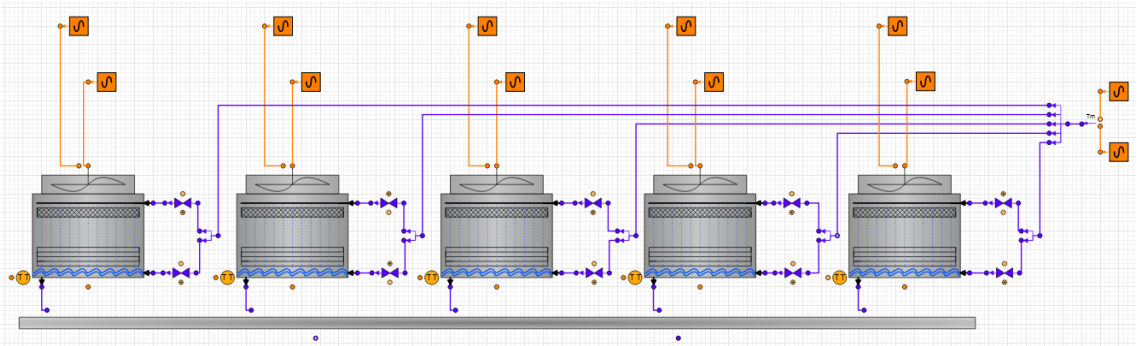

Figure 22: Schematic of the cooling tower complex in EcosimPro used in the open control loop simulations.

The design power of the heat recovery installation is 10 MW, which would contribute to a 3.2 $°C$ reduction in the hot primary cooling water temperature at design primary water flow of 2709 m^3/h. The simulation model consists of circuit with the cooling towers, clients contributing a constant power to the cooling water and heat recovery, that stops at the time of 00:30. The resulting transient is a step up of 3.2 $°C$ in the temperature to the state where the system would operate without the heat recovery.

Table 12 Likely scenarios for a loss of waste heat recovery (WHR) -event. ΔTs under design flow of 2709 m^3/h.

			Client		WHR	
Scenario	Season	T_{wb} $(°C)$	Q (MW)	ΔT $(°C)$	Q (MW)	ΔT $(°C)$
M1	Mid	12	20	6.4	6.3	2.0
M2	Mid	12	15	4.8	6.3	2.0
S1	Summer	21	20	6.4	1.6	0.5
S2	Summer	21	15	4.8	1.6	0.5
S3	Summer	21	10	3.2	1.6	0.5

Scenarios simulated (12) are based on a request from a team working with designing of the WHR installation. The scenarios represent anticipated operating conditions of the clients and waste heat recovery, and expected maximum worst case wet-bulb temperatures for each season. The worst case is high WHR with high client load at high ambient wet-bulb temperature. Clients are users of the primary cooling water at LHC point 8, which are the Large Hadron Collider (LHC) and LHCb experiment cryogenic refrigeration stations. Client heat load defines the delta T of the primary cooling water at client side. WHR load defines the cooling delta T of the waste heat recovery heat exchanger. Primary cooling water flow is kept stable at the design value.

Table 13 Initial system states and manual actions taken to maintain a sufficient supply temperature in a simulated WHR loss event.

	Initial number of towers at:			
Scenario	Bypass	Shower	Ventilation (Speed %)	Action after heat recovery
M1	0	4	1 (50%)	Ramp the first fan to full, start a second fan
M2	1	3	1 (0%)	Set bypass to showering, start a second fan
S1	0	0	5 (one at 50 %)	No action needed
S2	0	0	5 (0%)	No action needed
S3	0	1	4 (0%)	No action needed

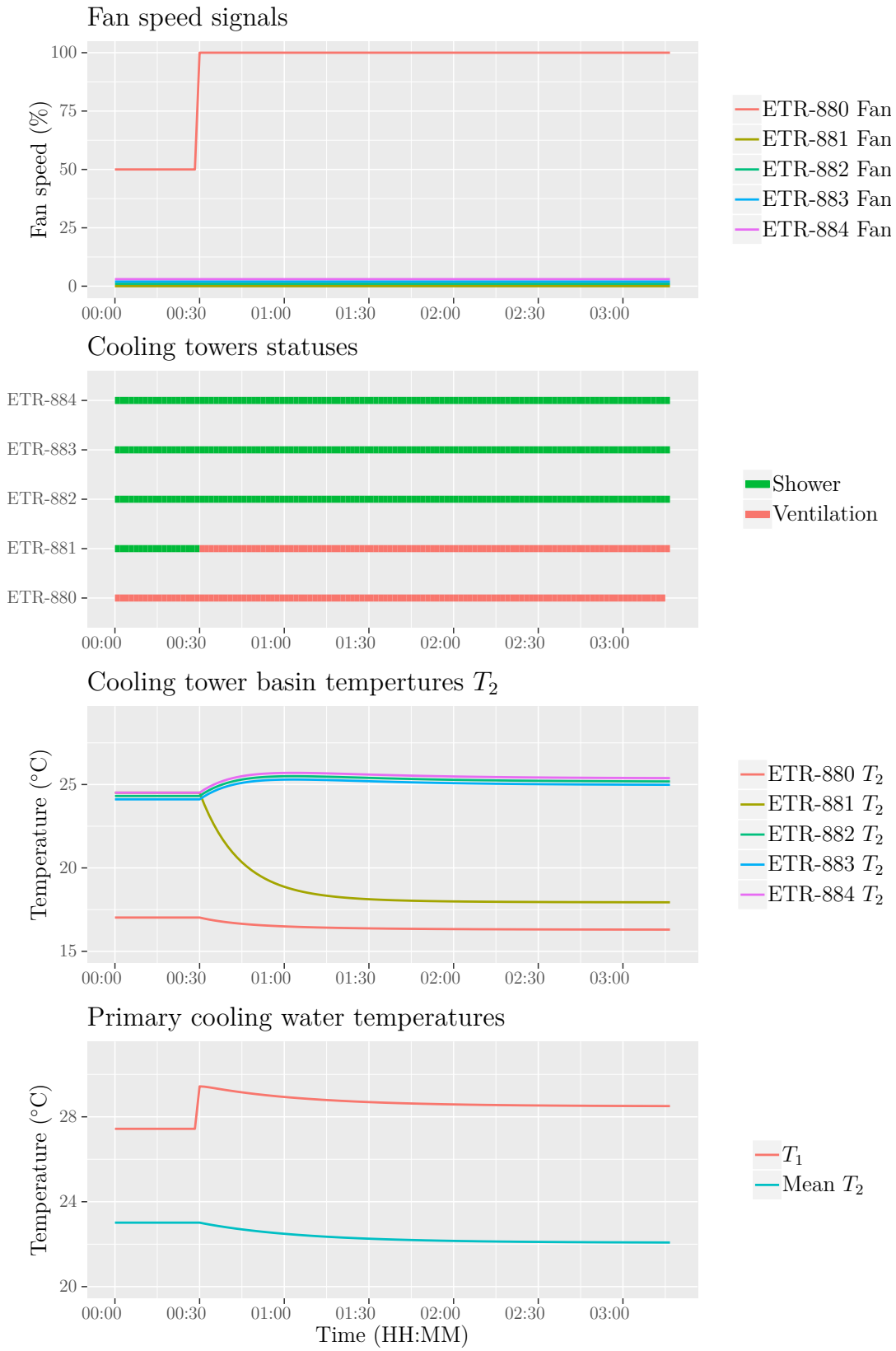

Figure 23: Simulation result plot for mid season scenario M1.

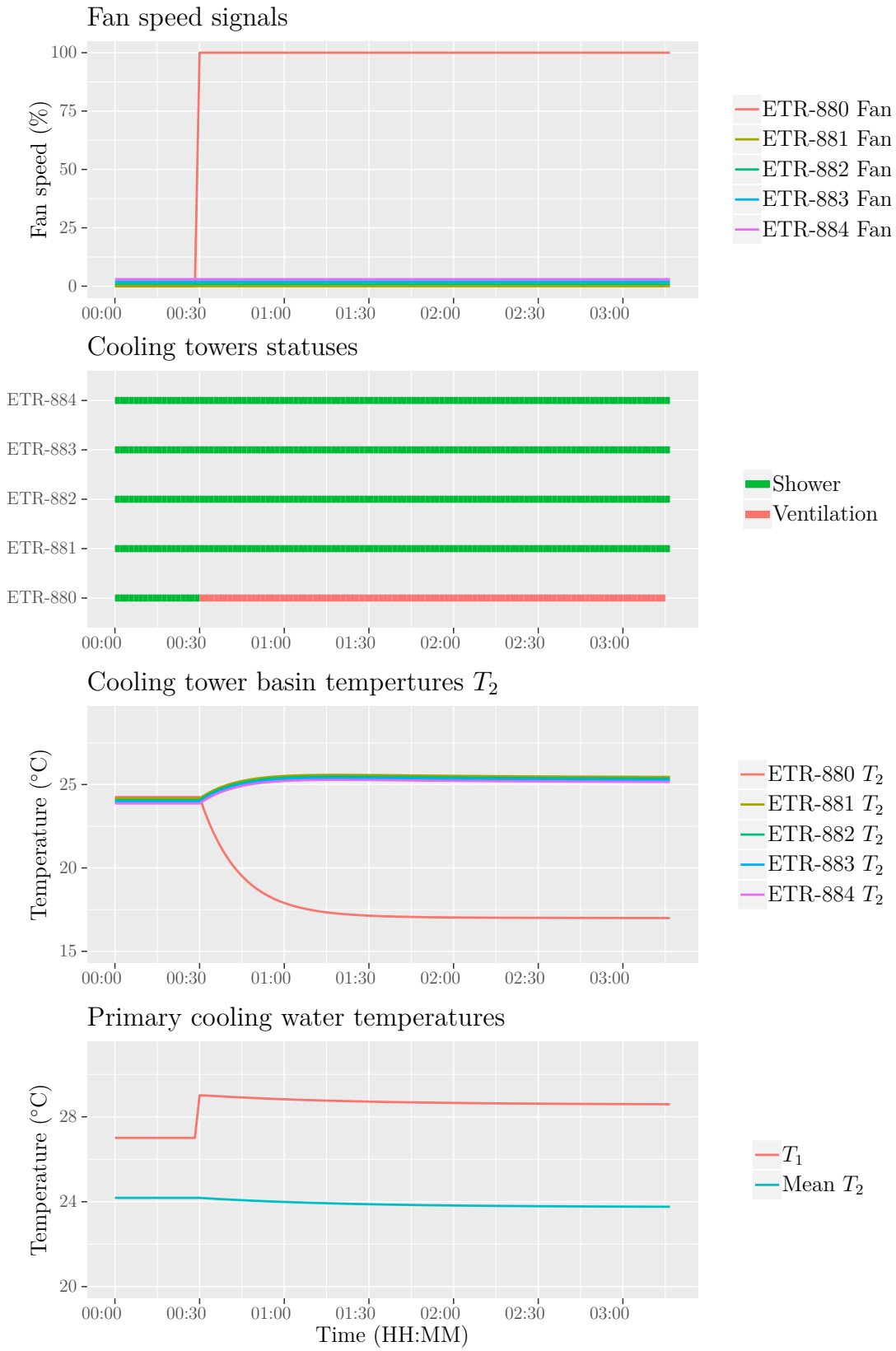

Figure 24: Simulation result plot for mid season scenario M2.

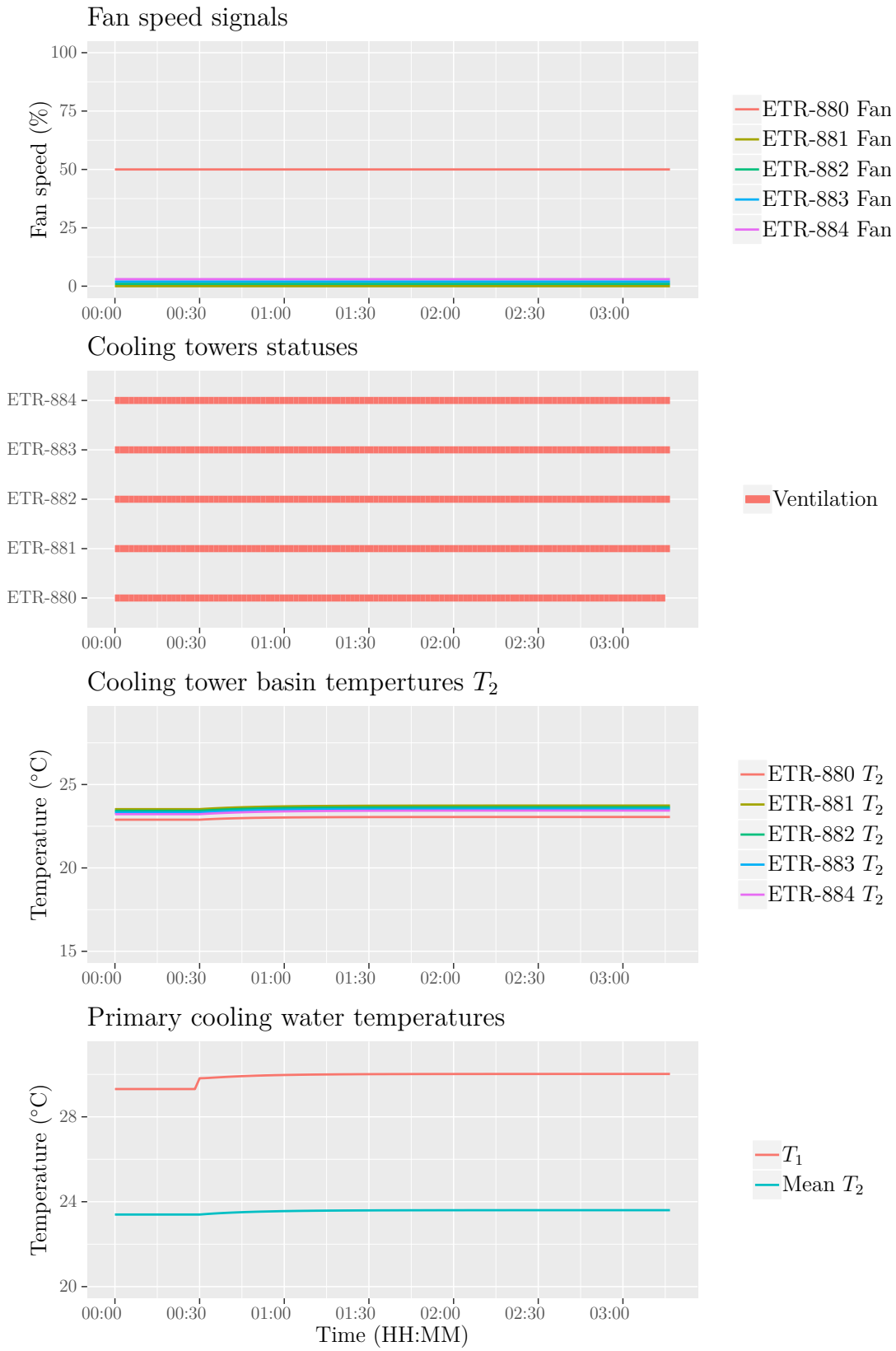

Figure 25: Simulation result plot for summer scenario S1.

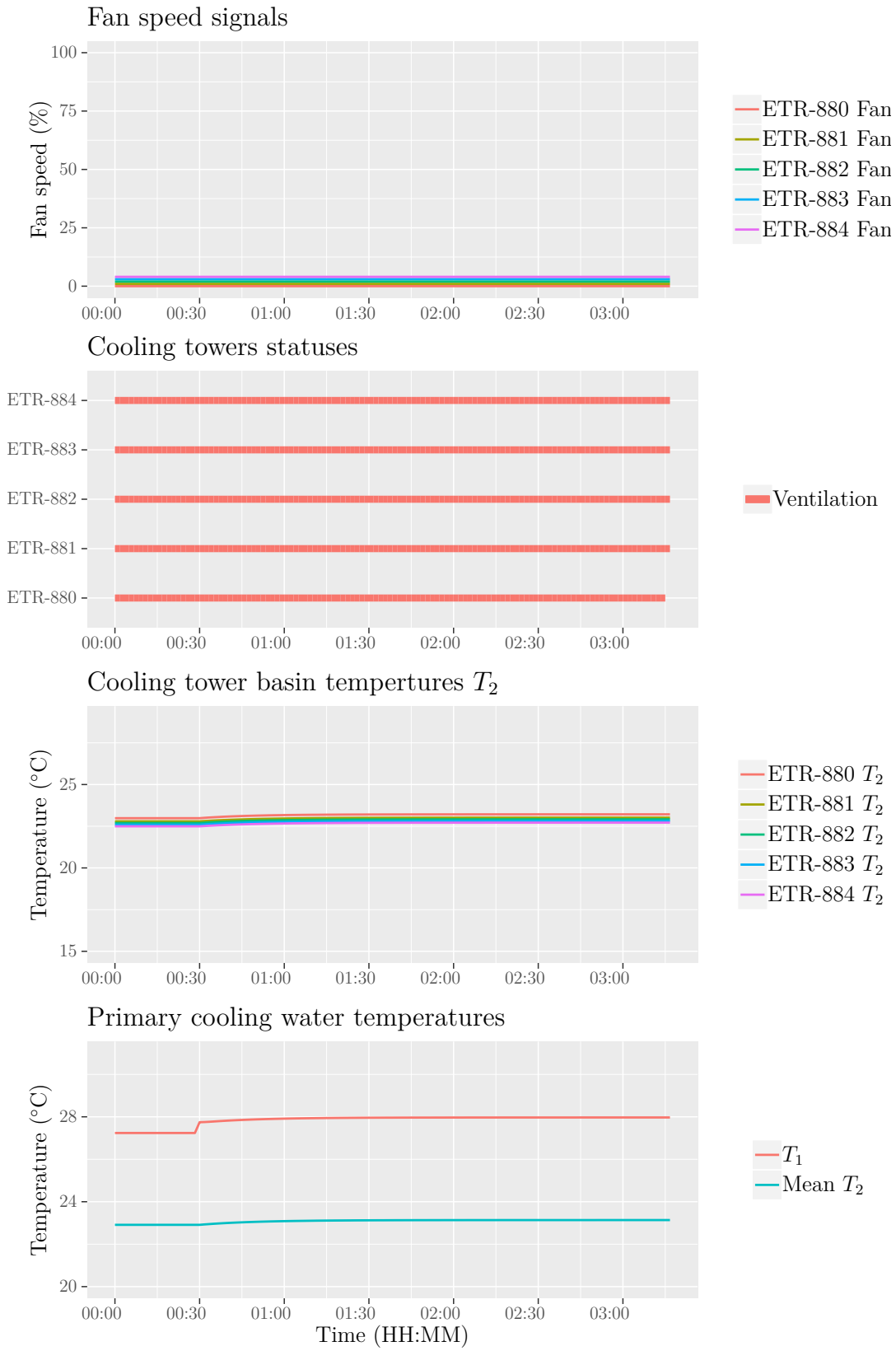

Figure 26: Simulation result plot for summer scenario S2.

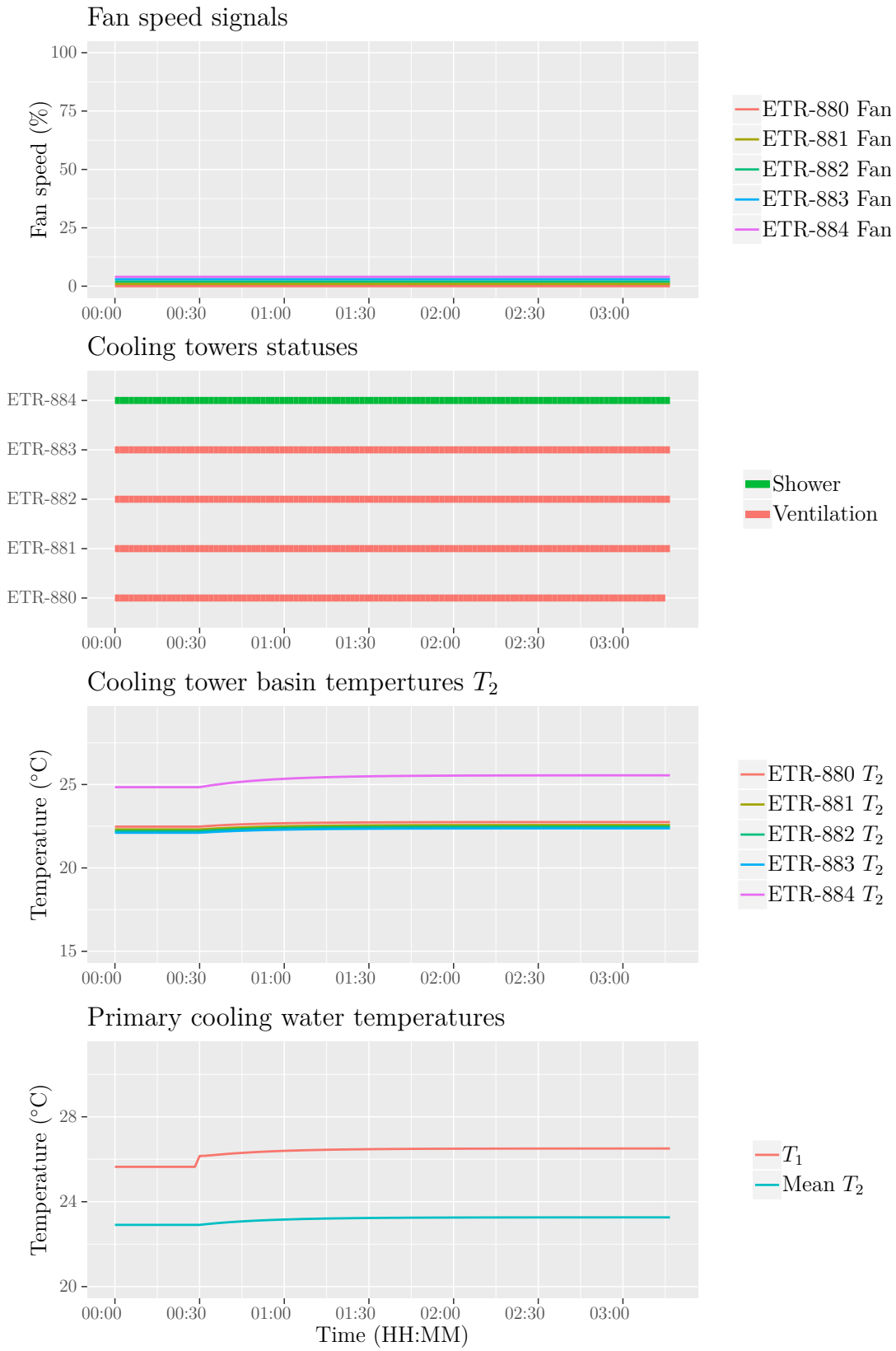

Figure 27: Simulation result plot for summer scenario S3.

Simulation results for each scenario are shown in figures, 23, 24, 25, 26 and 27. Figures include from top to bottom fan speed signals, cooling tower statuses, modeled responses in cooling tower basin temperatures T_2 for each of the tower basins and input T_1 - output Mean T_2 temperatures of the cooling tower complex. Changes in fan speed signals and in cooling tower statuses are control actions for damping the temperature step in general return temperature T_1. Identical lines are slightly offset vertically to make them visible. The simulations show that the cooling towers can easily damp the anticipated temperature transients, and the capacity nor the speed of the hardware itself is not a problem. If the actions defined in table (13) are taken right at the moment of WHR -loss without major delay, the towers would damp the transients very efficiently.

6.2 Virtual commissioning

Control configurations coded into a PLC can be tested and verified connecting the PLC with a simulation model of the real system, for which the control configurations is needed. This is called virtual commissioning, which is useful for systems which are critical or if the time available for commissioning and testing with the real system is limited or not possible (Booth et al. 2018).

In the closed control loop simulations presented here, the EcosimPro simulation is connected through the Open Platform Communication Unified Architecture (OPC UA) interface to a PLC in the lab, that runs a copy of the currently commissioned PLC code, which controls the real cooling towers. OPC is a standard for reliable exchange of data in the industrial automation context, developed and maintenanced by the OPC foundation (OPC Foundation 2018b). OPC-UA is a protocol which integrates all the functionalities of the independent OPC classic specifications (OPC Foundation 2018a).

The heat recovery loss event is simulated as in the open control loop simulations, but instead of manual initial system state and manual control actions, the real control algorithm running on a PLC is dynamically determining the cooling tower statuses and fan speeds. Virtual commissioning simulations here show how the current control configuration reacts to fast temperature transients in the input cooling water, and what is the magnitude and slope of the resulting response at the output water temperature.

Table 14 Likely scenarios for a loss of WHR -event simulated in virtual commissioning environment. ΔTs under design flow of 2709 m^3/h.

			Client		WHR	
Scenario	Season	T_{wb} $(°C)$	Q (MW)	ΔT $(°C)$	Q (MW)	ΔT $(°C)$
W3	Winter	10	10	4.8	10	3.2
M1	Mid	12	20	6.4	6.3	2.0
S1	Summer	21	20	6.4	1.6	0.5
S3	Summer	21	10	3.2	1.6	0.5

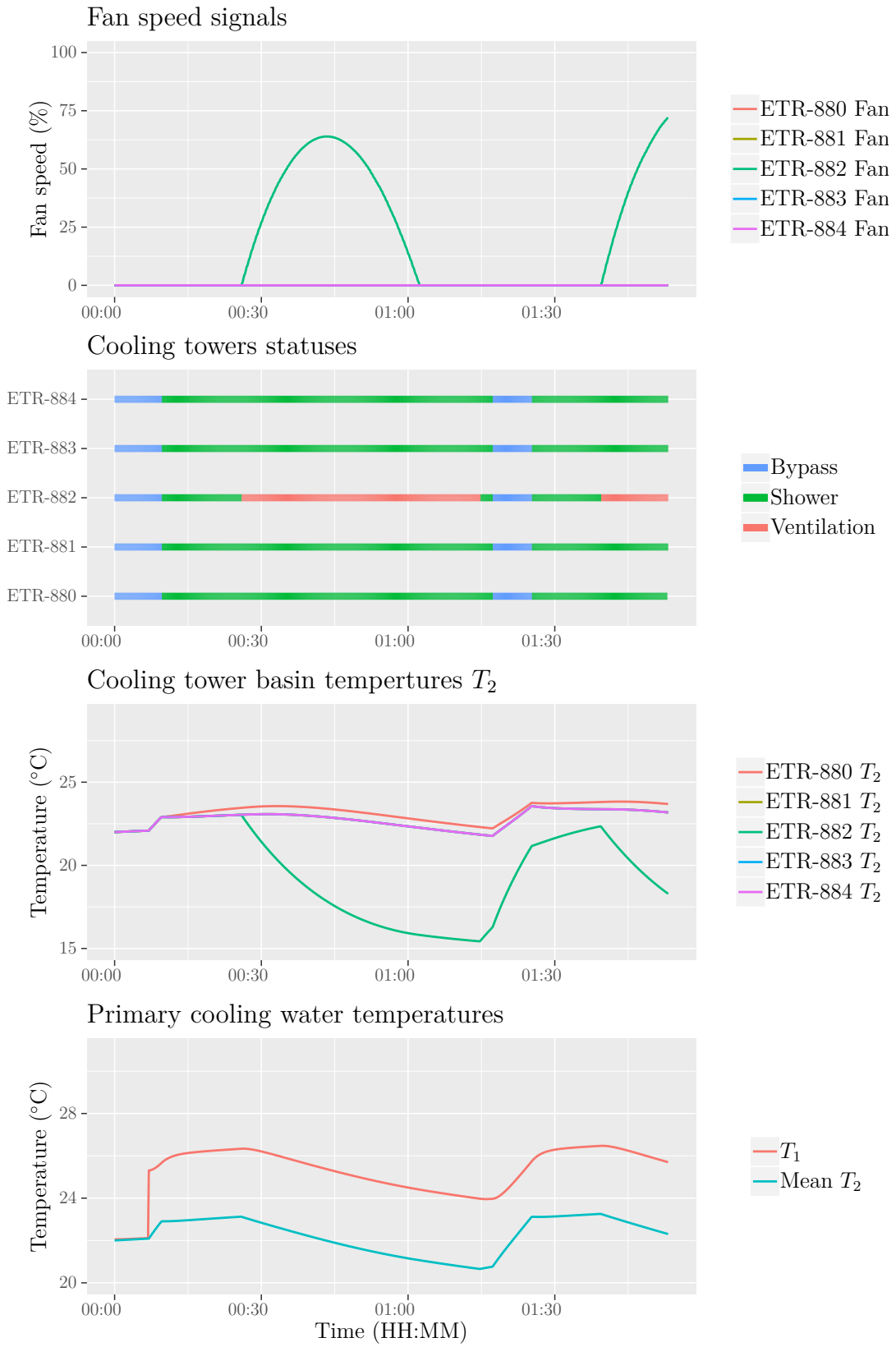

Figure 28: Scenario W3. Virtual commissioning control actions from real PLC for a winter scenario. It is seen that the control system switches from bypass to showering less than 5 minutes after the heat recovery loss event.

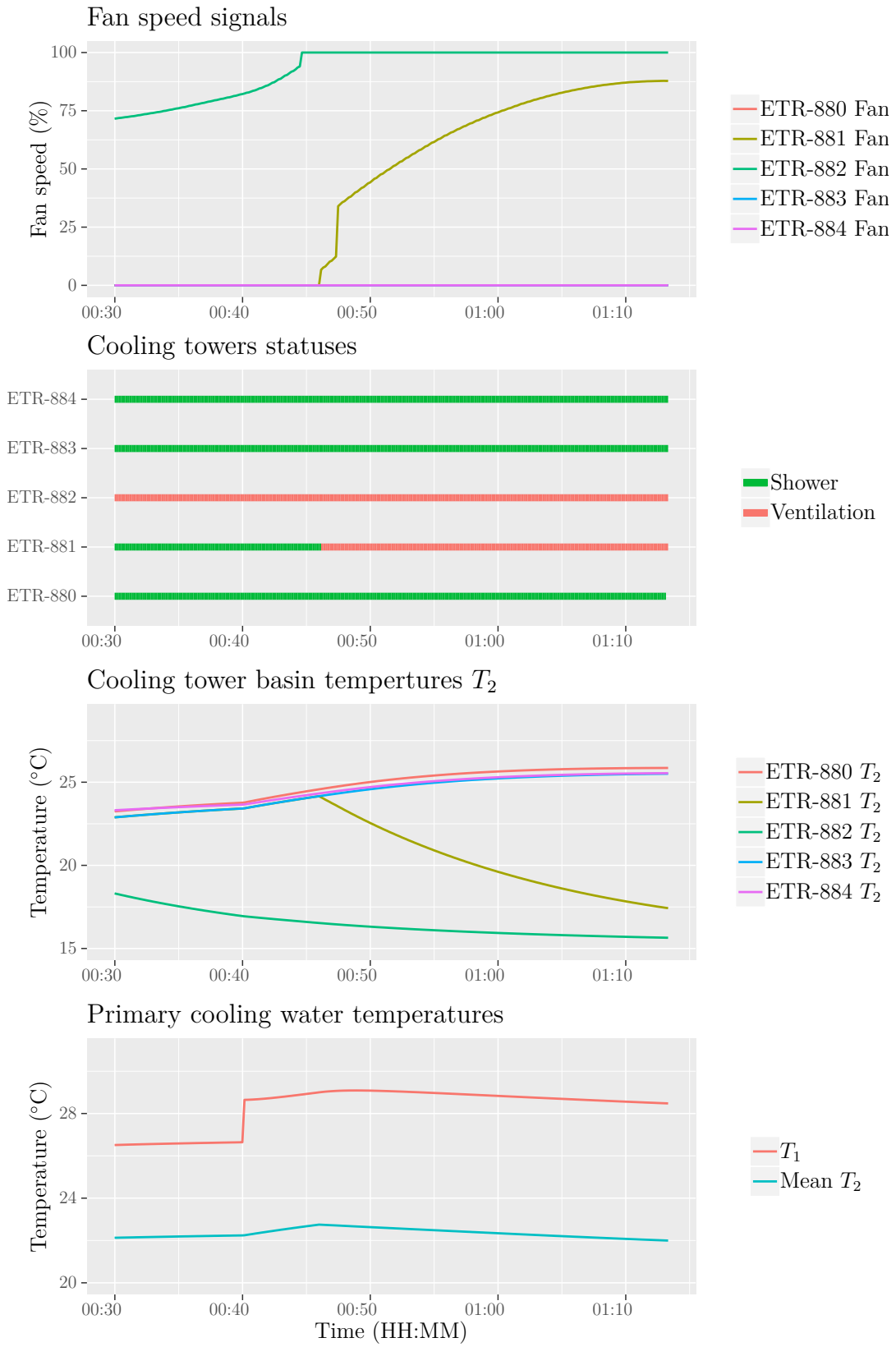

Figure 29: Scenario M1. Virtual commissioning control actions from real PLC for a winter scenario. It is seen that a new ventilator is started 5 minutes after the loss of heat recovery and the output temperature remains nominal.

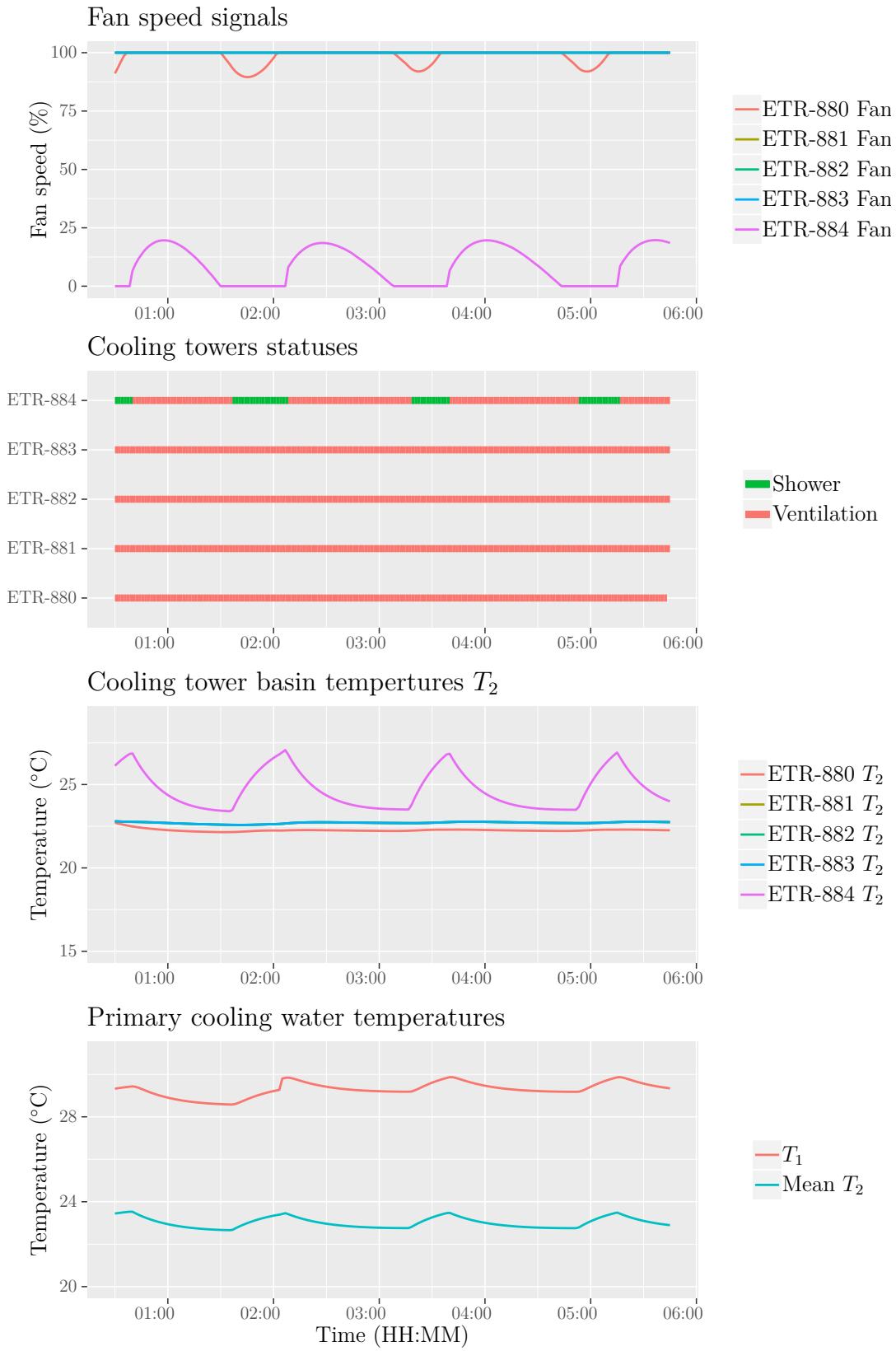

Figure 30: Scenario S1. The step in input temperature T_1 is insignificant compered to the normal oscillation of the system.

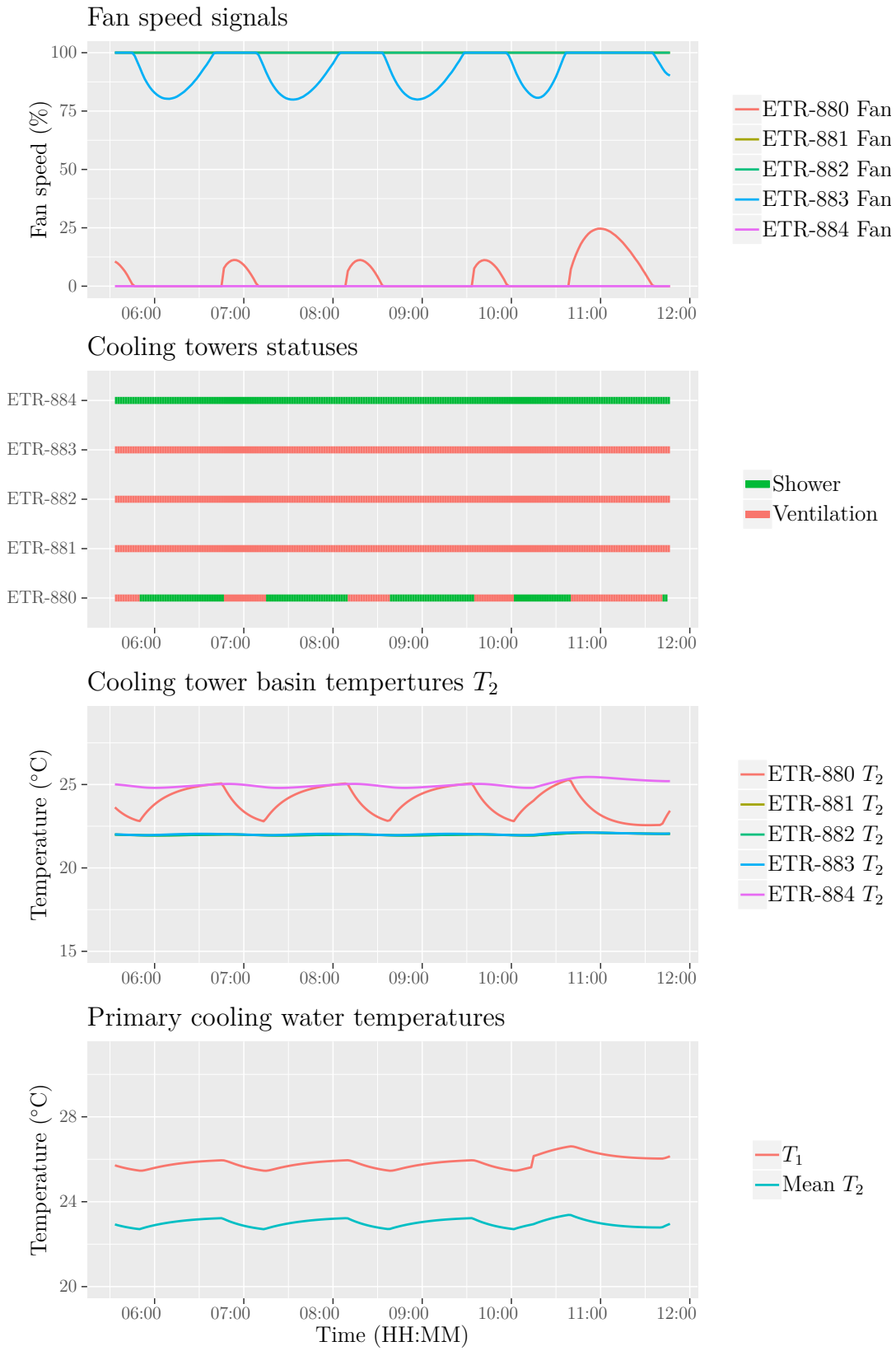

Figure 31: Scenario S3. The step in input temperature T_1 is insignificant compered to the normal oscillation of the system.

WHR -loss scenarios simulated are presented in figures (28), (29), (30) and (31). It is clear from the results that the fluctuations are damped well and do not raise concerns of the ability of the current control configurations performance. In figure (29) it is seen that the control system does not react immediately, but lets the basin temperatures go up for more than 5 minutes, before ramping up one more fan. Still the fluctuations are small and at acceptable level in the cooling water temperature Mean T_2 returned by the cooling tower complex.

In figures (30) and (31) the fluctuations are as small as the normal oscillation of the system. The oscillation seen in Mean T_2 and control actions are very similar as the normal operation and oscillation in the real system. The oscillation, which the model reproduces well, is due to the discrete steps in the cooling capacity when starting or shutting down cooling tower fans. The airflow at minimum fan speed is much higher than the free convection air flow during showering mode, thus the control region of the cooling rate is non-continuous. This forces the control system to oscillate around the setpoint.

7 Conclusions and development proposals

This chapters discusses and concludes the model developed in this thesis, the model reliability analysis and the results of the simulations. The results of the validation study, model accuracy in predicting the behaviour of the real system was presented in chapter (5). The results of simulations of heat recovery loss scenarios where presented in the chapter (6), and in section (6.2) the use of the model in the virtual commissioning environment, was shown to work satisfactory.

7.1 Model reliability, sensitivity and limitations

This Thesis presents how the evaporative cooling tower modeling method presented by Jin (2011) has been successfully implemented for an industrial application. The model validation shows that the model selection is good and it represents the real system well, and the model can thus be used to simulate the cooling towers at LHC point 8 for control system testing and verification purposes. The model was validated both against observed steady operation points and real dynamic data.

The data for model validation was extracted from the LHC logging system, where data was available from the last 5 years. The quality of the data was good and contained little or no outliers. The data had been archived using dead band filtering, which preserves major dynamics of the real signal but the smallest oscillations smaller than the dead band threshold are not included. After query, the data was re-sampled to 1Hz time series using forward filling, and was found to work well for both steady state and dynamic parameter identification.

The data was split into training and test data sets. Training data set was used to optimize the model steady state parameters and test data set was used to validate the parameters. The steady operation point validation showed minor systematic error, mean residual is 0.2 - 0.3 $°C$ below the observed basin temperatures, with approximately normally distributed residuals. Approximately normally distributed residuals indicate that the model is able to represent the characteristics of the real system and the error is random, and is not explained by some missing feature in the model.

Transient events available in the historical data were used to validate the dynamic performance of the model. In section 5.4.1 figures show the model estimate versus observed output temperatures. The model reproduces the dynamics in output temperature very well with root mean squared error (RMSE) between 0.75 and 1.25 °C in the simulated scenarios. The accuracy is not as good as what was reached in Jin (2011), which was expected as applying the method for an industrial application will be more challenging than for a smaller scale system with more thorough measurement instrumentation. This is affected by the restrictions in the available data and the

necessary assumptions made, mainly the air mass flow estimation.

The model, which in the original publication is used only for mechanical draft mode, was found to perform well also under free convection mode, and the model validation was conducted regardless the fan being on or off. Model validation showed root mean squared error of close to 1 $°C$. However under free convection mode the model has more uncertainty regarding the air mass flow, as the fan is not regulating the flow. If the model parameter optimization would be restricted to mechanical draft mode, or more accurate estimation of the air mass flow under free convection mode would be used, the accuracy of the model would get better. Bypass is modeled as a perfect mixing volume of water size of the LHC point 8 cooling tower basins. The dynamic validation scenarios show that the model also imitates the bypass mode well.

Alternative modeling approach would be to only use a steady state model for the cooling towers, and use a CFD simulation for the cooling tower basins. It's a more extensive modeling work compared to the approach of this thesis, but could possibly lead into more accurate results. This alternative approach would presumably predict the dynamics in the cooling towers well, as the cooling tower shower dynamics can be considered very fast compared to the dynamics in the basin.

7.2 The data

Gathering and working with the data, developing scripts to parse the data and identify steady operation points, has been a major part of the whole work, and has helped to build understanding of the system behaviour. The LHC-logging has proven very valuable, as all available data was easily accessible. The data was gathered to cooling tower data sets, which included the available ambient and system variables for each of the cooling towers. These data sets could be used early on to test the first prototypes of the model, and to monitor how the model accuracy got better after improvements.

The data also revealed a few important and interesting characteristics of the real system. The events in the data show that the towers react to transients very slowly, which was identified to be due to the large volume of water in the cooling towers basins. It was also noticed that there is a big step in the heat dissipation rate, between free convection mode and fan at minimal speed. This was later tracked down to an original design feature of the control system forced due to a high minimum speed limitation of the ventilator unit, resulting to frequency range of 33Hz - 50Hz or 990 - 1500 motor RPM.

7.3 Findings from the simulations

After comprehensive study on the available data, modeling methods proposed in the literature and model implementation and validation, the model could be used in simulations of the sudden loss of heat recovery, with a simplified representation of the heat load from the LHC and the experiments and heat absorption of the waste heat recovery in closed loop circuit. Different scenarios of the sudden loss of heat recovery were simulated, while applying selected manual control actions to increase the cooling capacity on the event of heat recovery loss. The closed loop simulation results show that the cooling towers have the capacity to damp the anticipated transients hardware wise.

The virtual commissioning was also proven to work satisfactorily. The model is able to handle all inputs of the control system in a right form and it provides all the necessary outputs for the control system. In the virtual commissioning environment the model reproduces well the slow oscillation experienced in the real system around the temperature set point, which further increases the confidence on the models ability to imitate the real system.

The virtual commissioning simulations show and verify that the current control algorithm is sufficient in damping anticipated temperature transients which may result after the operation of the heat recovery starts in 2020. Based on the results of the simulations run with model developed in this thesis, the engineers responsible for heat recovery project can go on with the installation and deployment knowing the current control configurations will work also after the introduction of waste heat recovery.

A recommended follow up and next use case of the model, is a more detailed look in to the current control configuration, and design of upgrades. The current control system is solely a proportional–integral–derivative (PID) feedback controller from the basin temperatures. The control is slow and allows oscillations and frequent fan start ups and shutdowns visible in the data and in the virtual commissioning simulations. The use of the model in control design allows exploring possibilities, fast prototyping, and more efficient and robust control configuration could be achieved. For example including the input temperature as a feed-forward signal would reduce oscillations, increase energy efficiency and improve robustness against temperature fluctuations in the input temperature. The model developed in this thesis can be then used to verify the upgraded control configuration and PLC -code prior to commissioning with a real system, to ensure reliable supply of primary cooling water to the LHC machine and the experiments.

8 Summary

In this thesis a dynamic evaporative cooling tower model is implemented based on the work of Jin (2011) and used in simulations of sudden temperature transients. The validation study shows that the developed model imitates the real system well. To the authors knowledge this Thesis is a first publication where this modeling method is applied for simulating real cooling towers. It is thus shown that the method can be successfully applied not only for the laboratory instrumentation but also for real industrial cooling towers. The virtual commissioning simulations conducted with the model show that the current cooling system and control configuration in use at LHC point 8 are sufficient in dampening the anticipated temperature fluctuations caused by the introduction of waste heat recovery (WHR).

After the installation and introduction of WHR in the cooling system in LHC long shutdown in 2018 - 2019, the WHR will start to absorb portion of the heat load from the LHC cryogenic cooling systems. The recovered waste heat is provided to a party outside the operations of CERN, the municipality of Ferney Voltaire. Thus CERN has to be able to adapt its cooling tower heat dissipation capacity in case of any malfunction by quickly absorbing the heat load, to ensure nominal cooling water temperature for sensitive and critical cryogenic cooling systems.

The literature review in this thesis is conducted to provide a basis for comparing and selecting an evaporative cooling tower modeling method that best fits the case. The author went through numerous relevant articles, and selected research studies on evaporative cooling and cooling towers are reviewed. It was found that the vast majority of the publications study cooling tower modeling only in steady state regime, and to the authors knowledge only one method was directly suitable for dynamic modeling. This hybrid modeling method combining physical formulation and empirical parameter optimization presented in Jin et al. (2007) and Jin (2011) is implemented in this Thesis. The method was chosen as it is well validated by the authors and can be accurately applied on a system which has historical operational data available for parameter optimization. This Thesis serves as a first publicly available proven use case of this modeling method.

The objective of developing a simulation model for the cooling towers at LHC point 8 is reached by developing a simulation model based on the work by Jin et al. (2007), and training it for the cooling towers at LHC point 8. To train the model by optimizing its four parameters, observations are needed for all of the four input variables and the output variable. Output variable, the cooling water output temperature, and input variables ambient wet-bulb temperature, input water temperature and flow are obtained from the LHC data logging archive. The fourth input variable, air mass flow, is not measured directly, and a linear regression model is used to estimate air mass flow from the fan speed control signal. The model is implemented in EcosimPro simulation software. The scripts for data mining, data visualization and parameter optimization are written in R-programming language. The model is cross-validated

by separating the data to training set for parameter optimization and testing set for model validation. The model is found to imitate the real system well.

To study the event of sudden loss of waste heat recovery, simulations are run in virtual commissioning environment. Virtual commissioning is a practise in which a system consisting of programmable logic controller (PLC) and a physical process, the real process is replaced by a simulation model running on a computer. It is concluded that the current control configuration is sufficient in damping the temperature transients also after the introduction of waste heat recovery. Simulations presented in this Thesis are simulated in EcosimPro which connects through an OPC UA interface to a PLC that contains a copy of the control code that is currently commissioned controlling the real cooling tower complex. These virtual commissioning simulations with a well performing model and real control actions determined by a PLC, gives a realistic picture of the system overall.

References

Atlas Collaboration, ed. (2015). *Mural of the Atlas detector*. URL: https://cds.cern.ch/record/2007504/files/2015-04-05_ATLAS-CR-FirstBeams_01.jpg?subformat=icon-1440.

Bazaraa, Mokhtar S., Hanif D. Sherali, and C. M. Shetty (2006). *Nonlinear Programming: Theory and Algorithms*. John Wiley and Sons, Incorporated. ISBN: 9780471787761.

Bille, R, M Perty, and M Marczukajtis (2002). *The LHC logging*. Tech. rep. Geneva: CERN. URL: http://lhc-logging.web.cern.ch/lhc-logging/docs/design/LHCLOG_AD.pdf.

Blanco, E and Ph Gayet (2007). "LHC Cryogenics Control System: Integration of the Industrial Controls (UNICOS) and Front-End Software Architecture (FESA) Applications". In: URL: http://accelconf.web.cern.ch/Accelconf/ica07/PAPERS/WOAA03.PDF.

Booth, William et al. (2018). "Virtual control commissioning for a large critical ventilation system: The CMS cavern use case". In: MODPL02. 7 p. URL: https://cds.cern.ch/record/2306216.

Bradu, Benjamin, Philippe Gayet, and Silviu-Iulian Niculescu (2009). "A process and control simulator for large scale cryogenic plants". In: *Control Engineering Practice* 17.12. Special Section: The 2007 IFAC Symposium on Advances in Automotive Control, pp. 1388–1397. ISSN: 0967-0661. DOI: https://doi.org/10.1016/j.conengprac.2009.07.003. URL: http://www.sciencedirect.com/science/article/pii/S0967066109001348.

Brüning, Oliver Sim et al. (2004). *LHC Design Report*. CERN Yellow Reports: Monographs. Geneva: CERN. URL: http://cds.cern.ch/record/815187.

CERN, ed. (2015). *The CERN accelerator complex*. URL: https://cds.cern.ch/record/2225847.

– ed. (2018a). *About CERN*. URL: https://home.cern/about.

– ed. (2018b). *CERN Accelerators*. URL: https://home.cern/accelerators.

– ed. (2018c). *CERN and the Environmnet*. URL: http://environmental-impact.web.cern.ch/environmental-impact/.

– ed. (2018d). *CERN Knowledge Transfer*. URL: https://kt.cern/about-us.

– ed. (2018e). *CERN Physics*. URL: https://home.cern/physics.

– ed. (2018f). *CERN Timelines*. URL: https://timeline.web.cern.ch/timelines/The-history-of-CERN.

– ed. (2018g). *Cryogenics: Low temperatures, high performance*. URL: https://home.cern/about/engineering/cryogenics-low-temperatures-high-performance.

– ed. (2018h). *Pulling together: Superconducting electromagnets*. URL: https://home.cern/about/engineering/pulling-together-superconducting-electromagnets.

CERN Engineering Department, ed. (2017a). *2017 Power Dissipated by the Cooling Towers*. URL: http://en.web.cern.ch/sites/en.web.cern.ch/files/EN-CV-Thermal_Energy_2017.pdf.

– ed. (2017b). *Consumption Flyers*. URL: http://en.web.cern.ch/consumption-flyers.

CERN Industrial Controls and Safety Group (ICS), ed. (2018). *UNICOS (UNified Industrial Control System)*. URL: http://unicos.web.cern.ch/.

CERN Outreach, ed. (-). *Beam*. URL: https://lhc-machine-outreach.web.cern.ch/lhc-machine-outreach/beam.htm.

CERN Technology Department, ed. (2015). *The CERN underground facilities*. URL: http://te-epc-lpc.web.cern.ch/te-epc-lpc/machines/lhc/pagesources/LHC-Underground-Layout.png.

Claudet, Serge (2017). *CERN Energy Management, Energy efficiency analysis and selected projects*. URL: https://indico.eli-np.ro/event/1/contributions/7/attachments/69/105/5_CERN_Energy_Claudet.pdf.

EcosimPro, ed. (2018). *Thermal, Thermal Network Simulation*. URL: https://www.ecosimpro.com/products/thermal/.

El Geneidy, Rami (2016-06-13). "Improving energy efficiency of passenger ships by discrete-event simulation; Matkustajalaivojen energiatehokkuuden parantaminen diskreetillä simuloinnilla". en. G2 Pro gradu, diplomityö, pp. 80+29. URL: http://urn.fi/URN:NBN:fi:aalto-201606172644.

Engineering ToolBox, ed. (2003). *Pump Affinity Laws*. URL: https://www.engineeringtoolbox.com/affinity-laws-d_408.html.

ESS, ed. (2013). *ESS to deliver waste heat to Kraftringen's district heating network*. URL: https://europeanspallationsource.se/ess-deliver-waste-heat-kraftringens-district-heating-network.

Fisenko, S.P., A.A. Brin, and A.I. Petruchik (2004). "Evaporative cooling of water in a mechanical draft cooling tower". In: *International Journal of Heat and Mass Transfer* 47.1, pp. 165–177. ISSN: 0017-9310. DOI: https://doi.org/10.1016/S0017-9310(03)00409-5. URL: http://www.sciencedirect.com/science/article/pii/S0017931003004095.

Gani, Rafiqul and Efstratios N Pistikopoulos (2002). "Property modelling and simulation for product and process design". In: *Fluid Phase Equilibria* 194-197. Proceedings of the Ninth International Conference on Properties and Phase Equilibria for Product and Process Design, pp. 43–59. ISSN: 0378-3812. DOI: https://doi.org/10.1016/S0378-3812(01)00680-X. URL: http://www.sciencedirect.com/science/article/pii/S037838120100680X.

Gesellschaft, VDI (2010). *VDI Heat Atlas*. VDI-Buch. Springer Berlin Heidelberg. ISBN: 9783540778769. URL: https://books.google.fi/books?id=0t-HrUf1aHEC.

Jin, Guang-Yu (2011). "Modeling and optimization of building HVAC systems." PhD thesis. Nanyang Technological University, School of Electrical Electronic Engineering. URL: https://dr.ntu.edu.sg/handle/10356/49960.

Jin, Guang-Yu et al. (2007). "A simplified modeling of mechanical cooling tower for control and optimization of HVAC systems". In: *Energy Conversion and*

Management 48.2, pp. 355–365. ISSN: 0196-8904. DOI: https://doi.org/10.1016/j.enconman.2006.07.010. URL: http://www.sciencedirect.com/science/article/pii/S0196890406002317.

Jurns, John M., Harald Bäck, and Martin Gierow (2014). "Waste heat recovery from the European Spallation Source cryogenic helium plants - implications for system design". In: *AIP Conference Proceedings* 1573.1, pp. 647–654. DOI: 10.1063/1.4860763. eprint: https://aip.scitation.org/doi/pdf/10.1063/1.4860763. URL: https://aip.scitation.org/doi/abs/10.1063/1.4860763.

Kloppers, J.C. and D.G. Kröger (2005). "A critical investigation into the heat and mass transfer analysis of counterflow wet-cooling towers". In: *International Journal of Heat and Mass Transfer* 48.3, pp. 765–777. ISSN: 0017-9310. DOI: https://doi.org/10.1016/j.ijheatmasstransfer.2004.09.004. URL: http://www.sciencedirect.com/science/article/pii/S0017931004004041.

Knauer, Jürgen et al. (2018). "Bigleaf—An R package for the calculation of physical and physiological ecosystem properties from eddy covariance data". In: *PLOS ONE* 13.8, pp. 1–26. DOI: 10.1371/journal.pone.0201114. URL: https://doi.org/10.1371/journal.pone.0201114.

Lee, Chi G. and Sang C. Park (2014). "Survey on the virtual commissioning of manufacturing systems". In: *Journal of Computational Design and Engineering* 1.3, pp. 213–222. ISSN: 2288-4300. DOI: https://doi.org/10.7315/JCDE.2014.021. URL: http://www.sciencedirect.com/science/article/pii/S2288430014500292.

Ljung, L. and T. Glad (1994). *Modeling of Dynamic Systems*. Prentice-Hall information and system sciences series. PTR Prentice Hall. ISBN: 9780135970973. URL: https://books.google.fi/books?id=zO9qQgAACAAJ.

Mairie de Ferney-Voltaire, ed. (2018). *La Zone d'Aménagement Concertée*. URL: https://www.ferney-voltaire.fr/politique-de-la-ville-projets/grands-projets/zac-ferney-geneve-innovation.

Mertens, Volker (2018). *Energy management and efficiency*. URL: https://indico.cern.ch/event/656491/contributions/2921120/attachments/1628667/2594902/FCC_EME_Amsterdam_VM_110418.pdf.

Naphon, Paisarn (2005). "Study on the heat transfer characteristics of an evaporative cooling tower". In: *International Communications in Heat and Mass Transfer* 32.8, pp. 1066–1074. ISSN: 0735-1933. DOI: https://doi.org/10.1016/j.icheatmasstransfer.2005.05.016. URL: http://www.sciencedirect.com/science/article/pii/S0735193305001041.

Al-Nimr, M.A. (1998). "Dynamic thermal behaviour of cooling towers". In: *Energy Conversion and Management* 39.7, pp. 631–636. ISSN: 0196-8904. DOI: https://doi.org/10.1016/S0196-8904(97)10006-1. URL: http://www.sciencedirect.com/science/article/pii/S0196890497100061.

OPC Foundation, ed. (2018a). *Unified Architecture*. URL: https://opcfoundation.org/about/opc-technologies/opc-ua/.

– ed. (2018b). *What is OPC?* URL: https://opcfoundation.org/about/what-is-opc/.

Qi, Xiaoni et al. (2016). "Performance prediction of a shower cooling tower using wavelet neural network". In: *Applied Thermal Engineering* 108, pp. 475–485. ISSN: 1359-4311. DOI: https://doi.org/10.1016/j.applthermaleng.2016.07.117. URL: http://www.sciencedirect.com/science/article/pii/S1359431116312509.

Roderick, C et al. (2009). *The LHC Logging Service : Handling terabytes of on-line data*. Tech. rep. CERN-ATS-2009-099. Geneva: CERN. URL: https://cds.cern.ch/record/1215574.

"A Celebrated Physicist With a Passion for Music" (2018). In: *The New York Times*. Ed. by The New York Times. URL: https://www.nytimes.com/2018/03/07/science/fabiola-gianotti-physics-cern.html (visited on 02/08/2018).

Todd, Benjamin et al. (2017). "LHC Availability 2017: Standard Proton Physics". In: URL: https://cds.cern.ch/record/2294852.

Viljakainen, Olli (2013). *Cooling Tower Modeling in Apros Software*. Espoo.